In compliance with the
Canadian Privacy Legislation
some supporting forms
may have been removed from
this dissertation.

While these forms may be included
in the document page count,
their removal does not represent
any loss of content from the dissertation.

UNIVERSITY OF ALBERTA

THE GENESIS AND EVOLUTION OF PRE-MISSISSIPPIAN BRINES IN THE WILLISTON BASIN, CANADA-U.S.A.

by

Heather Trudy Iampen ©

A thesis submitted to the Faculty of Graduate Studies and Research in partial fulfillment of the requirements for the degree of Master of Science.

DEPARTMENT OF EARTH AND ATMOSPHERIC SCIENCES

Edmonton, Alberta

Fall, 2003

National Library
of Canada

Acquisitions and
Bibliographic Services

395 Wellington Street
Ottawa ON K1A 0N4
Canada

Bibliothèque nationale
du Canada

Acquisisitons et
services bibliographiques

395, rue Wellington
Ottawa ON K1A 0N4
Canada

Your file Votre référence
ISBN: 0-612-87787-6
Our file Notre référence
ISBN: 0-612-87787-6

The author has granted a non-exclusive licence allowing the National Library of Canada to reproduce, loan, distribute or sell copies of this thesis in microform, paper or electronic formats.

L'auteur a accordé une licence non exclusive permettant à la Bibliothèque nationale du Canada de reproduire, prêter, distribuer ou vendre des copies de cette thèse sous la forme de microfiche/film, de reproduction sur papier ou sur format électronique.

The author retains ownership of the copyright in this thesis. Neither the thesis nor substantial extracts from it may be printed or otherwise reproduced without the author's permission.

L'auteur conserve la propriété du droit d'auteur qui protège cette thèse. Ni la thèse ni des extraits substantiels de celle-ci ne doivent être imprimés ou aturement reproduits sans son autorisation.

Canadä

UNIVERSITY OF ALBERTA

LIBRARY RELEASE FORM

NAME OF AUTHOR: Heather Trudy Iampen

TITLE OF THESIS: The Genesis and Evolution of Pre-Mississippian Brines in the Williston Basin, Canada-U.S.A.

DEGREE: Master of Science

YEAR THIS DEGREE GRANTED: 2003

Permission is hereby granted to the University of Alberta Library to reproduce single copies of this thesis and to lend or sell such copies for private, scholarly or scientific research purposes only.

The author reserves all other publication and other rights in association with the copyright in the thesis, and except as hereinbefore provided neither the thesis nor any substantial portion thereof may be printed or otherwise reproduced in any material form whatever without the author's prior written permission.

(Signed)

Date: January 24, 2003

UNIVERSITY OF ALBERTA

FACULTY OF GRADUATE STUDIES AND RESEARCH

The undersigned certify that they have read, and recommend to the Faculty of Graduate Studies and Research for acceptance, a thesis entitled **The Genesis and Evolution of Pre-Mississippian Brines in the Williston Basin, Canada-U.S.A.** submitted by **Heather Trudy Iampen** in partial fulfillment of the requirements for the degree of Master of Science.

Dr. Benjamin J. Rostron

Dr. Karlis Muehlenbachs

Dr. Hans Machel

Dr. Ian Hutcheon

Date: November 12, 2002

ABSTRACT

Variations in solute concentrations are used to constrain the genetic and evolutionary processes affecting formation waters in pre-Mississippian units of the Williston Basin (Canada-U.S.A.) to obtain a better understanding of fluid-flow. Three genetic endmembers were identified in the pre-Mississippian formations based on new major and minor ion data from 116 wellhead samples. Group A waters in the west, with TDS < 40,000 mg/L, are of meteoric origin. Group B, Na-Cl rich waters in the north and east, with TDS > 300,000 mg/L, are halite-derived. Group C, Ca-Cl rich waters in the basin center, with TDS > 300,000 mg/L, are evaporated seawaters that have undergone dolomitization, albitization and anhydrite cementation. Mixing between each of these three endmembers produces three distinct mixing zones, yielding six types of basinal waters in total. Spatial and chemical relationships indicate meteoric water has infiltrated into the basin for some time, eroding residual seawater through mixing, and dissolving halite.

To Ron Iampen, who set the standard, and in memory of Marilyn Iampen, who never imparted limits and ensured I had every opportunity.

ACKNOWLEDGEMENTS

Ben Rostron has afforded me much patience and understanding throughout my master's degree and it is most sincerely appreciated. I would like to thank him for the opportunities to attend conferences, especially Geofluids III, and for including me in his vision of the Williston Basin brine-sampling program. Many thanks are also extended to committee members Hans Machel, Karlis Muehlenbachs and Ian Hutcheon, who have supported my education both in courses and helpful discussion. I am grateful for the time you have spent reviewing this thesis. I also wish to express gratitude to Carl Mendoza for advice, positive challenges and much assistance in numerous capacities throughout my education in hydrogeology.

Sharing many courses, TA-experiences, conferences and discussions and lots of good laughs with members of the hydro group has made this experience a lot more enjoyable. I also am appreciative of the support provided by my family and by friends outside of the University who have encouraged me to keep going, particularly Robert Morley.

The support of John Duke who painstakingly adapted an analytical method to meet our needs was indispensable.

Berkley Petroleum and Wascana Energy/Canadian Occidental Petroleum provided funding for this research. Financial support for the sampling program was also provided in the form of an AAPG Grant-in-Aid awarded to H. Iampen and NSERC funding awarded to B. Rostron. Presentation of preliminary results at Geofluids III was made possible in part by a Mary Louise Imrie Scholarship awarded to H. Iampen. Graduate Teaching Assistantships from the Department of Earth and Atmospheric Sciences are also appreciated.

Many companies granted permission to sample wells on their leases including: Texakota, Jettison, Headington Oil, Cherryhill Resources, Berkley Petroleum, Williston Industrial Supply Corp., Wascana Energy, Westport Oil and Gas, Northrock Resources, Sceptre Resources, Continental Operating Corp., Colt Resources, Eland Energy, Burlington Resources, Petro Hunt LLC, Flying J Oil and Gas, Condor Petroleum, Summit Resources, Mayson Inc., Amerada Hess, Suncor, Berco Resources, Anderson Exploration, Stampeder, Cavell, Duce, Armstrong Operating, Wesco Operating, Best Pacific Resources, Lyco Energy, Upton Resources, Tarragon Oil and Gas, Shell, Panterra/Nance Petroleum, Ocean Energy, Trilink Resources, Luff Exploration, Husky Oil, BTA Producers, Omimex Petroleum, Founders Energy, Geo Resources, Eagle Operating.

The data set published in this thesis would not exist without the most kind and generous assistance provided by the operators and foremen of the above companies.

Contents

CHAPTER 1

1. Introduction 1
    - 1.1. Study rationale 1
    - 1.2. Current Thesis and Objectives 2

CHAPTER 2

2. Study Area 4
    - 2.1. Geological Overview 4
        - 2.1.1. Stratigraphy 5
        - 2.1.2. Hydrostratigraphy 7
    - 2.2. Regional Hydrogeology 8
    - 2.3. The Influence of Geologic Structure on Flow 10
    - 2.4. Summary 10

CHAPTER 3

3. Hydrogeochemistry 17
    - 3.1. Fluid Origin and Evolution 17
        - 3.1.1. Origin of Brines 18
            - 3.1.1.1. Depositional Implications for Brine Development 18
            - 3.1.1.2. Na-Cl-Br Systematics 19
    - 3.2. Previous Hydrogeochemical Studies 20
        - 3.2.1. Previous Study Conclusions and Interpretation 21
    - 3.3. Shortcomings of Previous Hydrogeological Work 23
    - 3.4. Problem Resolution 26

CHAPTER 4

4. Methodology 28
    - 4.1. Data Collection and Sampling Procedure 28
    - 4.2. Data Analysis 30
        - 4.2.1. Inductively Coupled Plasma Atomic Emission Spectroscopy 31
        - 4.2.2. Neutron Activation Analysis 32

CHAPTER 5

5. Results 36
    5.1. Solute Relationships 36
    5.2. Types of Formation waters 37

CHAPTER 6

6. Discussion of Brine Origin and Evolution in the Williston Basin 55
    6.1. Evidence of a Non-Brine Endmember 56
    6.2. Brines Derived from Salt Dissolution 57
        6.2.1. Major Ions in Group B Brines 57
        6.2.2. Minor Ions in Group B Brines 58
    6.3. Brines Derived from Evaporated Seawater 58
        6.3.1. Major Ions in Group C Brines 59
        6.3.2. Reactions Affecting Group C major Ions 60
        6.3.3. Minor Ions in Group C Brines 62
    6.4. Endmember Mixing 64
        6.4.1. Mixing Between Group A and B Endmembers 64
        6.4.2. Mixing Between Group A and C Endmembers 65
        6.4.3. Mixing Between Group B and C Endmembers 65
    6.5. Spatial Distribution of Endmembers and Mixtures 66
    6.6. Implications for Fluid Flow in the Williston Basin 67
    6.7. Summary of Origin and Evolution and Implications for Fluid Flow ...68

CHAPTER 7

7. Conclusions 84

REFERENCES 87

Appendix A – Well Location, Well Name, Well Operators and Comments ..93

Appendix B – Neutron Activation Analysis of Highly Saline Brines 96

Appendix C – Densities, Temperatures, Depths and Classification Data.........99

Appendix D – Minor Elements 103

Appendix E – Details of Reactions Possibly affecting Group C Major Ions 111

APPENDIX F – CALCULATIONS FOR ESTIMATING CA EXCESS, NA DEPLETION AND MG DEPLETION 116

LIST OF FIGURES

Figure 2.1. Significant physiographic features of the Williston Basin 12

Figure 2.2. The Williston Basin Study Area 13

Figure 2.3. Cross-section A to A' through the Williston Basin showing the subdivision of the pre-Mississippian portion of the basin 14

Figure 2.4. Pre-Mississippian stratigraphy and corresponding hydrostratigraphic units 15

Figure 2.5. Accepted present-day model of fluid flow in the Williston Basin 16

Figure 3.1. Relationship of TDS (g/L) in the Duperow Aquifer to Prairie Formation dissolution and subcrop against Cretaceous strata 27

Figure 4.1. Pre-Mississippian sample locations related to the Williston Basin Study Area boundary 34

Figure 5.1. TDS vs. depth 44

Figure 5.2. pH vs. depth 44

Figure 5.3. Bottom hole temperature vs. depth 44

Figure 5.4a-h. Chloride vs. TDS for pre-Mississippian hydrostratigraphic units 45

Figure 5.5a-h. Sodium vs. TDS for pre-Mississippian hydrostratigraphic units 46

Figure 5.6. Sodium vs. TDS 47

Figure 5.7. Calcium vs. TDS 47

Figure 5.8. Magnesium vs. TDS 48

Figure 5.9. Potassium vs. TDS 48

Figure 5.10. Strontium vs. TDS 49

Figure 5.11. Lithium vs. TDS 49

Figure 5.12. Bromide vs. TDS 50

Figure 5.13. Iodide vs. TDS 50

Figure 5.14. Sulphate vs. TDS 51

Figure 5.15. Bicarbonate vs. TDS 51

Figure 5.16. Calcium vs. TDS showing endmember groupings 53

Figure 5.17. Typical compositions for endmember groupings 54

Figure 6.1. Position of Group B endmember relative to the 1:1 halite dissolution line 70

Figure 6.2. Group B endmember Na/Br and Cl/Br molar ratios compared to seawater 70

Figure 6.3. The behavior of solutes during progressive seawater evaporation 71

Figure 6.4. Comparison of Group C chloride, sodium and potassium concentrations with the seawater evaporation trend 71

Figure 6.5. Comparison of Group C calcium, sulphate and magnesium concentrations with the seawater evaporation trend 72

Figure 6.6. Calcium vs. sulphate in Group C waters 72

Figure 6.7. Log ($Ca+Mg-SO_4$) vs. Log Br for Group C values 73

Figure 6.8. Ca excess vs. Mg depletion compared to evaporated seawater 73

Figure 6.9. Ca excess vs. Na depletion in Group C samples compared to evaporated seawater 74

Figure 6.10. Group C endmember Na/Br and Cl/Br molar ratios compared to seawater 74

Figure 6.11. Bromide vs. chloride for the group C endmember relative to seawater evaporation 75

Figure 6.12. Endmember groupings and mixtures on a sodium vs. chloride plot 75

Figure 6.13. Endmember groupings and mixtures on a calcium vs. TDS plot 76

Figure 6.14. Mix AB Na/Br and Cl/Br molar ratios compared to seawater 76

Figure 6.15. Mix AC Na/Br and Cl/Br molar ratios compared to seawater 77

Figure 6.16. Mix BC Na/Br and Cl/Br molar ratios compared to seawater 77

Figure 6.17. Ca vs. Cl/Br for saline endmembers and intermediate compositions compared to seawater 78

Figure 6.18. Ca excess vs. Mg depletion in WB samples compared to evaporated seawater..79

Figure 6.19. Ca excess vs. Na depletion in WB samples compared to evaporated seawater..80

Figure 6.20. Spatial distribution of endmember and mixtures 82

Figure 6.21. Cl/Br and Na/Br molar ratios for all pre-Mississippian samples 83

Figure 7.1. Schematic drawing of new flow model and brine composition 86

LIST OF TABLES

Table 4.1. Numbers of samples, sample locations and collection date 35

Table 5.1. Results for major and minor ions with concentrations > 1 mg/L.......... 40

Table 5.2. Classification scheme for pre-Mississippian waters based on TDS and calcium concentration in by milliequivalents per liter 52

Table 6.1. Summary of water and mixing group classifications 81

CHAPTER 1

1. INTRODUCTION

Large volumes of saline fluids in sedimentary basins, including brines with Total Dissolved Solids > 100 g/L (Carpenter, 1978), are an important part of fluid flow systems that affect diagenesis, hydrocarbon migration and ore deposit formation. Geochemical characterization of the origin and evolution of brines can constrain the rates and patterns of regional fluid flow (Tóth, 1984). However, brines can evolve quite extensively from initial compositions during the progression toward equilibrium with the host-rock, making brine origin somewhat difficult to discern. Movement or mixing of fluids within the host rock requires that new chemical equilibria are satisfied and may guarantee that equilibrium is never achieved. Mappable present-day fluid compositions represent the sum of the interactions and processes during fluid history. Conservative chemical tracers must be employed to track fluids back through successive evolutionary processes in order to determine the origin of brines.

1.1. STUDY RATIONALE

Hydrogeochemistry has been combined with hydrogeological studies to obtain a more accurate description of fluid flow in many sedimentary basins (Clayton et al., 1966; Hitchon and Friedman, 1969; Connolly et al., 1990; Stueber et al., 1998, and others). In the same manner, geochemical patterns, when combined with hydrogeological systems, can be used to delineate some of the large-scale geological processes in the Williston Basin, Canada-USA. This particular basin was chosen for study for the following reasons.

1) Basin geology and portions of the hydrogeological system are well-documented (Sloss, 1987; Downey et al., 1987; Hannon, 1987; Gerhard

and Anderson, 1988; Mossop and Shetsen, 1994; Bachu and Hitchon, 1996). A regionally active flow system exists with well-defined recharge and discharge areas (Downey, 1984; Gosnold, 1990; Bachu and Hitchon, 1996) and exploration and production of petroleum has provided abundant geological data and active wells from which to sample (Berg et al., 1994).

2) Plentiful economic resources also exist in the basin. Continuing hydrocarbon exploration can be aided by knowledge of fluid flow driving petroleum migration. Additionally, the potential of formation waters as a source of bromine, iodide and lithium has been shown (Kreis et al., 1991).
3) Previous studies have poorly constrained the origin and evolution of formation waters in the Williston Basin. The major difficulties with previous studies include: i) the areal restriction of studies based on international and national boundaries; ii) the poor definition and correlation of hydrostratigraphic units; iii) the principles underlying culling methods and number of data points used in studies; iv) the undetermined rates of flow in the deepest, highest Total Dissolved Solids (TDS) portion of the basin; and v) the lack of comprehensive analysis of samples, especially bromine data, to allow for a valid investigation of brine origin. Only one truly basin-wide study with detailed hydrostratigraphy used chemical data from Drill Stem Tests (DST's) to show major trends in formation water composition and classify groups of waters (Benn and Rostron, 1998). Unfortunately that study also lacked bromine data, and could not infer brine origin.

1.2. CURRENT THESIS AND OBJECTIVES

This thesis presents new geochemical data from the Cambrian through Bakken formations across the Williston Basin from 116 wells. The project had the following objectives:

1) To better understand the geochemistry of Williston Basin formation waters by collecting high quality data from producing wells.
2) To trace the origin of pre-Mississippian formation waters in the Williston Basin, especially the highly saline brines.
3) To discern and describe evolutionary processes affecting formation water compositions in the basin, both in the past and presently.
4) To combine the knowledge of processes controlling the genesis and evolution of pre-Mississippian waters to generate a preliminary outline of present and paleo fluid migration in the Williston Basin.

CHAPTER 2

2. STUDY AREA

The Williston Basin is a roughly circular intracratonic sedimentary basin centred in northwestern North Dakota that extends radially outward into regions of Saskatchewan, Manitoba, South Dakota and Montana (Figure 2.1). Geographically, it covers approximately 518,000 km^2, straddles the Canada-U.S.A. border, and extends from approximately 98.5^0 W to 108.5^0 W longitude and 45^0 N to 51.5^0 N latitude (Brown and Brown, 1987). The basin is bounded on the west and southwest by a series of Tertiary age uplifts (Sloss, 1987) and bounded on the east by the erosional edge at the Precambrian Shield (Figure 2.1). Previously, the basin had been delineated by an arbitrary zero elevation of the Cretaceous Dakota sandstone and equivalents in this area (Laird, 1952) (Figure 2.1). However, for the purpose of this study a basin outline defined by the 100m isopach of Ordovician through Silurian strata (Benn and Rostron, 1998) was used (Figure 2.2). The Red River Formation represents the maximum extent of deposition in the Paleozoic, and is more appropriate for a study related to the pre-Mississippian formations because pre-Mississippian formations are more areally extensive than Cretaceous units (Benn and Rostron, 1998).

2.1. GEOLOGICAL OVERVIEW

The regional geology of the Williston Basin has been well-documented, e.g. Gerhard and Anderson (1988), Mossop and Shetsen (1994) and many others. Only a summary of the geology, in the context of hydrogeochemistry, will be presented here. In the basin center, sediments covering the Precambrian basement reach over 4 km in depth and range in age from Cambrian to Cretaceous (Fuller, 1961; Peterson and MacCary, 1987) (Figure 2.3). The boundary separating pre-Mississippian units from the remaining Paleozoic and Mesozoic rocks has been placed above the upper black shale of the Bakken Formation (Carlson, 1967) (Figure 2.3). This boundary was chosen as the vertical limit for the study because the upper shale portion of the Bakken is thought to isolate the pre-Mississippian somewhat from the Mississippian formations, as indicated by the different formation water chemistry above and below the Bakken shale (Busby et al., 1995; Bachu and Hitchon, 1996).

2.1.1. STRATIGRAPHY

On a regional scale, pre-Mississippian strata can be divided into a lower clastic sequence, overlain by a carbonate sequence, capped by interbedded carbonates, shales and salt (Figure 2.3).

The lower clastic sequence consists of shales and sandstones of the Deadwood Formation (Upper Cambrian) and Winnipeg Formation (Middle Ordovician). The Deadwood Formation is composed of up to 270 m of quartz-sandstone interbedded with dolomitic limestone and shale (LeFever, 1996), deposited on the Precambrian basement. Rocks of the Deadwood Formation have a slightly smaller regional extent than the study area boundary and thin to a zero edge at the eastern perimeter of the basin (Kreis et al., 1991). Unconformably overlying the Deadwood Formation is the Winnipeg Formation. It consists of up to 135 m of medium grained sandstone and shale. The sandstone is highly porous except in the basin center due to compaction and silica cementation (LeFever, 1996). Less permeable shales of the upper Black Island, Icebox and Roughlock members cap the sandstone in much of the basin (Paterson, 1988).

Above the lower clastic sequence is a series of mainly dolostones and limestones ranging from Middle Ordovician to Upper Silurian in age. Lowermost, lying directly on the shales of the Icebox Member (over most of the basin), is the Red River Formation (Ordovician). It consists of a lower package of fractured limestone and dolomite and an upper package of three evaporite units of fractured limestone and anhydrite (Fuller and Porter, 1962). Red River strata thicken to 200 m in the basin center (Haidl et al., 1996). In Canada, the lower package in the Red River Formation is referred to as the Yeoman Formation and the upper package as the Herald Formation (Haidl et al., 1996). This study will observe the Canadian nomenclature, as the sub-division is consistent with observed hydrogeologic properties (Benn and Rostron, 1998). Conformably overlying the Red River, is the Stony Mountain Formation composed of up to 60 m of carbonate, shaly carbonate and anhydrite beds (Carlson and Eastwood, 1962). Next in succession is the Stonewall Formation (Upper Ordovician to Lower Silurian), which consists of 40 m of finely crystalline limestone and dolomite with two thin anhydrite beds in the central basin area (Carlson and Eastwood, 1962). Conformably overlying the Stonewall Formation is the Interlake Formation (Middle Silurian), which ranges from finely crystalline dolomites to calcareous dolomite and dolomitic limestone, thickening to 330 m (Carlson and Eastwood, 1962).

More diverse Devonian sediments comprise the upper-most pre-Mississippian sequence between the Stonewall Formation and Mississippian strata (Peterson and MacCary, 1987). The Devonian section is bounded on the bottom by a thin (6-15 m) shale unit termed the Ashern Formation (Edie, 1959). The overlying Winnipegosis Formation contains reef (maximum 40 m) and off-reef (maximum 12 m) deposits composed of dolostone (Edie, 1959). Next in the section, the Prairie Formation contains up to 200 m of halite, minor anhydrite and shale, as well as potash salts near the top (Gerhard and Anderson, 1988). Overlying the Prairie Formation, is the Dawson Bay Formation consisting of 30 to 60 m of dolomitic shales, limestones and mixed evaporites (Edie, 1959). Calcareous dolomite and anhydrites of the Souris River Formation overlie the Dawson Bay Formation (Sandberg and Hammond, 1958). The overlying Duperow Formation contains calcareous dolomite and is capped by thin shale equivalent to the Ireton shale in the Alberta Basin (Gerhard and Anderson, 1988). Covering the Duperow Formation, is the Birdbear Formation, which contains mainly limestone with some dolostone, and is followed by the Three Forks Formation containing massive dolostone (Gerhard and Anderson, 1988). At the top of the section, the Bakken Formation is composed of three layers, a basal shale, a middle sandstone and an upper shale (Gerhard and Anderson, 1988). The upper Bakken Shale at the top of the Devonian section represents the vertical limit of this study.

2.1.2. HYDROSTRATIGRAPHY

A hydrostratigraphic unit is described as a package of rock with similar hydraulic properties e.g., porosity, permeability (Seaber, 1997). To achieve the necessary detail required in hydrogeochemical differentiation of the pre-Mississippian units, these units have been grouped and/or classified into 15 hydrostratigraphic units (summarized in Figure 2.4) based on hydraulic properties and the general geology and lithology presented above.

In this study, relatively high permeability clastics of the Deadwood and Winnipeg formations have been grouped into one aquifer: the Cambro - Ordovician Aquifer. Separating these lower clastics from overlying sequences, the upper Winnipeg Formation shale members represents a less permeable cap referred to as the Winnipeg Aquitard. The Yeoman Formation limestones and dolomites are considered an aquifer. These limestones and dolomites are separated by the low permeability Herald Formation evaporite unit, referred to as the Herald Aquitard, from the Upper Ordovician to Lower Silurian limestones and dolomites termed the Ordo-Silurian Aquifer. Low permeability Ashern Formation shales comprise the Ashern Aquitard. Porous dolomite and reefal deposits of the Winnipegosis Formation are designated as the Winnipegosis Aquifer. The Prairie Formation evaporites form the significant Prairie Aquitard. The relatively permeable dolomites of the Dawson Bay and Souris River formations (part of the Manitoba Group) form the Manitoba Aquifer. The upper portion of the Souris River Formation, which contains more anhydrite, and is less permeable, forms the Souris River Aquitard. Limestones and dolostones of the Duperow Formation contain significant permeability and are referred to as the Duperow Aquifer. The thin overlying shale is referred to as the Ireton Aquitard. The porous Birdbear Formation limestones are designated as the Birdbear aquifer. The more permeable sandy portion of the Bakken Formation represents the upper-most aquifer of the section: the Bakken Aquifer. Finally, the upper Bakken Shale caps the section with a low permeability unit referred to as the Bakken Aquitard.

2.2. REGIONAL HYDROGEOLOGY

The Great Plains aquifer system, of which the Williston Basin is a part, is recognized as the largest, well-studied aquifer system in North America (Hannon, 1987). Previous hydrogeological studies in the Williston Basin, of varying scopes, fit into two major categories: (1) hydrogeological studies in the Canadian portion of the basin (Hannon, 1987; Bachu and Hitchon, 1996) and (2) hydrogeological studies in the US portion of the basin (Downey, 1982; Bredehoeft et al., 1983; Downey, 1984; Downey et al., 1987; LeFever, 1998). These previous studies focused mainly on groundwater evaluation in terms of water supply (Downey, 1982; Bredehoeft et al., 1983; Downey, 1984; Downey et al., 1987; Busby et al., 1995), rather than fluid flow relating to geologic processes. However after 90 years of study (Darton, 1906), data on both American and Canadian sides of the border have elucidated present-day regional flow paths and rates, and resulted in well-defined recharge and discharge areas.

The present hydrodynamic regime in the Williston Basin arose during the Laramide Orogeny (Bachu and Hitchon, 1996), which took place in the Late Cretaceous and

Early Tertiary (Sloss, 1987; Lisenbee and Dewitt, 1993). As a result of this orogeny, relief features formed, including: the Black Hills of South Dakota and the Pryor Mountains, Bighorn Mountains, Beartooth Mountains and Little Rocky Mountains of Montana (Figure 2.1), which affected the hydrogeology of the Williston Basin. While the Bighorn Mountains and the Black Hills contribute significant recharge to the aquifers, the other uplifted areas seem to contribute little water (Downey et al., 1987; Busby et al., 1995). Outcrops of the major aquifers in the Black Hills and the Bighorn Mountains are 1000-1600 maMSL (Downey, 1984; Gosnold, 1990), while elevations along the Canadian Shield average 300 maMSL (Gosnold, 1990).

Gravity-driven fluids move along a flow system that extends more than 965km and constitutes one of the largest confined aquifer systems in the world (Downey, 1984; Hannon, 1987; Gosnold, 1990). Studies focused on the Canadian side document fluid flow from southeastern Saskatchewan to western Manitoba (Bachu and Hitchon, 1996). Studies on the American side document flow from Montana and South Dakota to North Dakota. When combined, the complete regional picture created by the studies evokes flow from southwest to northeast (Figure 2.5). Meteoric water infiltrates aquifers directly at southwestern uplifts and flows downward into the basin in the southwest. As it continues down dip into the basin it is believed to dissolve the Prairie salt unit and form dense brines (Chipley and Kyser, 1991; Busby et al, 1995). Migration continues to the east and northeast where discharge occurs at outcrops and subcrops along the Canadian Shield (Downey et al., 1987). The eastward slope causes a corresponding slope in the potentiometric surface (with a maximum gradient of approximately 0.0013m/m NE) in pre-Mississippian aquifers and hence the driving force for large-scale regional flow (Hannon, 1987). A modelling study notes that flow in deeper pre-Mississippian aquifers is generally faster, but potentiometric data and modeled fluid flow velocities suggest fluid flow is very slow in all formations, especially within the brines (Downey et al., 1987) (Figure 2.5).

2.3. THE INFLUENCE OF GEOLOGIC STRUCTURE ON FLUID FLOW

Geologic structure may govern the rates and direction of flow to some degree, perhaps even on a regional basis (Downey et al., 1987). There are abundant lineaments and fault structures in the Williston Basin (Downey et al., 1987; Zhu and Hajnal, 1993). Faults and lineaments can provide paths of increased water movement, when they occur along the flow direction and are permeable, or they can impede flow when they are normal to the flow direction or are non-permeable. Recharge from the Bighorn Mountains appears to be channeled by geologic structure associated with major lineament zones. This recharge moves northeastward across the northern part of Powder River Basin to join the flow system from the Black Hills recharge area. The flow direction continues around the southern part of the Williston Basin to the northeast where it discharges in Manitoba and northeastern North Dakota.

2.4 SUMMARY

Centered in North Dakota, the Williston Basin study area coincides with the 100m isopach of Ordovician through Silurian strata. Regional geological units have been grouped or classified singularly as hydrostratigraphic units. Eight aquifers, predominately clastic or carbonate in composition, and eight aquitards, including shales, evaporites and cemented breccias, comprise the pre-Mississippian hydrostratigraphic section (Figure 2.4). Both aquifers and aquitards are laterally discontinuous, which may compartmentalize flow to some degree. With recharge at uplifts in the west and southwest, a gravity-driven flow system drives fluids from southwest to northeast to discharge in the vicinity of the Canadian Shield. Fluid movement is on the order of m/yr (Downey et al, 1987) and may be affected to some degree by geologic structure.

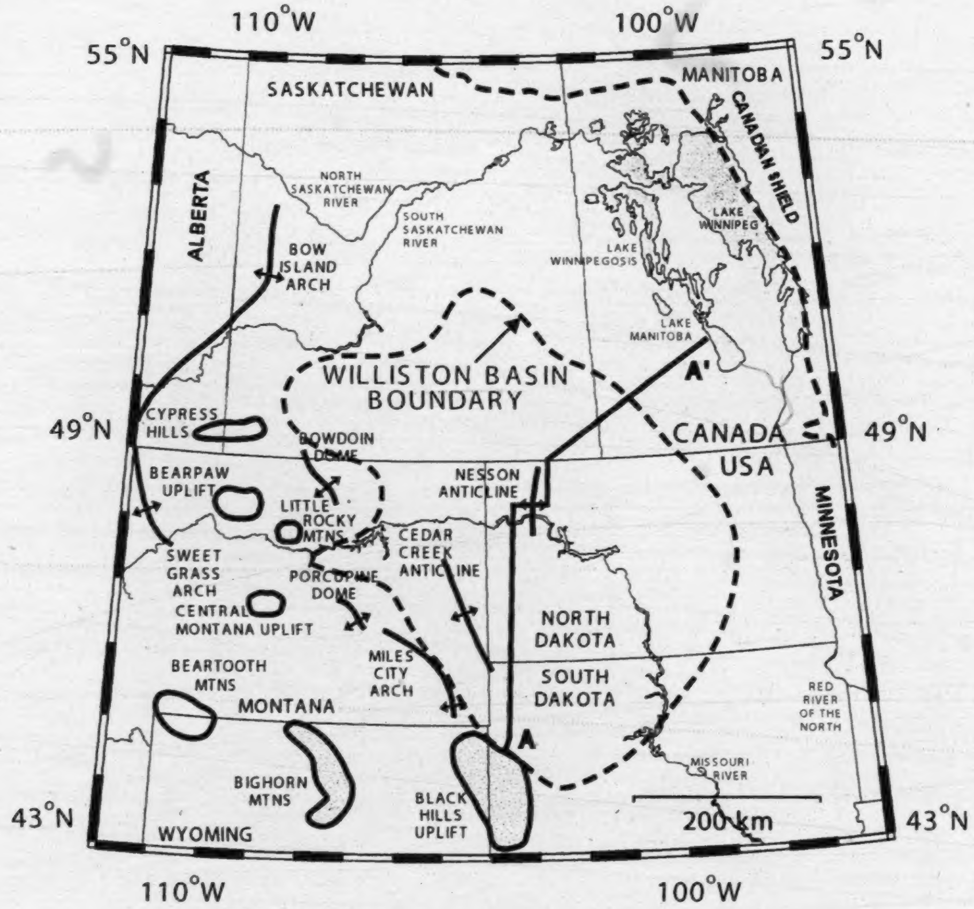
110°W
100°W
55°N
55°N
SASKATCHEWAN
MANITOBA
CANADIAN SHIELD
ALBERTA
NORTH SASKATCHEWAN RIVER
SOUTH SASKATCHEWAN RIVER
LAKE WINNIPEG
LAKE WINNIPEGOSIS
LAKE MANITOBA
BOW ISLAND ARCH
WILLISTON BASIN BOUNDARY
A'
CYPRESS HILLS
49°N
49°N
BOWDOIN DOME
CANADA
USA
BEARPAW UPLIFT
NESSON ANTICLINE
LITTLE ROCKY MTNS
MINNESOTA
CEDAR CREEK ANTICLINE
SWEET GRASS ARCH
PORCUPINE DOME
CENTRAL MONTANA UPLIFT
NORTH DAKOTA
BEARTOOTH MTNS
MILES CITY ARCH
SOUTH DAKOTA
MONTANA
RED RIVER OF THE NORTH
A
MISSOURI RIVER
BIGHORN MTNS
BLACK HILLS UPLIFT
200 km
43°N
43°N
WYOMING
110°W
100°W

Figure 2.1. Significant physiographic features of the Williston Basin (boundary after Laird, 1952), modified from Benn and Rostron, 1998. The location of cross-section A to A' (Figure 2.3) is shown. The green dashed line signifies the limit of the Canadian Shield. Stipled uplifts signify major recharge areas.

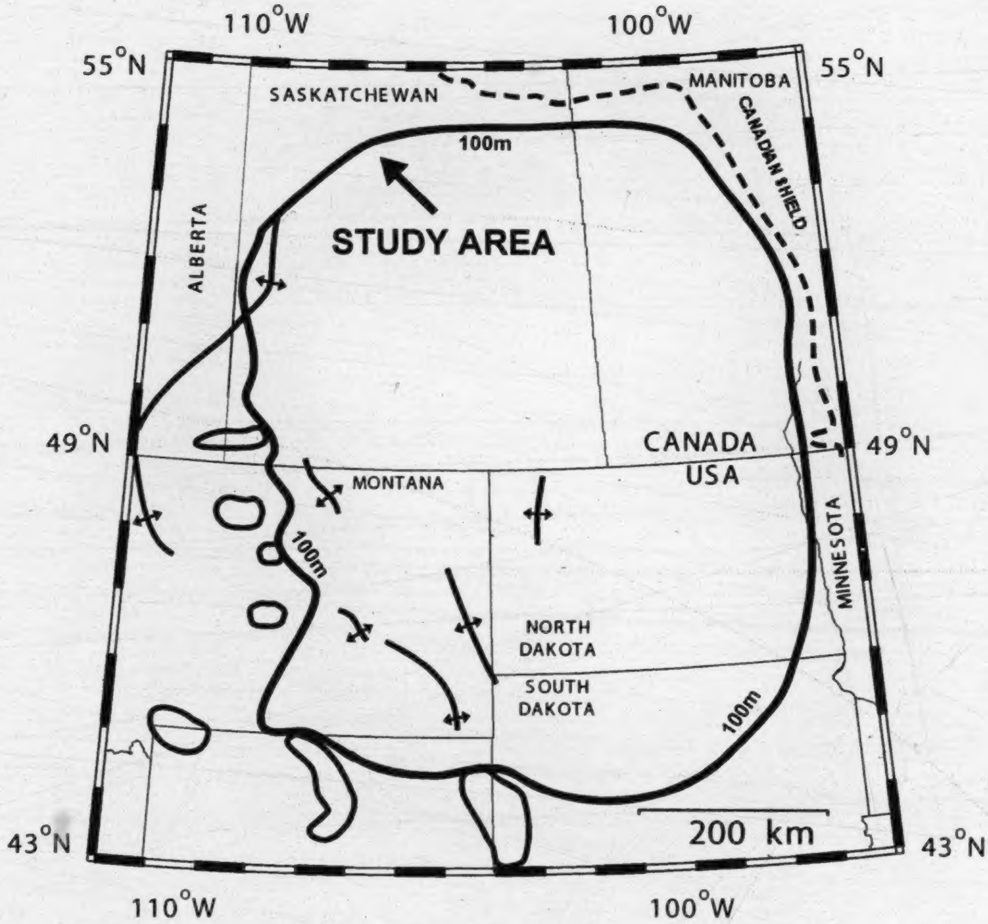
110°W
100°W
55°N
55°N
SASKATCHEWAN
MANITOBA
CANADIAN SHIELD
100m
STUDY AREA
ALBERTA
49°N
49°N
CANADA
USA
MONTANA
MINNESOTA
100m
NORTH DAKOTA
SOUTH DAKOTA
100m
200 km
43°N
43°N
110°W
100°W

Figure 2.2. The Williston Basin Study Area as defined by the 100m isopach of Ordovician through Silurian strata (after Benn and Rostron, 1998).

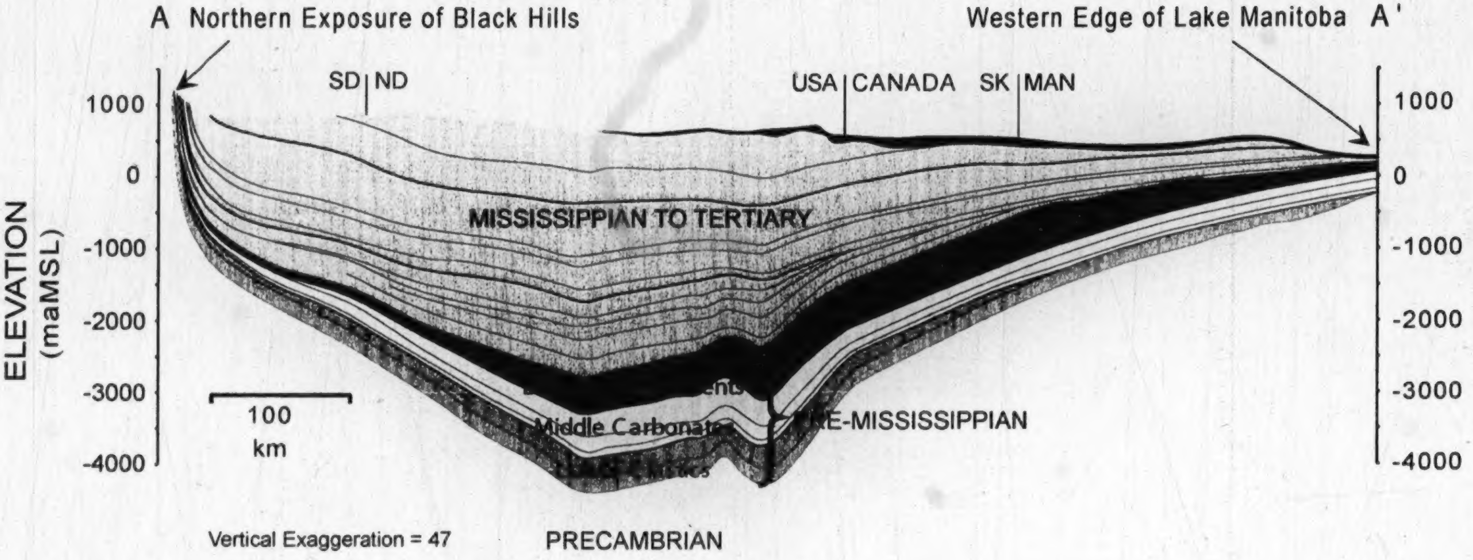
A Northern Exposure of Black Hills
Western Edge of Lake Manitoba A'
SD | ND
USA | CANADA
SK | MAN
1000
0
-1000
-2000
-3000
-4000
ELEVATION (maMSL)
MISSISSIPPIAN TO TERTIARY
Middle Carbonate
PRE-MISSISSIPPIAN
100 km
Vertical Exaggeration = 47
PRECAMBRIAN

Figure 2.3. Cross-section A-A' through the Williston Basin showing the subdivsion of the pre-Mississippian portion of the section, modified from Benn and Rostron, 1997. Location of cross-section is shown in Figure 2.1. The boundary between the pre-Mississippian and Mississippian strata is the upper Bakken Shale.

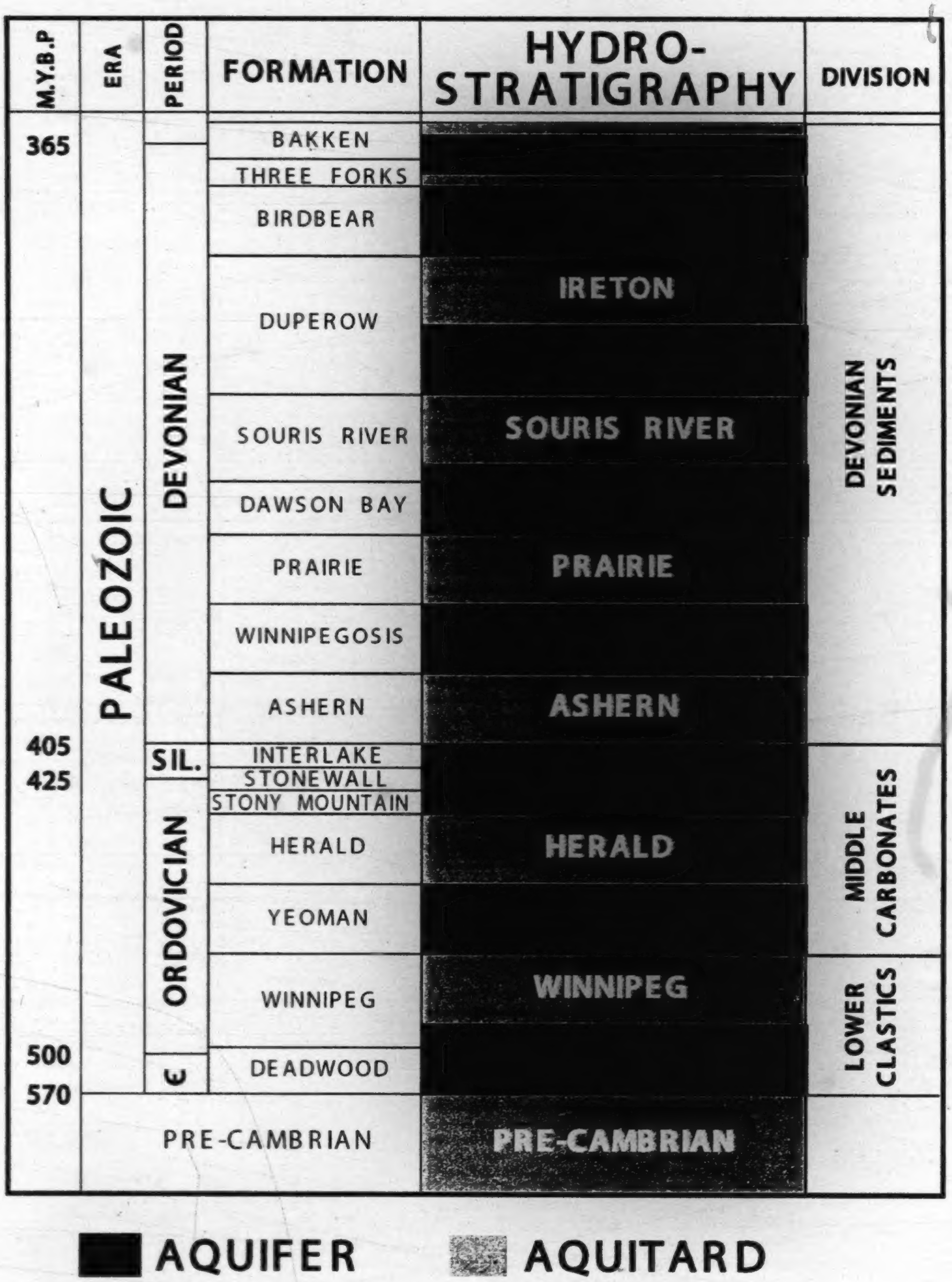

M.Y.B.P	ERA	PERIOD	FORMATION	HYDRO-STRATIGRAPHY	DIVISION
365	PALEOZOIC		BAKKEN		DEVONIAN SEDIMENTS
		DEVONIAN	THREE FORKS		
			BIRDBEAR		
			DUPEROW	IRETON	
			SOURIS RIVER	SOURIS RIVER	
			DAWSON BAY		
			PRAIRIE	PRAIRIE	
			WINNIPEGOSIS		
			ASHERN	ASHERN	
405		SIL.	INTERLAKE		MIDDLE CARBONATES
425		ORDOVICIAN	STONEWALL		
			STONY MOUNTAIN		
			HERALD	HERALD	
			YEOMAN		
			WINNIPEG	WINNIPEG	LOWER CLASTICS
500		Є	DEADWOOD		
570	PRE-CAMBRIAN			PRE-CAMBRIAN	

■ AQUIFER ▨ AQUITARD

Figure 2.4. Pre-Mississippian stratigraphy and the corresponding hydrostratigraphic units (modified from Rostron and Holmden, 2000).

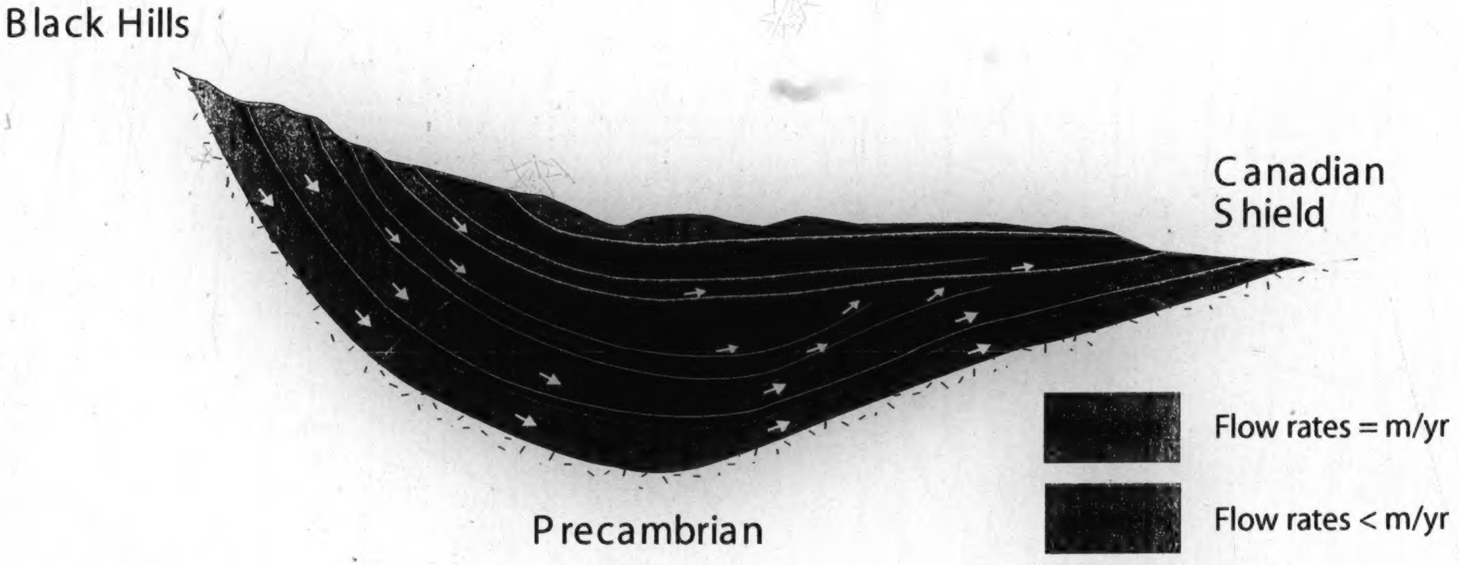
Black Hills
Canadian
Shield
Precambrian
Flow rates = m/yr
Flow rates < m/yr

Figure 2.5. Accepted present-day model of fluid flow in the Williston Basin for Cambrian to Cretaceous strata (after Bachu and Hitchon, 1996, flow rates from Downey et al., 1987).

CHAPTER 3

3. HYDROGEOCHEMISTRY

Hydrogeochemistry in sedimentary basins has been studied for decades since it is inexorably coupled to the driving forces, rates and directions of flow (Clayton et al., 1966; Davisson and Criss, 1996). Variable geochemical patterns detected in basins develop during genesis and evolution of deep basinal fluids. However, in many cases, fluid sources and systems of reactions controlling major and minor constituent concentrations have not been determined (Davisson and Criss, 1996). This is true in the Williston Basin as well. Variable geochemical patterns involving both fresher water and brines in the pre-Mississippian were highlighted in a previous study that gathered DST data (Benn and Rostron, 1998), but this and other previous hydrogeochemical studies were unable to assign an incontestable origin to the brines, nor surmise non-conflicting explanations of brine evolution. This study has placed an emphasis on resolving the origin and evolution of these brines since they may yield an interesting story regarding fluid flow.

3.1. FLUID ORIGIN AND EVOLUTION

Fluid origin in sedimentary basins can involve a number of sources including: i) fresh water e.g., meteoric, glacial, streamflow, shallow groundwater etc., ii) seawater, iii) igneous, and iv) metamorphic e.g., compaction, dewatering (Collins, 1967; Fisher and Kreitler, 1987; Ingebritsen and Sanford, 1998). Of these sources, some form of fresh water or seawater is most commonly responsible for the origin of sedimentary fluids (Wilson and Long, 1993). Depending on origin, prior to any water-rock interaction or mixing, each fluid has a discrete starting composition. This initial composition may be considered the "original chemical endmember" from which groundwaters evolve.

Factors that alter the starting composition of formation waters include: 1) changes in basin configuration and fluid input (i.e., tilting, uplift, faulting, fracturing, glaciation) causing migration and mixing of fluids, 2) solubility, 3) temperature and pressure, 4) contact area between water and rock, 5) rock to water ratios, 6) residence time, 7) traveled length of flow path, 8) amount and distribution of soluble salts (Tóth, 1984). Fortunately, geochemical tracers can be used to discern between endmembers even after they have evolved and increased or decreased in total dissolved solids over time.

3.1.1 ORIGIN OF THE BRINES

Brines are commonly thought to form in one of two ways (Hanor, 1994; Stueber and Walter, 1994). Fresher water can interact with the rock and increase in TDS, e.g., evaporite dissolution as fresher water moves through salt units and becomes saturated with respect to the salt. Alternatively, brines can develop from evaporation of seawater at surface or subaerially (Hanor, 1994). Both evaporite dissolution and evaporative concentration can be active within one basin (Stueber and Walter, 1994) and this fact has not been considered in most previous Williston Basin studies. This study examines whether both brine-forming mechanisms play a role in the Williston Basin, or whether brines can be specifically attributed to either evaporite dissolution or seawater evaporation.

3.1.1.1 DEPOSITIONAL IMPLICATIONS FOR BRINE DEVELOPMENT IN THE WILLISTON BASIN

Abundant carbonate and anhydrite units throughout the pre-Mississippian section are potential sources of the solutes HCO_3^-, Mg^{2+}, Ca^{2+} and SO_4^{2-}. The Prairie Evaporite is the most significant source of soluble salts, potentially increasing Na^+, K^+ and Cl^- concentrations in addition to concentrations of the above ions. Collapse anomalies in the approximately 200 m thick Prairie deposit suggest that dissolution of these evaporites may account for at least some of the salinity within the basin (Chipley and Kyser, 1991). The western edge of the Prairie Evaporite coincides with a freshwater tongue near the recharge areas and borders a high TDS zone to the east, closer to the basin center (Benn and Rostron, 1998) (Figure 3.1). For this reason many authors attribute the deep basinal brines to the dissolution of anhydrite, halite and dolomite found within the Prairie Formation (Wittrup and Kyser, 1990; Chipley and Kyser, 1991; Busby et al., 1995). Some authors even believe dissolution of Prairie salt has been ongoing since the Devonian (Wittrup and Kyser, 1990 and references therein).

Aside from abundant chemical precipitates throughout the section, salinity may also be derived from the original formation water included at deposition. Deposition of the carbonates and sulphates in epeiric and shallow lagoonal environments (Gerhard and Anderson, 1988) would require salinity values greater than the average 35 g/L TDS seawater composition (TDS = 125 to 300 g/L) (McCaffrey et al., 1987). Deposition of halite and bittern salts would require even more evaporation (TDS = 300 to 400 g/L), producing large volumes of brines in order to deposit thick units of salt (McCaffrey et al., 1987). Evidence exists for seawater evaporation past halite saturation, not only during deposition of the Prairie, but also during Ordovician and Silurian times, as confirmed by salts, red bed formation and desiccation features (Haidl, 1990). The resulting highly concentrated brines may have been incorporated in the sediments. Subaerially evaporative environments also existed during the pre-Mississippian allowing buried, slightly concentrated seawater to evaporate further and form highly saline brines (Sandberg and Hammond, 1958; LoBue, 1982).

3.1.1.2 NA-CL-BR SYSTEMATICS

Relative Na, Cl and Br concentrations provide a superior way to discriminate between evaporite dissolution and seawater evaporation (Carpenter, 1978).

Plotting Cl/Br vs. Na/Br on a molar basis can distinguish the two processes (Kesler, 1995) because of bromine's conservative nature (Hanor, 1994; Worden, 1996). Prior to halite saturation, these solute ratios are constant during the progressive evaporation of seawater since all three solutes increase in concentration by the same factor. After halite saturation, Na and Cl are removed from solution, mainly excluding Br. During further evaporation this results in Cl/Br and Na/Br ratios lower than those of normal seawater. Na/Br and Cl/Br values in excess of normal seawater plotting on a 1:1 line are generally considered to be indicative of surface or subsurface dissolution of halite by the fluids (Land, 1987, Hanor, 1994, Kesler et al., 1995). Low Na/Br values coupled with high Cl/Br values are believed to indicate the dissolution of halite followed by Na loss through the formation of albite during rock-water interactions (Spencer, 1987, Kesler et al., 1995). Although some authors have pointed out shortcomings associated with this technique during recrystallization (Stoessell and Moore, 1983; Stoessell and Carpenter, 1986), it is thought that except in cases of very low water to rock ratios, endmember identification is still possible (Stoessell and Moore, 1983; Stueber and Walter, 1994).

3.2. PREVIOUS HYDROGEOCHEMICAL STUDIES

The origin of the brines in the Williston Basin has been the subject of previous study. One group of authors has considered both sources (dissolution and evaporation) of salinity (Kreis et al., 1991; Bernatsky, 1998; LeFever, 1998). Others have only narrowly pursued the origin of brines, assuming the dissolution of evaporites is the only mechanism by which brines can have formed (Wittrup and Kyser, 1990; Chipley and Kyser, 1991; Busby et al., 1995; Bachu and Hitchon, 1996). Chemical studies of the Williston Basin formation waters have mainly utilized DST data, but in some cases have included a small number of wellhead samples. None have included a detailed chemical analysis involving major and minor elements from all parts of the basin. For these reasons, previous hydrogeochemical studies have not furthered knowledge of basin paleohydrogeology, instead focusing on the hydrogeology of the present-day flow system. Worse, unlike in the hydrogeological studies, conclusions of prior hydrogeochemical studies of the Williston Basin were not in accord even within regional boundaries. Both postulated brine formation mechanisms and subsequent geochemical controls on formation water evolution vary between studies but can be divided into three main groups.

3.2.1 PREVIOUS STUDY CONCLUSIONS AND INTERPRETATION

The first group of authors maintains Williston Basin formation waters are derived from meteoric recharge, suggesting meteoric water evolves to form brine in the deep portion of the basin during the dissolution of sodium chloride in the Prairie Formation. This interpretation is based on results indicating that all basinal brines up to and greater than 300 g/L are Na-Cl in type (Busby et al., 1995; Bachu and Hitchon, 1996). Sources of ions other than Na and Cl are attributed to anhydrite dissolution and dedolomitization (Busby et al., 1995). However, in the same study, a trend toward calcium waters from magnesium-dominated waters is cited to represent conversion of di-octahedral to tri-octahedral clays or dolomitization (Busby et al., 1995). With no spatial or temporal context given this is confusing since dolomitization and dedolomitization cannot be concurrent processes. Further evolutionary processes believed to affect the evolution of fresh water to current basinal compositions include sulphate reduction and mixing (Bachu and Hitchon, 1996). These processes are also not described as location specific.

The second group of authors construe that many formation water origins are possible in the Williston Basin including: glacial recharge, waters derived from thermal Ca-Cl_2 brines from the Precambrian basement, paleo-stream input (Kreis et al., 1991), 'connate' seawater (LeFever, 1998) and evaporated seawater (Bernatsky, 1998). These authors believe that the origin of brines is uncertain and complex, nevertheless acknowledging it likely involves dissolution of evaporite minerals in the Prairie Formation to some degree (Kreis et al., 1991; LeFever, 1998). Evolution to present-day geochemical compositions, specifically low Mg and high Ca concentrations, is attributed to either dolomitization (Kreis et al., 1991; Bernatsky, 1998) or an alternate idea suggesting calcium-rich brines are derived from Devonian fluids associated with the recrystallization of the evaporites (Wittrup and Kyser, 1990). Objectives for this second group of studies involved determining formation water origin, fluid flow systems and the potential for exploiting high ion concentrations in the saline brines. Because of these objectives, these studies tended to include a more complete suite of major and minor ions. Na-Cl-Br systematics were applied in two cases to solve the problem of brine origin (Wittrup and Kyser, 1990; Bernatsky, 1998); however, small numbers of samples and sample locations restricted to evaporite horizons, left results pointing to residual seawater remaining in the basinal brines to be verified by further work. Wittrup and Kyser, 1990, (whose data Bernatsky used) obtained anomalously high bromine concentrations, leaving questions as to the validity of the analytical method (Ion Selective Electrode) used to determine bromine on the samples (Rostron, personal communication, 1999; Duke and Rostron, 2002).

A third type of study utilized DST-derived data, compiled and plotted for the Lower Paleozoic section (Benn and Rostron, 1998). This is the sole Williston Basin hydrogeochemical study to date that was not restricted by political boundaries. Results showed that three classes of waters are present in the Williston Basin and despite widely disparate ages and lithologies, the overall patterns of TDS are similar for pre-Mississippian aquifers (Benn and Rostron, 1998). The first class is predominantly Ca-Mg-SO_4 in type and < 30,000 mg/L. It is found in the brackish water tongue entering at southwestern Saskatchewan and northeastern Montana.

The second class of water, Na-Cl in type, ranging from 100,000-200,000 mg/L TDS, is found in the northern, northwestern and eastern parts of the basin. The third class of brine comprised of Ca-Na-Cl waters is located in the center of the basin and has TDS > 300,000 mg/L, with very low sulphate concentrations.

3.3. SHORTCOMINGS OF PREVIOUS HYDROGEOCHEMICAL WORK

As mentioned above, except for the regional DST study, the whole basin has never been studied as a single unit and similar to previous hydrogeological studies, previous hydrogeochemical studies have been restricted to parcels within the Williston Basin region. Groundwater flow crosses political boundaries, yet studies have been of a political nature and controlled by national and state/provincial boundaries (LeFever, 1998; Benn and Rostron, 1998). Different hydrostratigraphic divisions and different suites of chemical data within those divisions has made it difficult to integrate study results to obtain a complete hydrogeological and hydrogeochemical picture that is truly representative of Williston Basin formation waters.

Furthermore, the vertical hydrostratigraphic division of previous studies has been too coarse and has not yielded enough hydrogeological and hydrogeochemical detail. Evidence exists that each aquifer is isotopically unique, (Rostron et al., 1998) suggesting that other hydrogeochemical properties and fluid flow may also be formation specific and as such, certainly deserve detailed investigation. In a long-term USGS hydrogeological study, the entire stratigraphic section was divided into 5 aquifers and 4 aquitards. The Paleozoic formations were grouped 8 to 10 at a time to become either the Cambro-Ordovician Aquifer or Silurian-Devonian Aquitard (Downey et al., 1987), with the 'aquitard' including porous carbonates and substantial reefal material. In an attempt to integrate results to obtain a regional picture, a later Canadian study based its hydrostratigraphic division upon the USGS groupings, and only increased resolution slightly by adding one additional aquifer system in the Silurian to Devonian interval to their conceptual model (Bachu and Hitchon, 1996). These groupings represent invalid generalizations based on hydrogeologic properties. In a regional formation water study it is important to refine further to a smaller scale and examine the strata in small packages if groupings are invalid on a larger scale, to properly evaluate solute sources and hydrogeologic properties.

Samples used for geochemical interpretation in previous studies have been too few and often limited in location; additionally, valid data points have been rejected based on incorrect criteria. In the major American geochemical study, waters with a pH less than 6.5 were deleted as they were thought to represent poor data (Busby et al., 1995). Since groundwater pH in sedimentary basins decreases as depth and salinity increase and has often been observed in the range of 3 to 6 at depths 3 to 5 km (Land and Macpherson, 1992; Hanor, 1994), use of the remaining data to interpret the geochemical system created a systematic error as the most saline data points were rejected. In fact the remaining 57 samples focused on the southwest portion of the basin, away from the most saline brines in the basin center. The Canadian study (Bachu and Hitchon, 1996) incorporated just over 300 data points in the chemical evaluation of the pre-Mississippian units, but these DST analyses did not include bromine data and were grouped according to the coarse hydrostratigraphic divisions. Yet another study utilized fluid inclusions in the Prairie Formation to assess whether pure seawater or evaporated seawater could be found in the basin (Chipley and Kyser, 1991). However, analyzed fluid inclusions only came from the Canadian side, where fluid flow events causing recrystallization that produced those fluid inclusions may have flushed any seawater.

Although a clear picture of regional southwest to northeast flow has been established through the many studies, and flow rates around the brines are accepted to be on the order of m/yr, it has not yet been established whether the brines are moving at all. This is an important topic since it is relevant to petroleum migration in the pre-Mississippian formations. The USGS non-density dependent modelled flow rates of the brine are less than 1m/yr (Downey et al., 1987), and, by admission in this study, do not unequivocally establish flow within the brine slug. The USGS study suggests three reasonable hypotheses including: 1) the brine is static, diverts fresher water over and around it and is located up dip due to the pressure of the freshwater column; 2) the brine, formed by freshwater dissolution of salt, is slowly moving in the same west to east direction as the freshwater itself, 3) the brine is flowing and attempting to adjust to changes in recharge and discharge associated with the Pleistocene glaciation (Downey et al., 1987). The most viable of these three hypotheses has yet to be determined (Downey et al., 1987) and will be examined on a geochemical basis in this study.

Finally, previous studies used bulk TDS values to devise an appropriate conceptual model. While TDS values yield information on present-day less active flow regions, the lack of detailed chemical analysis by formation, low sample numbers and limited suite of analyzed species in many cases do not allow for proper investigation of processes controlling brine origin and evolution. The paucity of good bromine data particularly inhibited the ability of previous studies to consider anything but halite dissolution with respect to the origin of the brines. As a result, the currently accepted present-day, gravity-driven flow model neglects discussion of potential salinity prior to uplift.

3.4. PROBLEM RESOLUTION

This thesis was conducted to resolve the aforementioned problems. Sampling was carried out all across the basin, irrespective of international or national boundaries. Furthermore, sampling was conducted so as to preserve the hydrogeochemical distinctiveness of each formation as much as possible. Often single formations comprised one aquifer in the study and similar permeabilities and lithologies were ensured before formations were grouped into hydrostratigraphic units. This study aimed to obtain the best possible data by collecting samples from the wellhead and collecting them at least in pairs at the same time as extending sample locations outward as much as possible to capture regional transition areas. Formation water chemistry prior to the Laramide uplifts will be considered and therefore its influence on post-Laramide fluid migration will be taken into account. By considering how original formation waters were derived, as well as how they have evolved into the waters seen today, a much clearer picture of past and present regional fluid flow in the Williston Basin is presented.

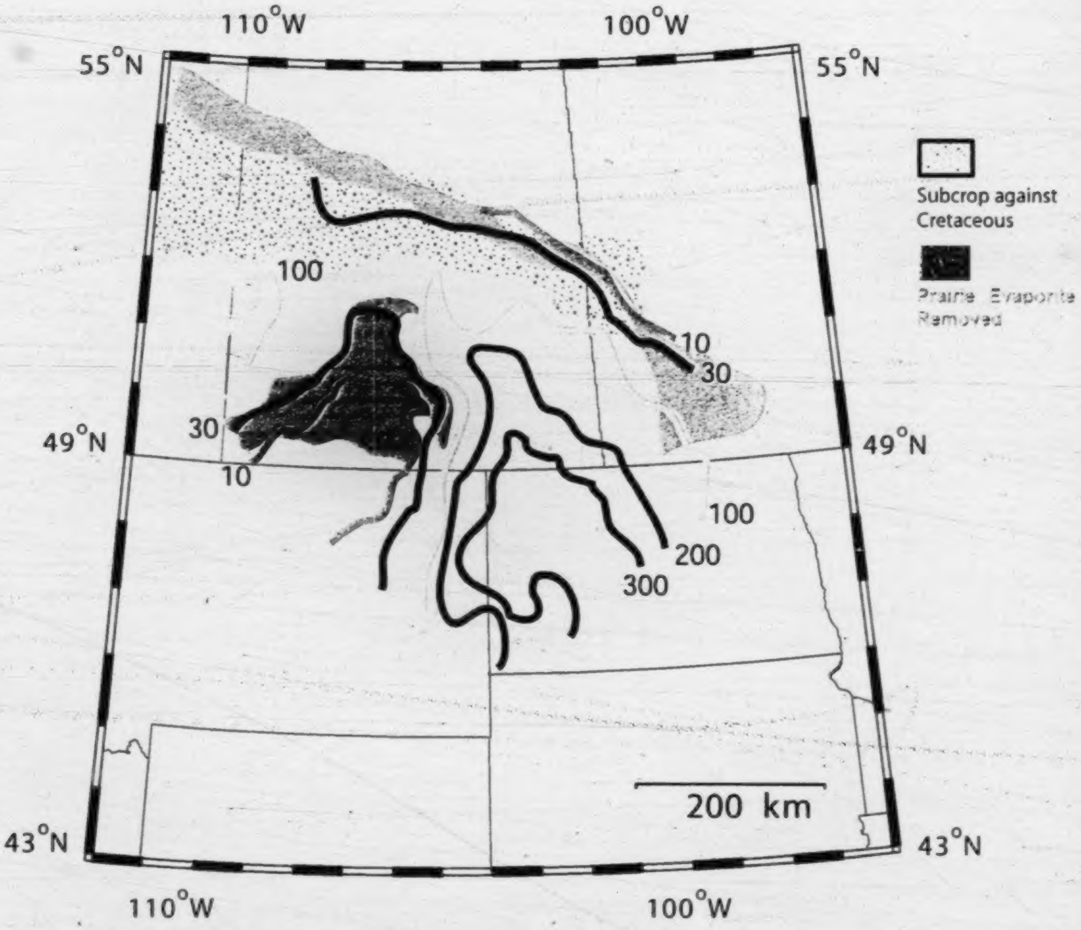
110°W
100°W
55°N
55°N
Subcrop against Cretaceous
Prairie Evaporite Removed
100
10
30
30
10
49°N
49°N
100
200
300
200 km
43°N
43°N
110°W
100°W

Figure 3.1. Relationship of TDS (g/L) in the Duperow Aquifer to Prairie Formation dissolution and sub-crop against Cretaceous strata (after Benn and Rostron, 1998). Areal extent of Prairie Formation based on Mossop and Shetsen (1994).

CHAPTER 4

4. METHODOLOGY

Data presented in this thesis were collected as part of the on-going Williston Basin brine-sampling program (Rostron et al. 1999). The main portion of data collection was conducted during the summers of 1998 and 1999. Samples collected over this two-year period were supplemented with pre-Mississippian samples collected in 1996, 1997 and 2000 from southern Saskatchewan. The total number of samples collected for this study was 122 (Table 4.1). Six suspect samples were omitted in data interpretation as they fell below 30,000 mg/L TDS in areas and depths uncharacteristic of fresher water (according to Benn and Rostron, 1998). Well locations (Figure 4.1), well operators, producing formations, depths and comments on methodology are listed in Appendix A. Well sampling locations do not extend to the Study Area boundary as the basin shape and decreasing formation depth toward the margins limits the number of actively producing oil fields.

4.1. DATA COLLECTION AND SAMPLING PROCEDURE

Obtaining quality samples was a multi-stage process. Well selection was the first step in obtaining representative samples of formation waters from each hydrostratigraphic unit. Industry standard petroleum databases and regulatory databases were used to select wells. For Canada, the CDPubCo Geovista database (June 1999 version) was used to identify appropriate wells. The North Dakota Industrial Commission production information volumes from 1998 and 1999 were used to select wells in North Dakota. Similarly in South Dakota, the South Dakota Department of Environment and Natural Resources provided a production volume for 1999. The Montana Board of Oil and Gas provided a disk from their database of Montana production current to 1999. Oil wells producing from pre-Mississippian strata were identified from each of these data sources and list of potential locations was created. Final well selection was based on producing zone, location, water cut and lack of water flooding in the area. Generally wells with water cuts greater than 50% were selected, although all of the above considerations were weighed and less commonly produced formations were given priority, as were sample locations that would help extend the total sampled area of the Williston Basin. Selection of sample pairs (two samples, same formation, close proximity) when possible increased confidence in the data. After selection, companies operating the selected wells were contacted to confirm producing intervals, absence of a water flood and to ensure fresh water was not run back into the well to reduce salt build-up on the well bore.

Once selected, each well was sampled as follows (based on the sampling protocol from Lico et al, 1996, but modified for this study):

1) Any injected well-production enhancement chemicals were turned off for periods of 3 days to 1 hour prior to sampling if necessary. Produced emulsions (oil and water) were collected directly from the wellhead into 8 or 12 L high-density, polyethylene jugs. Approximately 2.5L of water was collected.
2) Oil/water emulsions were allowed to separate in the jug for a period of time ranging from 1 minute to 3 days. Generally samples were separated, filtered and bottled (below) in less than 3 hours.
3) Water was pre-filtered through quartz wool packed into a large plastic funnel. The sample was passed through the filter until oil droplets were no longer visible (generally 4-10 cycles). The quartz wool was replaced during many pre-filtrations to absorb oil droplets and expedite particulate filtration.
4) 500mL of water was filtered through a 0.45 micron polyethylsulfone, 90mm disposable filter attached to a hand-operated vacuum pump. Suction was applied at 30-40 cm Hg.

5) The filtered water was then split for analysis.

5.1) Immediately after the first 500ml was filtered, splits for bicarbonate and isotopic analysis were taken in non-coated, non-additive Becton-Dickinson brand 20ml vacutainers.

5.2) Field pH and temperature were determined to a 10^{-2} and 10^{-1} precision respectively using a VWR Scientific Model 2000 portable (VWR 43105-002) pH meter and a Ag/AgCl gel-filled combination electrode with thermistor for Automatic Temperature Compensation (VWR 34105-032). Density was determined to a 10^{-4} precision using VWR brand, 325 mm precision specific gravity hydrometers (VWR 34627-35X).

5.3) Splits for cation and anion determination were obtained by filtering water through the 90mm filter until two 1L bottles could be filled or at least 400ml of each was obtained. The bottle for anion determination was tightly sealed and stored in a cool dark area for analysis. The bottle for cation determination was acidified with triple distilled 2.8N HNO_3 by 10% of the cation split volume (e.g. 1L sample, 10ml acid) to a pH < 1.

Items collected for each well, but not reported here include: an oil sample in a 125ml Amber Qorpak bottle, an organic acid sample in 125ml Amber Qorpak bottle containing 60 mg of sodium azide, a stable isotope sample in 20ml vacutainers or 125ml low-density poly-ethylene bottles. The sampling protocol included on-site titration for bicarbonate early in the brine-sampling program (1997), which was later omitted, as little alkalinity (< 100 mg/L) was found.

4.2. DATA ANALYSIS

Due to the complex nature of the brines and problems with interferents, different elements were analyzed using different methods. Major and minor cations were analyzed using Inductively Coupled Plasma Atomic Emission Spectroscopy (ICP-AES) at a commercial lab (Norwest Laboratories, Edmonton, AB). Some neutral species were also analyzed via ICP-AES. Reproducibility difficulties using the ICP-AES technique for the elements Na, Cl and Br necessitated the adaptation of an epithermal Neutron Activation Analysis determination for these elements during which time is was found the technique could also be applied to Sr and I.

4.2.1. INDUCTIVELY COUPLED PLASMA ATOMIC EMISSION SPECTROSCOPY

Cations, in particular dissolved metals, were detected using a commercial ICP-emission spectrometer with APHA 3120:B specifications. The ICP-AES technique employs argon gas ionized by a radio frequency. A sample aerosol is injected into this ionized gas subjecting the atoms to temperatures averaging 7000K. The high temperature causes almost a complete dissociation of molecules and excites atomic emission efficiently, reducing chemical interference. Ionization of a high percentage of these atoms produces ionic emission spectra at wavelengths characteristic of each element. Emission wavelengths are examined to determine the concentration of each element present in the sample. This method is applicable to all of the elements although care must be taken when dissolved solids exceed 1500 mg/L.

To successfully analyze elements of such varying concentration, samples in this study had to undergo successive dilution (ranging from 1:10 to 1:500) compared to ion concentration in the original 1L sample bottles. Dilutions were performed as aliquots were pipetted into volumetric flasks and diluted with deionized water. A 5 μL portion of this dilution product was aspirated, nebulized and carried into the plasma through an injector tube to be analyzed for concentration. The large amount of dissolved solids in these brines and large dilutions resulted in problems with the determination of some species. Listed sensitivity ranged from ppm to ppb, but this did not seem to be the case. For the ions present in the highest concentrations, namely Cl and Na, repeatability discrepancies were sometimes greater than 10%.

During the course of the project, the determination of the anions Cl, I, and Br as well as the cations Sr and Na displayed problems during the typical ICP-AES analysis, and the applicability of a new method was tested and utilized. Neutron Activation Analysis (NAA) of highly saline brines proved to be both efficient and accurate due to its species-specific nature, lack of masking effects and exceptionally low detection limits. A summary of the theory and technique developed at the University of Alberta will be presented here, and a more thorough discussion presented in Appendix B written by Dr. John Duke, but the reader is directed to a more detailed paper, Duke and Rostron, 2002, for a description of this new analytical technique.

4.2.2. NEUTRON ACTIVATION ANALYSIS

Irradiating samples in a nuclear reactor resulted in gamma-ray emissions. For each sample the energies of released gamma rays were used to identify the elements present, while the intensity or number of gamma rays detected was used to determine the concentration of elements. Using this method of analysis (referred to as Neutron Activation Analysis, or NAA) the *SLOWPOKE* nuclear reactor facility at the University of Alberta analyzed samples for a number of elements simultaneously. Analytical sensitivity was in many instances at the part per million (ppm) to part per billion (ppb) level.

The experimental procedure for the analysis of the brine sample (taken from Appendix B) is as follows. Aliquots of the brine samples measuring 250 µL were pipetted into polyethylene micro-centrifuge tubes previously washed in nitric acid, rinsed in deionized water and hermetically sealed. Individual samples were placed in the central cavity of a B_4C shield and irradiated at a nominal thermal neutron flux of 1×10^{11} n cm^{-2} s^{-1} in the University of Alberta SLOWPOKE Nuclear Reactor for 360 seconds (6 mins). Following irradiation, the samples were permitted to decay for 10-15 minutes, during which time the irradiated sample was removed from the irradiation shield and placed in front of a gamma-ray detector at a sample-to-detector distance of 5 mm. Following the timed decay period each sample was counted for 360 seconds (6 mins) using a 41% hyperpure Ge detector housed in a 10 cm lead cave. This procedure allowed dependable concentrations of Na, Cl, Br, Sr and I to be obtained for Williston Basin brines.

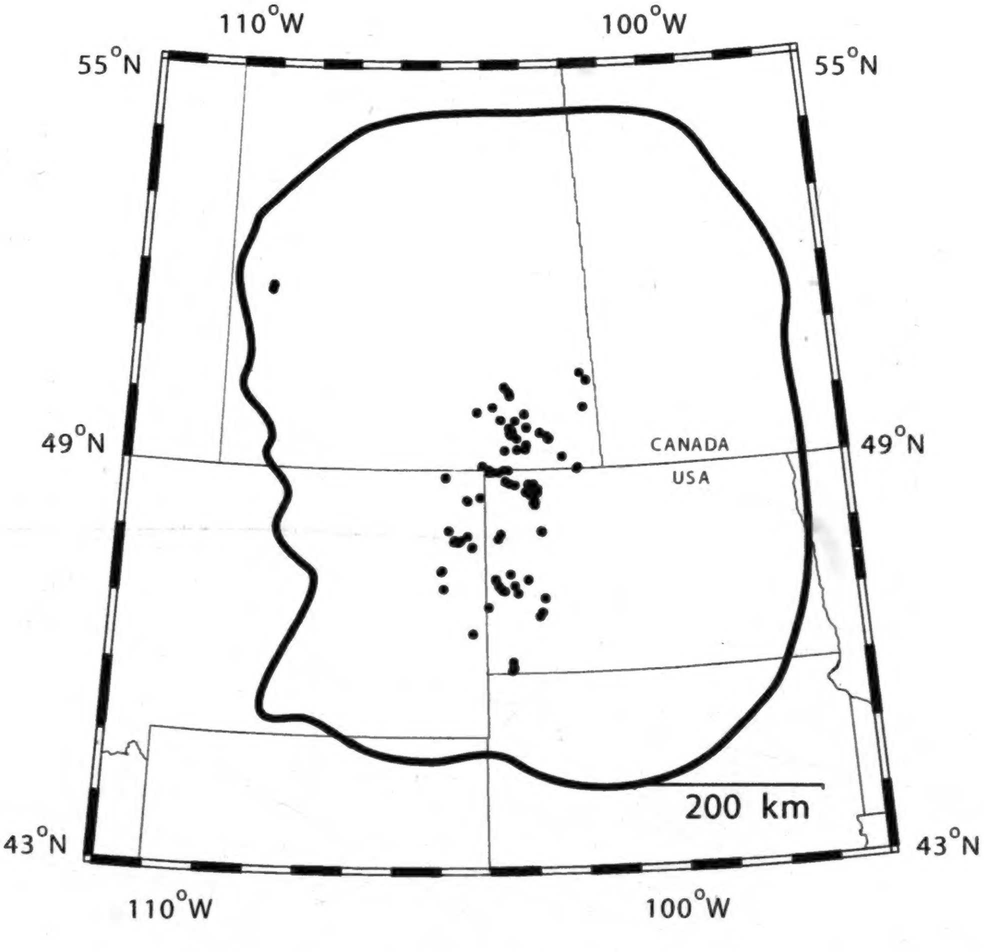
110°W
100°W
55°N
55°N
49°N
49°N
CANADA
USA
200 km
43°N
43°N
110°W
100°W

Figure 4.1. Pre-Mississippian sample locations related to the Williston Basin Study Area boundary.

Year	Saskatchewan	North Dakota	South Dakota	Montana	Total
1998	19	12	-	-	31
1999	16	26	1	18	61
1996/1997/2000	24	-	-	-	24
Total	59	38	1	18	116

Table 4.1. Numbers of samples, sample locations and collection dates.

CHAPTER 5

5. RESULTS

Results for 116 samples illustrate pre-Mississippian formation water characteristics. Key chemical data, TDS values and charge balance errors are presented in Table 5.1. Sample charge balance errors are usually less than 1% and reach a maximum of 6% (Table 5.1). TDS values of the samples range from 28,000 to 365,000 mg/L with most exceeding a TDS value of 100,000 mg/L (Figure 5.1). Samples were obtained from depths ranging from 1000 m to 4000 m (Figure 5.1). Formation water pH ranges from 5.19 to 7.11 (Figure 5.2) and formation water temperatures in the sampling area range from 37^0C to 134^0C (Figure 5.3). Densities, temperatures and depths corresponding to sample locations are shown in Appendix C. Minor elements other than Sr, Li, Br, I and B are presented in Appendix D but not included in the results discussion.

A maximum depth in the basin of just over 4000 m (Figure 2.3) corresponds to the basin center. Quite a few sample depths approach 4000 m and represent data from the deepest portion of the basin (Figure 5.1). TDS increase with depth in pre-Mississippian formations is dramatic up to 1500 m, but relatively independent of depth thereafter (Figure 5.1). pH decreases gradually with depth in pre-Mississippian formations (Figure 5.2). Formation temperatures increase with depth in pre-Mississippian formations (Figure 5.3). Therefore, the highest TDS values, highest temperatures and lowest pH values can generally be found in the center or deepest part of the basin (Figures 5.1, 5.2 and 5.3).

5.1 SOLUTE RELATIONSHIPS

These data show many direct correlations between solute concentrations and TDS, especially between two of the most dominant ions, chloride and sodium. Chloride concentrations vary linearly with TDS in every pre-Mississippian formation (Figure 5.4a to 5.4h), showing chloride increases as total concentrations increase for the whole section. The behavior of sodium with respect to TDS (or chloride) is similar in all formations (Figures 5.5a to 5.5h), but a lower number of data points in some formations does not allow the relationship to be seen clearly until formations are grouped together (Figure 5.6). Sodium concentrations vary linearly with TDS up to approximately 175,000 mg/L TDS, but then deviate from the line (Figure 5.6).

Major ion concentrations other than Na and Cl, and some minor ion concentrations, do not show a linear variation with TDS (or chloride). Ca, Mg, K, Sr, Li and Br increase non-linearly with increasing TDS, and have like profiles. The trend for these ions is similar in each formation and each can be shown as a group for the pre-Mississippian section (Figures 5.7 to 5.12). Iodine data can also be grouped for the section, and show a similar non-linear variation with TDS, with the exception of data from the Bakken Formation (Figure 5.13). SO_4 and HCO_3 concentrations have a less systematic variation with TDS. SO_4 concentrations start at less than 1000 mg/L, rise to a peak of 6500 mg/L (corresponding to 200,000 mg/L TDS), and then fall back down to less than 1000 mg/L (Figure 5.14). HCO_3 concentrations generally decrease as TDS increases (Figure 5.15).

5.2 TYPES OF FORMATION WATERS

Comparisons of TDS values and relative abundances of solutes allow waters to be organized into groups indicating possible endmembers. Distinct cutoffs between the endmember groupings and data which are not considered to be endmembers are subjective for reasons that will be discussed in the next chapter, and are chosen for illustrative purposes; however, visible extremes in the chemistry data do support such division.

Not all formation waters are brines: seven samples have TDS < 100,000 mg/L, and of these, four have less than 40,000 mg/L TDS (Table 5.2). These four samples approximately match the compositions of fresher water to the west and southwest mapped previously (Busby et al., 1995; Benn and Rostron, 1998). For this study, these freshwaters, with TDS < 40,000 mg/L, are termed Group A (Figure 5.16). Unfortunately, sampling did not extend far enough to the west and southwest to collect more of these fresher waters, specifically those of the Ca-Mg-SO_4 type identified from DST data by Benn and Rostron (1998).

The remaining samples are brines (TDS > 100,000 mg/L), and have been grouped based on both TDS and Ca values (Table 5.2). TDS in some samples exceed 300,000 mg/L, the approximate concentration for halite saturation in sedimentary basins (Hanor, 1994). Two extremes can be observed for TDS values above 300,000 mg/L (Figure 5.16). Waters containing less than or equal to 500 meq/L calcium are subjectively termed Group B, while waters having greater than 2000 meq/L calcium are subjectively termed Group C (Figure 5.17). A typical stiff diagram for Group B waters depicts the dominance of Cl (100% of anions) and Na, with Na concentrations comprising 90% of total the cations (Figure 5.17). In contrast, a typical stiff diagram for Group C waters again shows Cl comprising 100% of the anions, but Na and Ca each comprising about 50% of the cation composition. These two types of waters comprise two more endmembers in addition to Group A waters.

Ranges of compositions in between these endmembers can be found and have been termed Mix AB, Mix AC and Mix BC. The endmembers and the intermediate compositions have been organized into the six groups presented in Table 5.2. The three main groups (A, B and C) confirm results of the previous hydrogeochemical DST study that proposed three major types of waters are present in the Williston

Basin although the classification scheme is very different and has been extended to include the secondary groups Mix AB, BC and AC.

Table 5.1. Results in mg/L for major ions and minor ions with concentrations >1 mg/L, nd = not determined.

Sample ID	Formation	TDS	Na	Ca	Mg	K	Cl	SO_4^*	HCO_3	Li	Sr	I	Br	B	% Charge balance
UofA 9969	Bakken	282750	91053	12100	1420	5160	170988	306	nd	47	531	70	630	294	-0.03
UofA 9948	Bakken	289804	87878	15700	1710	6110	175407	327	nd	43	1160	76	827	249	-0.25
UofA 9951	Bakken	308577	83516	30200	2140	3900	186427	191	nd	71	1020	11	755	163	1.71
UofA 9979	Bakken	30350	11973	250	236	220	17422	146	nd	5	60	1	17	17	6.16
UofA 9978	Bakken	36806	11166	849	369	210	16279	5910	nd	6	66	1	15	16	-3.49
UofA 9977	Bakken	35688	11353	898	388	200	15191	5700	nd	6	58	1	16	17	0.58
UofA 9821	Bakken	239574	89376	2190	478	1960	141789	2148	232	20	72	27	233	119	0.39
UofA 9820	Bakken	254917	95790	2270	396	1910	151349	1809	189	18	100	13	240	72	0.55
UofA 9856	Bakken	255320	97300	2400	409	1920	150000	1827	208	18	68	9	235	74	1.81
UofA 9843	Bakken, 3 Forks	308646	88814	19800	1530	6370	188910	285	5	47	1330	82	934	334	-1.56
UofS 9723	Bakken	247037	92047	2510	484	2130	146530	1836	236	20	53	20	241	102	0.51
UofA 9986	Birdbear	285201	95715	10600	1290	3830	171593	405	nd	28	566	35	600	333	0.60
UofA 9925	Birdbear	290218	88627	17300	1740	5750	174458	300	nd	50	543	68	800	386	0.94
UofA 9981	Birdbear	209053	77368	1750	628	1260	119088	6510	nd	15	100	10	156	78	0.25
UofS 9727	Birdbear	209305	74676	1910	659	1240	121740	6360	169	15	100	10	172	84	-2.32
UofA 9839	Birdbear	262512	92359	7530	1070	2900	156603	663	91	34	309	25	389	226	1.43
UofS 9616	Birdbear	285325	99000	7920	1060	3250	172000	642	125	31	379	15	378	190	0.13
UofS 9714	Birdbear	284131	95480	10300	1330	3220	171870	408	67	33	453	29	496	236	0.11
UofS 9732	Birdbear	301036	99739	10600	1350	3280	184132	426	69	33	436	30	480	246	-1.29
UofA9842	Duperow	307771	96672	15500	1750	4870	186515	477	76	164	505	28	691	268	0.04
UofA 9829	Duperow	285334	87204	18000	2240	5050	170402	312	80	35	780	41	681	276	2.11
UofA 9841	Duperow	308859	94429	18700	2160	4570	186462	363	109	165	619	28	762	247	0.93
UofA 9995	Duperow	289814	79262	23200	1500	7210	175561	262	nd	82	1130	53	889	446	-0.14
UofA 9828	Duperow	309669	87915	25400	2850	6790	183954	303	64	49	957	39	763	353	3.04
UofA 9942	Duperow	274447	66437	30400	1990	6800	165398	531	nd	102	1140	18	963	411	1.06
UofA 9973	Duperow	299443	71517	33200	3090	6390	181599	250	nd	184	1580	22	1110	368	1.10
UofA 9947	Duperow	233675	42281	35700	2750	8470	140548	846	nd	133	1410	20	849	305	1.54
UofA 9926	Duperow	308109	71441	36700	2870	7290	186203	250	nd	113	1440	21	1190	437	1.37
UofA 9941	Duperow	279507	52672	42100	2920	7910	169568	227	nd	172	1960	22	1280	437	1.13
UofA 9946	Duperow	281670	50227	43000	3040	8370	173049	290	nd	209	1690	25	1196	397	-0.31
UofA 9950	Duperow	288596	53519	43300	2930	8990	176239	474	nd	132	1350	19	1060	348	0.22

* [SO4] is estimated from [total S] by factor 96.06/32.06. This is based on the assumption all S exists as SO4, and may slightly overestimate SO4 concentrations.

Table 5.1. Results in mg/L for major ions and minor ions with concentrations >1 mg/L, nd = not determined.

Sample ID	Formation	TDS	Na	Ca	Mg	K	Cl	SO_4^*	HCO_3	Li	Sr	I	Br	B	% Charge balance
UofA 9940	Duperow	335952	66766	47300	3480	9240	204598	312	nd	121	1740	37	1490	585	0.49
UofA 9996	Duperow	355287	66576	54600	3650	10300	215138	303	nd	172	2130	32	1540	574	1.41
UofA 9949	Duperow	348362	60935	54800	4810	9810	213034	306	nd	113	2360	39	1540	394	0.66
UofA 9953	Duperow	347034	58830	56000	3710	10300	212835	292	nd	198	2450	25	1597	534	-0.10
UofA 9952	Duperow	346356	58532	58700	4750	10900	208622	318	nd	159	1990	34	1630	459	2.59
UofA 9980	Duperow	194561	71377	2280	801	1520	111982	4710	nd	18	100	9	179	83	0.76
UofS 9711	Duperow	195133	65874	3930	1470	3600	116082	2712	111	40	100	9	265	37	-0.94
UofA 9840	Duperow	320961	111609	5880	805	9450	191099	507	108	134	285	27	622	156	0.68
UofA 9966	Duperow+Nisku	289399	82515	23000	2430	6400	172223	339	nd	66	1000	45	841	351	2.61
UofA 00201	Dawson Bay	177344	46561	12600	1310	3660	111351	399	nd	39	498	9	577	172	-4.66
UofA 9957	Dawson Bay	284993	82651	18800	1710	7780	171737	235	nd	78	683	13	916	243	0.47
UofA 9956	Dawson Bay	289963	83009	19100	1750	8350	175406	251	nd	80	693	13	908	234	-0.09
UofA 9967	Winnipegosis	184952	69638	2070	248	1990	108376	1782	nd	11	120	2	57	28	1.68
UofA 9971	Winnipegosis	259106	94979	3870	337	3540	154969	687	nd	17	257	3	112	45	0.70
UofA 9991	Winnipegosis	277467	104061	4330	540	3930	163029	777	nd	20	266	5	151	50	2.92
UofA 9993	Winnipegosis	284097	101471	6180	766	4280	170078	570	nd	26	201	5	215	63	0.93
UofA 9975	Winnipegosis	302924	104768	7330	2120	5340	181680	489	nd	46	347	17	421	88	1.06
UofA 9982	Winnipegosis	278282	96051	8130	1260	5130	166329	318	nd	43	295	9	440	78	1.37
UofS 9731	Winnipegosis	272028	90600	10000	1170	4710	164000	351	78	37	400	7	384	77	0.36
UofA 9990	Winnipegosis	299221	102253	10300	1380	4790	179084	369	nd	38	372	8	380	83	1.46
UofS 9731	Winnipegosis	266904	88856	10400	1170	4570	160313	339	76	36	355	10	499	80	0.85
UofA 9983	Winnipegosis	310179	105183	10500	1570	6160	185117	299	nd	47	538	10	496	92	1.64
UofA 9848	Winnipegosis	312477	104300	11100	1520	5290	188630	402	76	41	366	9	433	89	0.30
UofS 9725	Winnipegosis	312782	106363	11300	1290	5230	187098	333	50	45	339	9	445	104	1.46
UofS 9728	Winnipegosis	325160	102299	14500	1660	5640	199262	312	55	46	599	11	495	105	-1.41
UofS 9726	Winnipegosis	326326	101383	15500	2050	5560	200113	299	56	49	564	10	479	97	-1.26
UofA 9992	Winnipegosis	328122	105582	15700	1960	5180	197958	294	nd	46	670	10	497	96	0.88
UofA 9846	Winnipegosis	245021	69070	18900	1620	4570	148849	330	53	28	840	14	435	124	0.13
UofA 9845	Winnipegosis	257673	62187	28800	1910	6410	156482	246	35	41	728	5	461	195	0.70
UofA 9858	Winnipegosis	305078	103000	6440	4480	5700	183665	606	39	52	362	5	346	88	1.27
UofA 9936	Interlake	275770	81477	18700	1440	6050	166206	180	nd	39	727	12	691	128	0.82

* [SO4] is estimated from [total S] by factor 96.06/32.06. This is based on the assumption all S exists as SO4, and may slightly overestimate SO4 concentrations.

Table 5.1. Results in mg/L for major ions and minor ions with concentrations >1 mg/L, nd = not determined.

Sample ID	Formation	TDS	Na	Ca	Mg	K	Cl	SO_4^*	HCO_3	Li	Sr	I	Br	B	% Charge balance
UofA 9961	Interlake	311184	92628	19600	1640	6520	188781	231	nd	48	603	10	769	228	-0.04
UofA 9935	Interlake	282747	83182	20400	1510	6010	169286	261	nd	51	880	16	784	228	1.61
UofA 9934	Interlake	295937	78299	27600	1960	5630	180128	217	nd	55	807	14	925	189	0.25
UofA 9955	Interlake	291755	79747	28400	2050	3710	175460	259	nd	68	1000	12	747	155	2.21
UofA 9937	Interlake	28306	9016	844	110	650	16234	942	nd	10	100	2	55	61	-1.96
UofA 00200	Interlake	92949	30415	3380	432	1780	55718	528	nd	23	142	4	192	125	-0.23
UofA 9963	Interlake	263443	96093	4410	529	3800	157255	651	nd	24	182	4	153	59	1.06
UofA 9970	Interlake	325289	69597	44700	4520	5540	196397	315	nd	40	2610	47	1050	308	2.50
UofA 9851	Yeoman	275526	95441	9030	1160	3170	165128	432	71	36	391	7	341	72	1.29
UofA 9852	Yeoman	282820	97603	9390	1250	3760	169257	483	72	40	250	10	313	79	1.40
UofA 9850	Yeoman	314448	102620	13000	1620	6130	189209	369	87	57	435	12	542	113	0.66
UofA 9836	Yeoman	283235	92973	13900	1790	3130	169670	375	70	41	521	7	464	90	1.89
UofA 9832	Yeoman	311380	100242	14300	1670	3210	190309	351	53	40	471	7	458	85	-0.65
UofA 9847	Yeoman	311638	101265	14500	1810	5350	186908	369	67	56	448	10	508	115	1.38
UofS 9720	Yeoman	282286	89115	14700	1740	3000	172032	330	50	39	577	5	436	86	-0.15
UofS 9716	Yeoman	293688	93133	15100	1860	3500	178375	336	59	43	515	6	476	96	0.22
UofS 9719	Yeoman	299775	95081	15300	1860	3200	182655	348	65	41	487	6	446	89	-0.12
UofS 9715	Yeoman	289198	90706	15400	1760	2940	176816	321	53	38	456	5	448	78	-0.48
UofA 9825	Yeoman	295780	93740	15600	1770	3320	179570	324	51	41	563	7	502	92	0.29
UofA 9833	Yeoman	296496	91832	18700	2120	3340	178663	318	43	45	642	8	530	86	1.55
UofA 9831	Yeoman	308147	95599	19600	2240	3520	185361	318	61	47	620	6	496	93	1.80
UofA 9830	Yeoman	292360	89113	19900	2250	3390	175879	287	46	46	633	6	531	92	1.89
UofA 9838	Yeoman	321232	97084	22200	2320	3400	194192	330	51	44	766	6	573	84	1.30
UofA 9962	Red River	266843	74991	20300	1410	6780	161329	85	nd	85	872	10	646	175	0.45
UofA 9835	Red River	314823	88752	25700	1640	3550	192949	148	5	34	1010	9	756	1	-0.46
UofA 9959	Red River	298437	81563	29000	2150	3720	179628	192	nd	68	1050	11	764	148	2.19
UofA 9958	Red River	310014	84267	29400	2360	3720	187801	190	nd	67	1140	10	786	146	1.42
UofA 0093	Red River	249820	90423	3170	601	3270	150512	1185	nd	19	80	2	107	26	-0.55
UofA 0094	Red River	244277	88215	3390	603	3160	147073	1143	nd	20	99	3	128	29	-0.43
UofA 0092	Red River	247100	89819	3670	638	3010	148244	1032	nd	22	155	2	120	32	0.21
UofA 0090	Red River	266085	96253	3780	681	3020	160675	993	nd	22	140	3	134	32	-0.47

* [SO4] is estimated from [total S] by factor 96.06/32.06. This is based on the assumption all S exists as SO4, and may slightly overestimate SO4 concentrations.

Table 5.1. Results in mg/L for major ions and minor ions with concentrations >1 mg/L, nd = not determined.

Sample ID	Formation	TDS	Na	Ca	Mg	K	Cl	SO_4^*	HCO_3	Li	Sr	I	Br	B	% Charge balance
UofA 9930	Red River	137854	48944	3990	492	1720	81126	657	nd	39	164	7	223	168	2.43
UofA 9987	Red River	264354	95903	4350	632	3280	158512	882	nd	26	225	3	149	42	0.44
UofA 0091	Red River	258766	92693	4360	739	2900	156503	846	nd	24	194	3	148	38	-0.50
UofA 00189	Red River	298291	98505	11500	1390	3640	181741	384	nd	32	435	6	422	67	-0.55
UofA 00192	Red River	292076	89397	16100	1850	3140	179840	375	nd	39	634	6	458	77	-1.39
UofS 9729	Red River	306023	82935	28500	3080	3680	185739	271	49	58	817	6	623	99	1.46
UofA 9927	Red River A,B,C,D	291847	63177	36900	2750	6520	179850	271	nd	42	1031	15	1003	144	-0.69
UofA 9931	Red River B	99295	35537	2030	253	1600	58039	990	nd	22	100	7	179	236	1.46
UofA 9994	Red River 'B'	76640	26144	2020	315	1010	45102	1194	nd	21	100	5	162	228	-0.39
UofA 9939	Red River B,C,D	314061	76363	33300	2930	7270	190800	262	nd	98	1250	42	1153	421	0.54
UofA 9964	Red River C	273395	64703	32600	3370	3850	166503	312	nd	38	890	6	771	96	1.43
UofA 9965	Red River C	302524	74738	34200	3510	4210	183422	283	nd	41	1020	7	809	104	1.90
UofA 9834	Red River 'C'	340287	76400	40400	4140	4740	212000	216	14	47	1190	5	900	112	-1.29
UofA 9928	Red River D	318009	70345	44100	3130	3910	193295	199	nd	50	1400	13	1250	122	1.78
UofA 9960	Red River	304817	92472	19600	1620	6660	182267	232	nd	47	773	10	785	227	1.70
UofA 9972	Red River	322709	85426	31800	2570	5440	195011	218	nd	55	1080	9	811	149	1.58
UofA 9976	Red River	285501	88813	17100	1970	3270	172569	324	nd	42	622	6	473	88	1.07
UofA 9989	Winnipeg	267058	100456	3810	705	2250	158207	879	nd	25	100	3	179	27	2.14
UofA 9810	Winnipeg	289535	103000	8450	908	2780	173000	456	5	30	372	3	283	44	1.69
UofA 9824	Winnipeg	301728	102970	10900	1030	2890	182430	417	5	30	345	6	348	46	0.35
UofS 9609	Deadwood	305110	113280	3240	914	1450	184310	1095	38	12	129	4	188	21	-0.21
UofA 9822	Deadwood	329579	92393	31400	2140	3530	197950	278	5	26	713	8	623	55	2.45
UofA 9823	Deadwood	323161	85843	35300	2160	3570	193957	372	5	23	788	7	628	47	2.70

* [SO4] is estimated from [total S] by factor 96.06/32.06. This is based on the assumption all S exists as SO4, and may slightly overestimate SO4 concentrations.

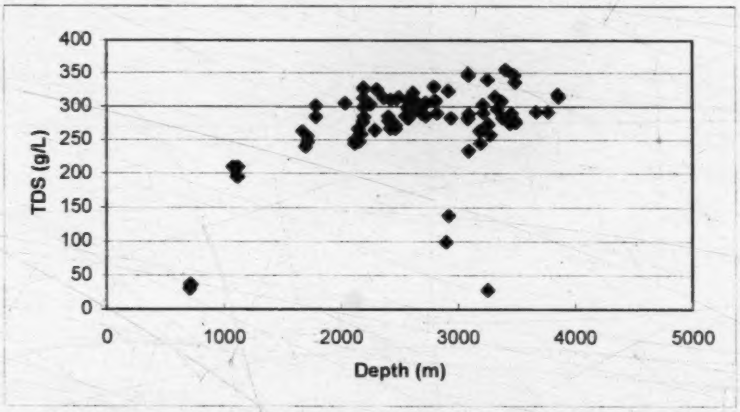

Figure 5.1. TDS vs depth. The three outlying samples around 3000 m could not be omitted based on sample quality or isotopic criteria.

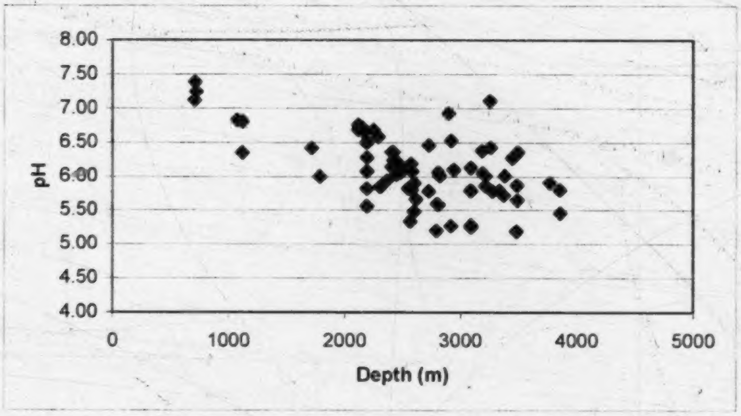

Figure 5.2. pH vs. depth.

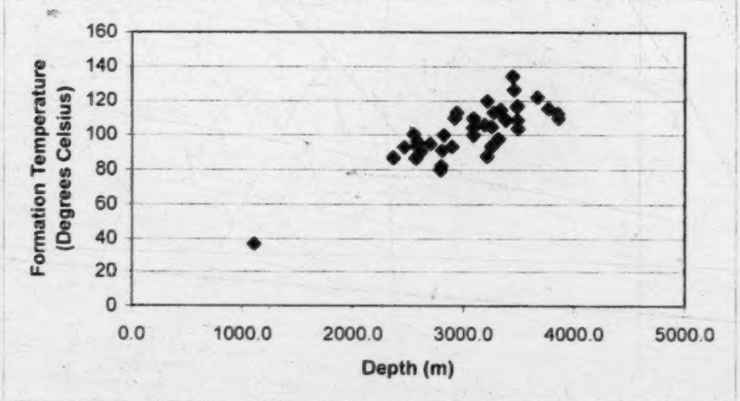

Figure 5.3. Bottom hole temperature vs. depth. Some data not available.

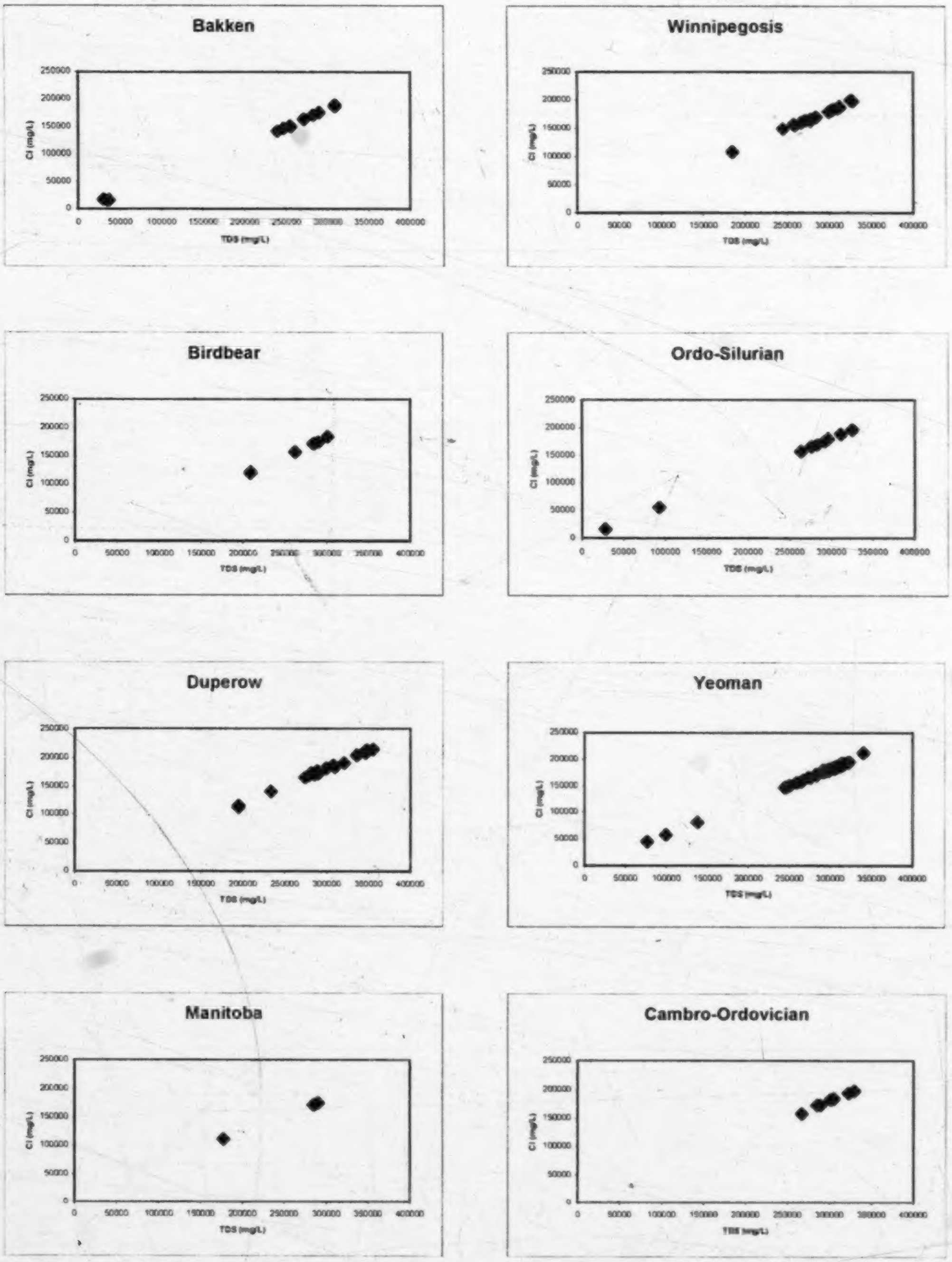

Figures 5.4a to 5.4h. Chloride vs. TDS for pre-Mississippian hydrostratigraphic units. Note: R^2 values for the above plots range from 0.994 to 0.9999.

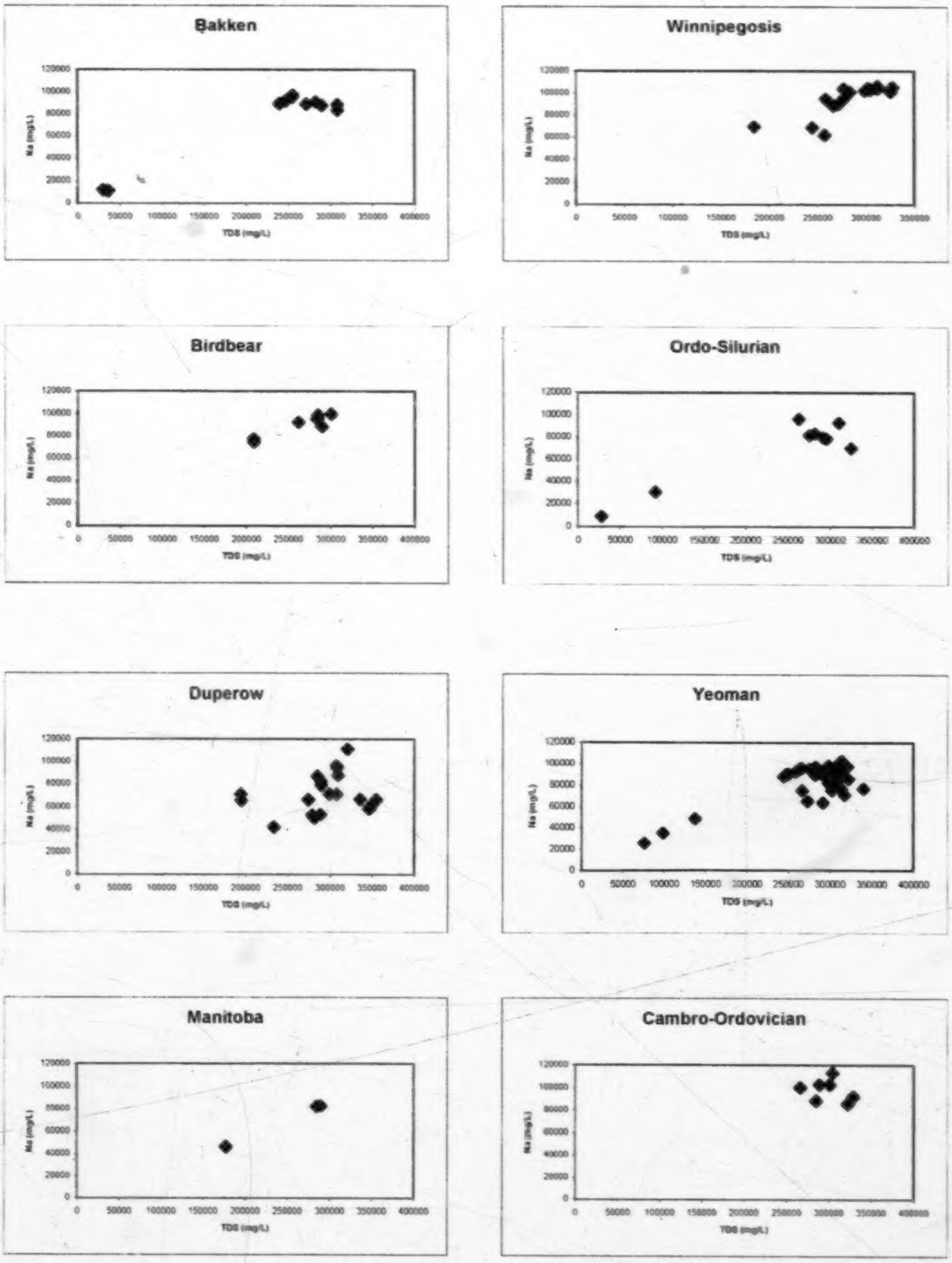

Figures 5.5a to 5.5h. Sodium vs. TDS for pre-Mississippian hydrostratigraphic units.

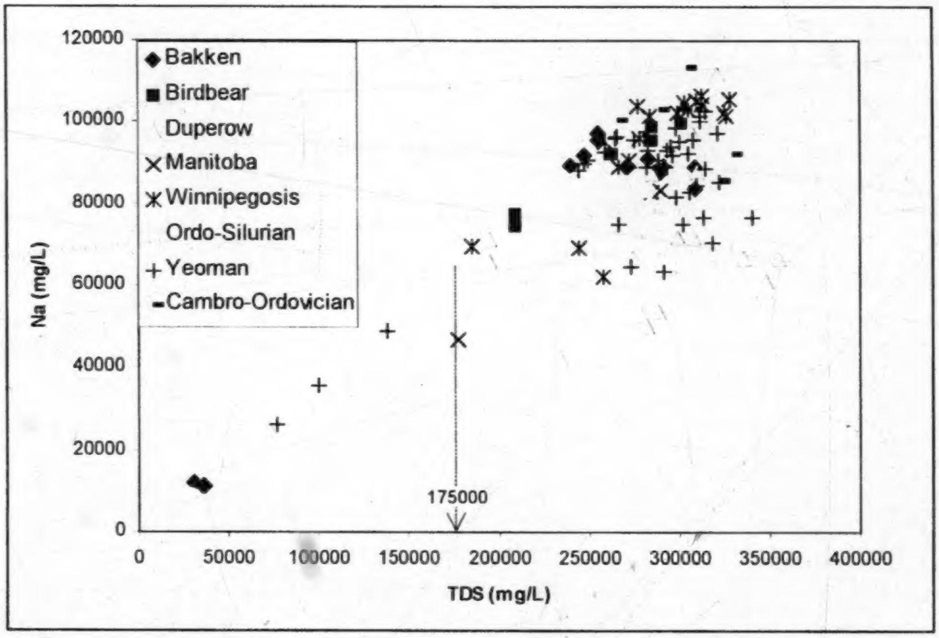

Figure 5.6. Sodium vs. TDS.

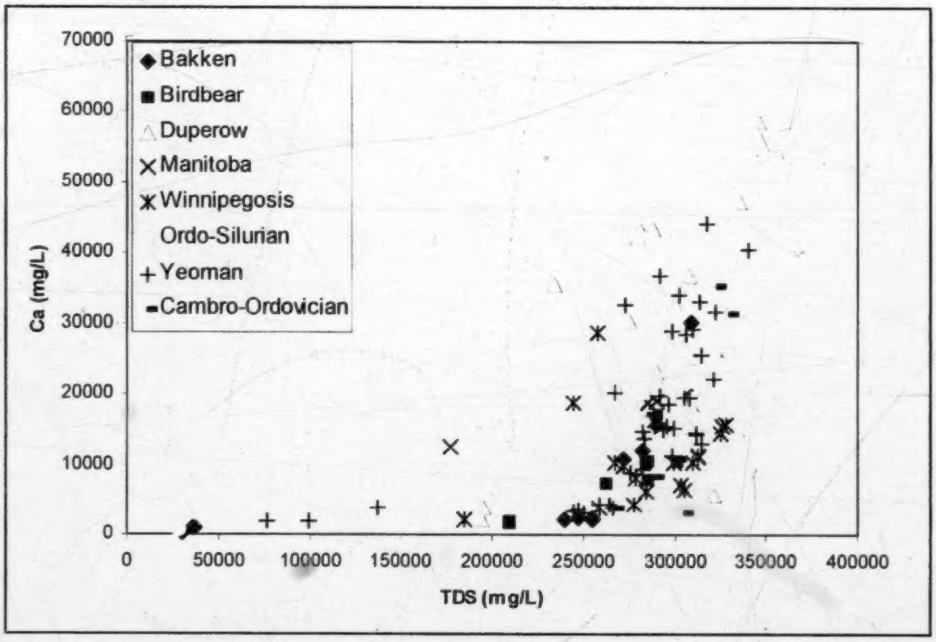

Figure 5.7. Calcium vs. TDS.

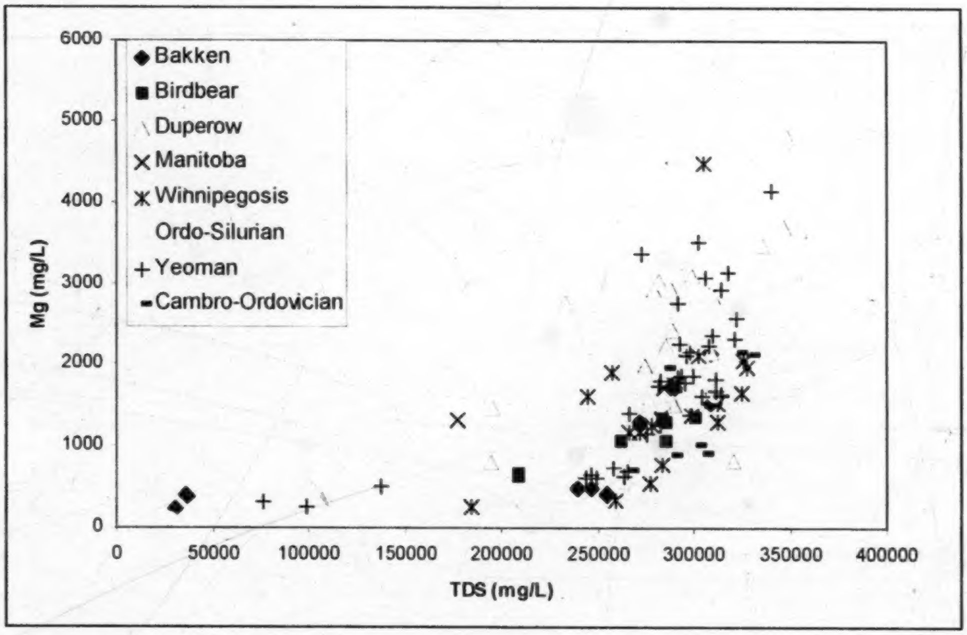

Figure 5.8. Magnesium vs. TDS.

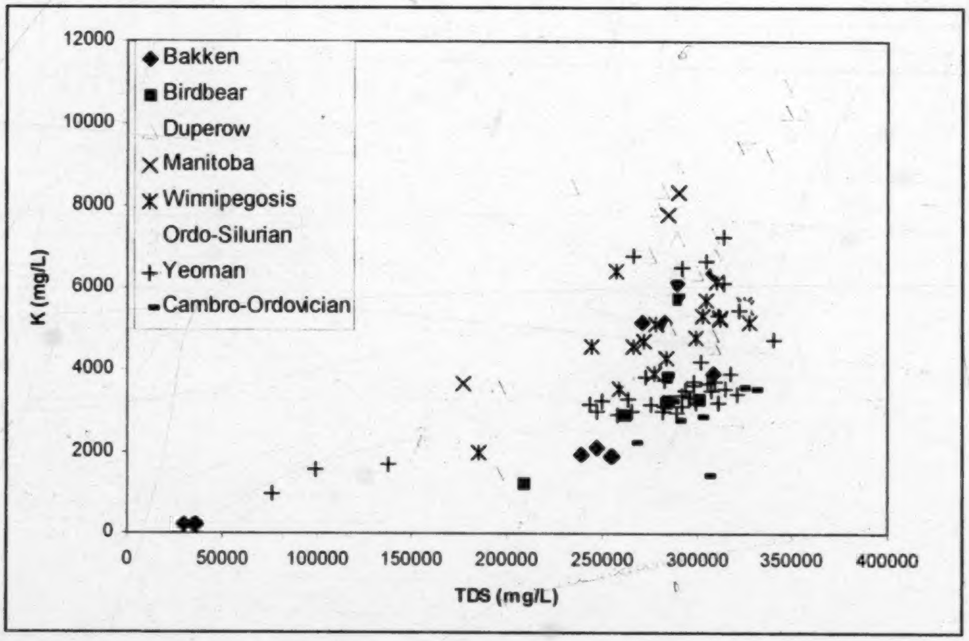

Figure 5.9. Potassium vs. TDS.

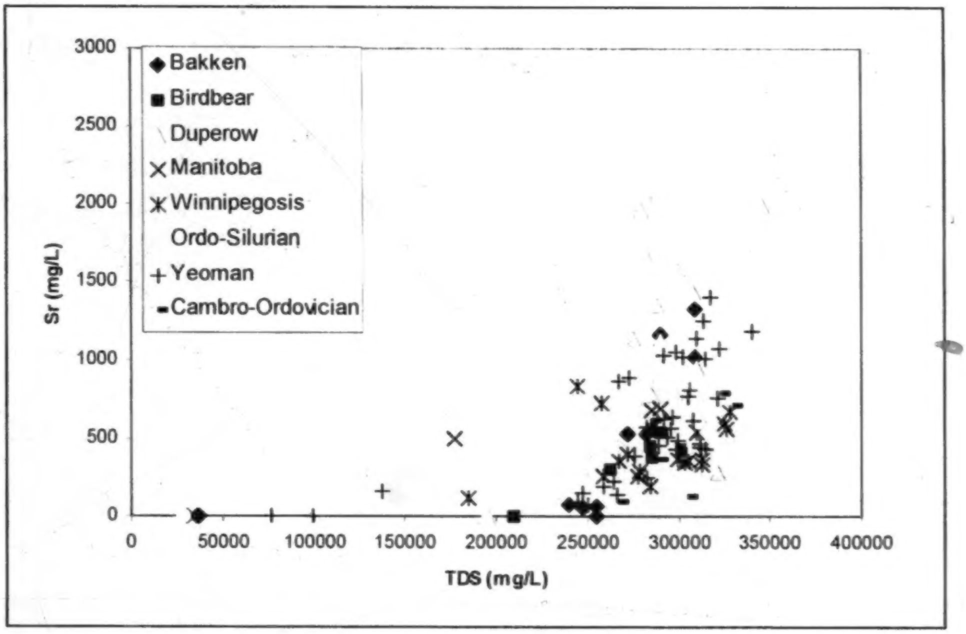

Figure 5.10. Strontium vs. TDS.

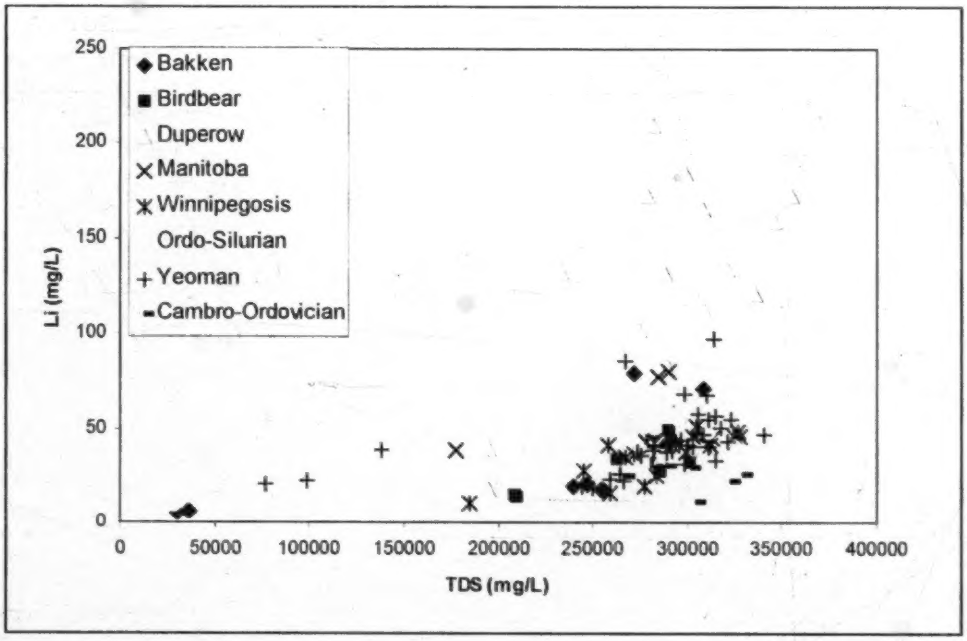

Figure 5.11. Lithium vs. TDS.

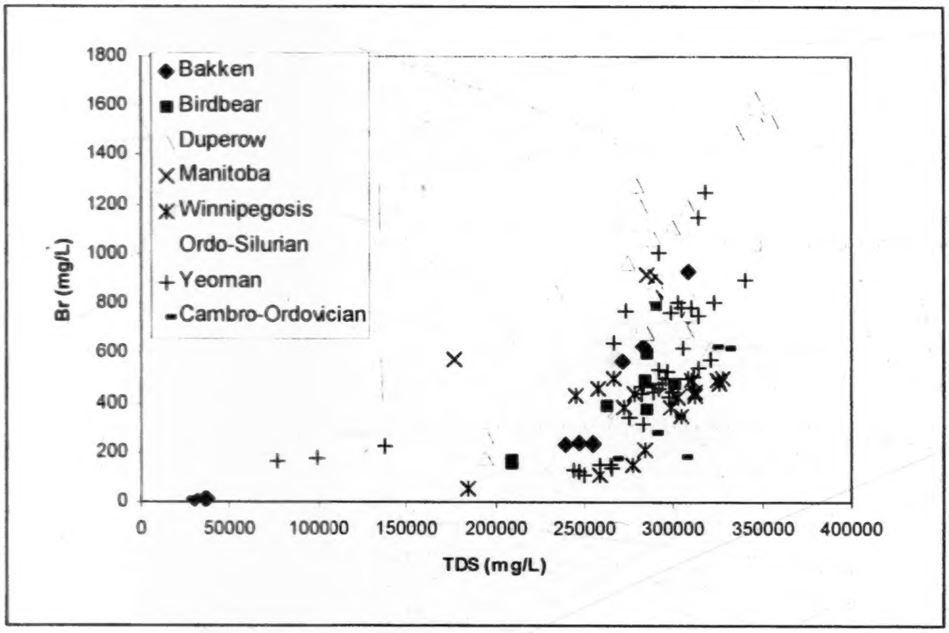

Figure 5.12. Bromide vs. TDS.

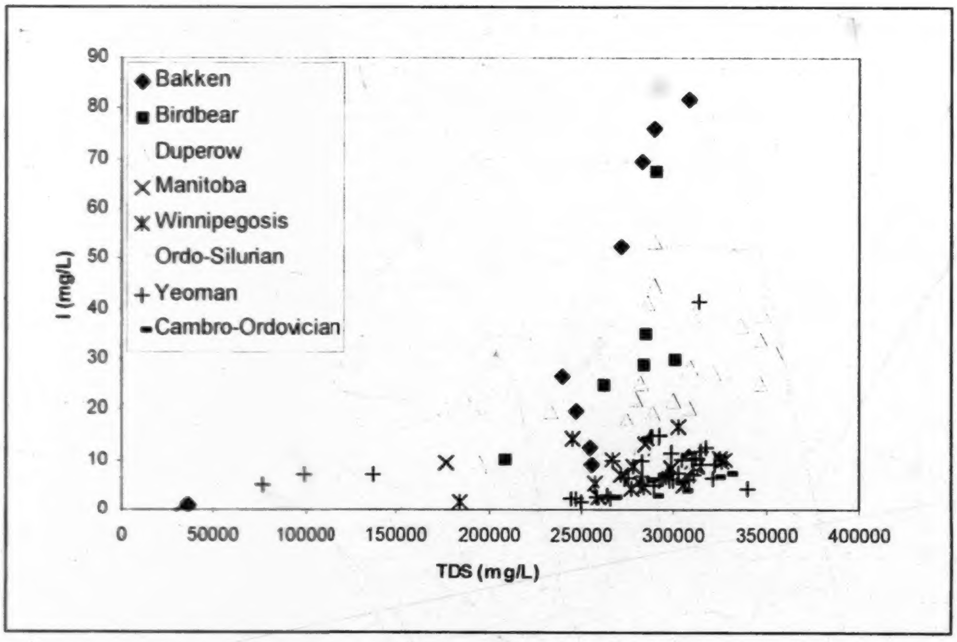

Figure 5.13. Iodide vs. TDS.

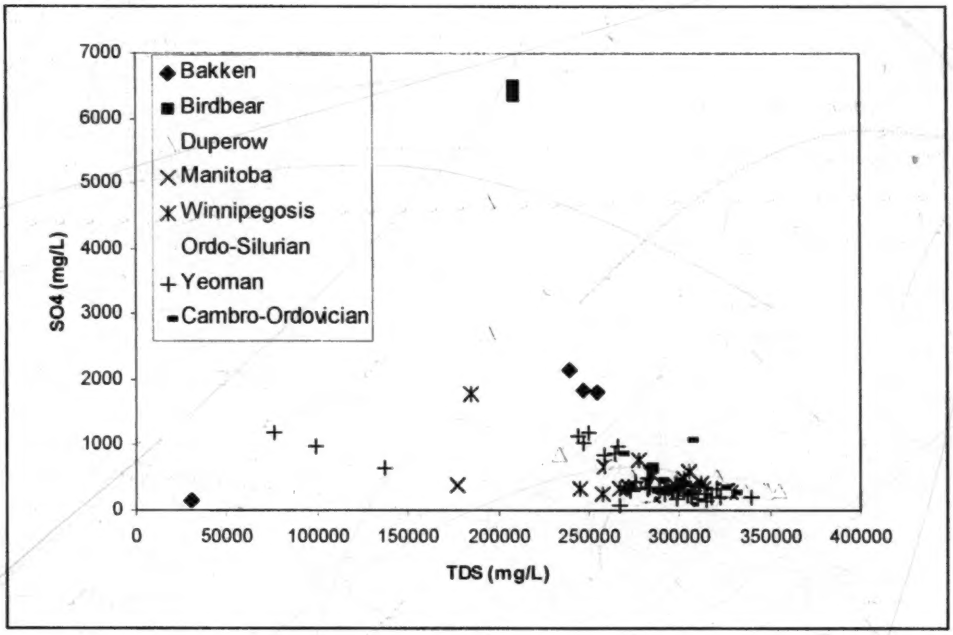

Figure 5.14. Sulphate vs. TDS.

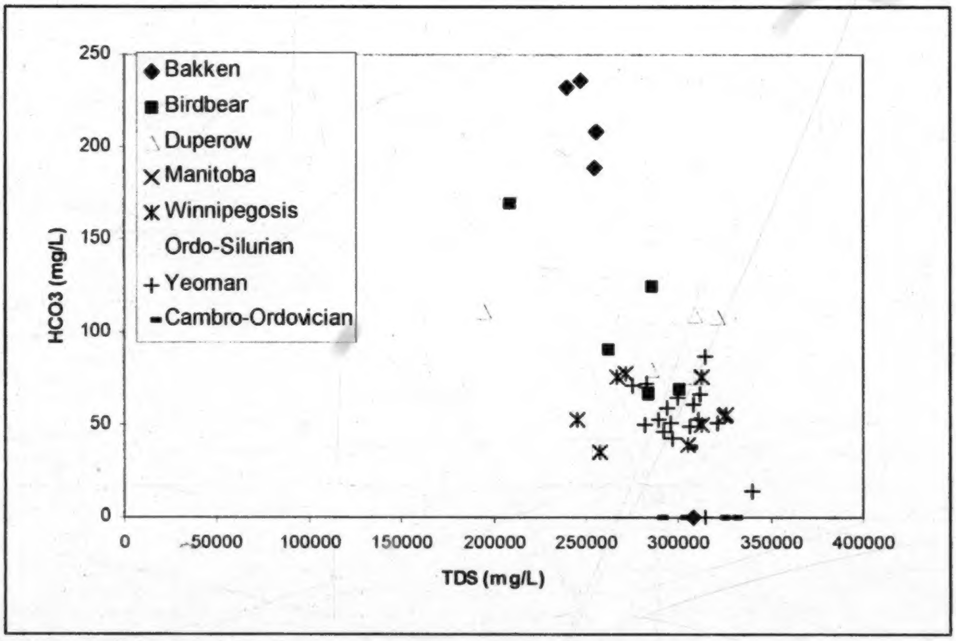

Figure 5.15. Bicarbonate vs. TDS.
Note: HCO_3^- data for low TDS samples are absent from plot because they were not measured.

Group	A	Mix AB	B	Mix BC	C	Mix AC
Type	Na-Ca-Mg-Cl-SO_4	Na-Cl	Na-Cl	Na-(Ca)-Cl	Ca-Na-Cl	Na-Ca-Cl
Ca (meq/L)	50	50-500	<500	500 - 2000	> 2000	500 - >2000
TDS (mg/L)	<40,000	40,000 - 300,000	> 300,000	200,000 - 300,000	> 300,000	200,000 - 300,000

Table 5.2. Classification scheme for pre-Mississippian formation waters based on TDS and calcium concentration in milliequivalents per liter.

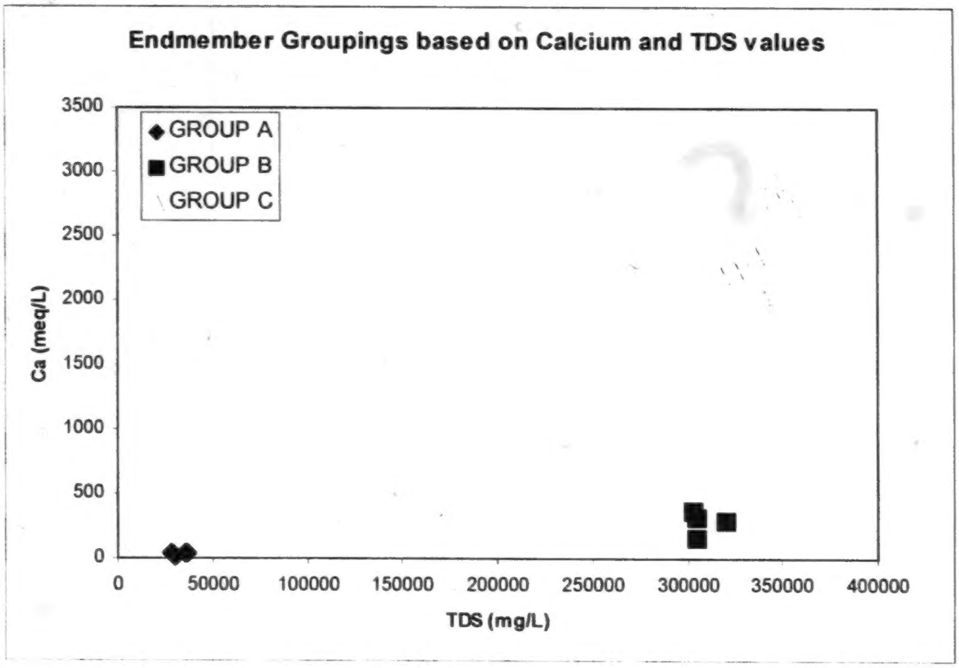

Figure 5.16. Calcium vs. TDS showing Endmember Groupings.

Figure 5.17. Typical Compositions for Endmember Groups

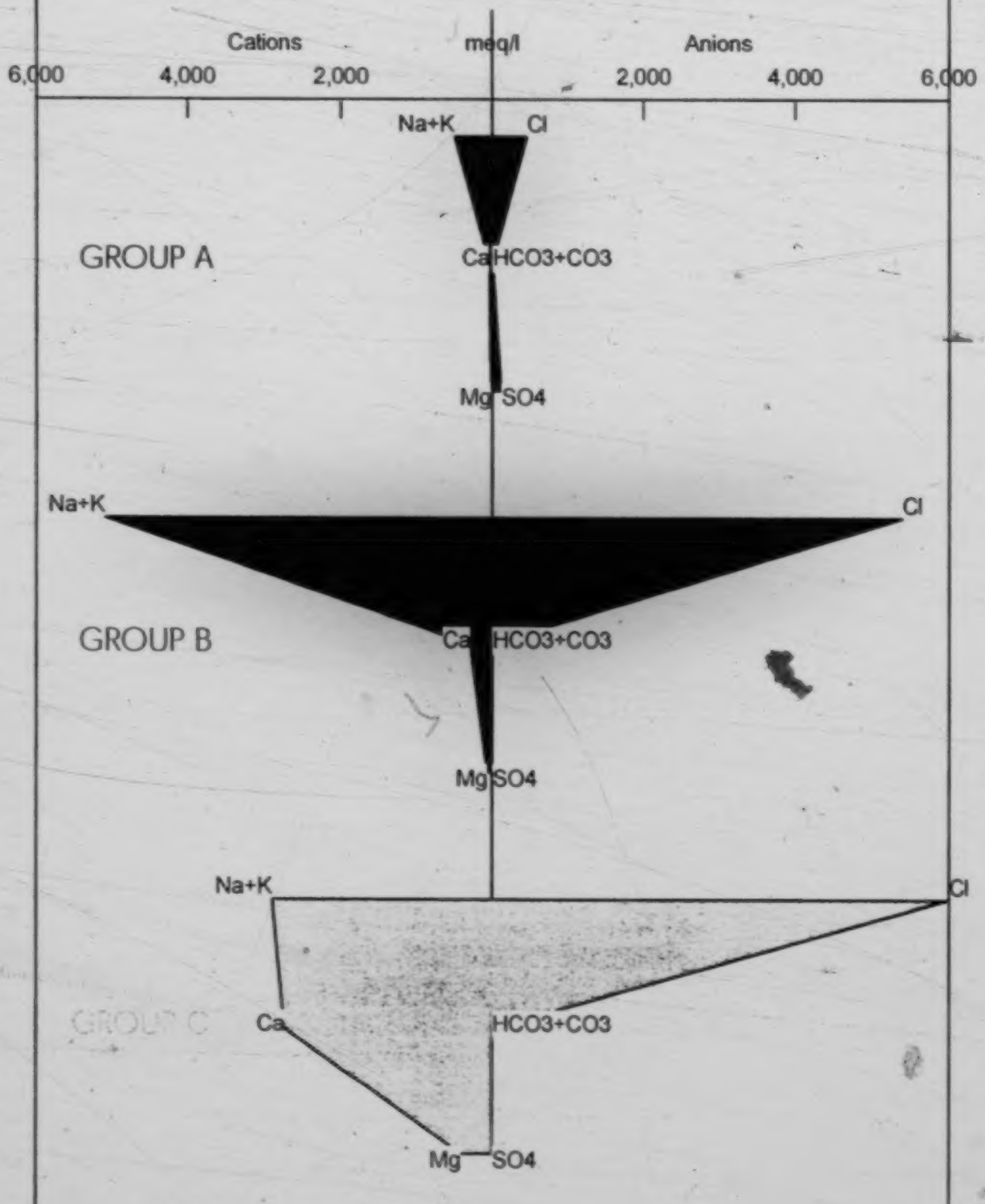

CHAPTER 6

6. DISCUSSION OF BRINE ORIGIN AND EVOLUTION IN THE WILLISTON BASIN

Spatial variation in brine composition suggests the involvement of different water and solute sources. Theoretically, water from many sources can enter a sedimentary basin (see Section 3.1). In the Williston Basin, the primary sources of fluids are seawater and meteoric water due to the past depositional environment and current structure consisting of an intracratonic basin bordered by perimeter uplifts. Sedimentary waters can also theoretically accumulate solutes in many different ways, e.g., during burial of original sediment-forming fluids, during introduction of solute-containing fluids after burial and during rock-water interaction. In the Williston Basin, the possible sources of solute are primarily restricted to solutes introduced as residual seawater (remaining seawater, after evaporation and deposition, buried within sediment), or formation water dissolution of chemical precipitates, particularly $NaCl_{(s)}$ due to its abundance and solubility.

The origin of two types of brines, each with a range of solute concentrations and types of solute, will be evaluated in the explanation of solute composition and abundance in the Williston Basin. Brines can result from the processes described above, e.g., when meteoric water and seawater undergo reaction or concentration, or both. Reactions other than dissolution, including precipitation, oxidation-reduction and cation exchange, can affect the evolution of brine compositions. Brine chemistry can also evolve during mixing to form intermediate compositions. Both the original brine forming mechanisms and indications of mixing and reactions may have implications for fluid flow.

6.1 EVIDENCE OF A NON-BRINE ENDMEMBER

Prior to discussion of the brines predominantly sampled in the basin, it must be acknowledged that a few pre-Mississippian formation water samples (Group A) indicate the presence of fresher water in the basin. Although the Group A TDS range of 28,000 to 36,000 mg/L spans the average seawater salinity of 35,000 mg/L (Carpenter, 1978), this group does not represent buried seawater. Group A chloride concentrations are less than 18,000 mg/L, while those for seawater are approximately 20,500 mg/L (McCaffrey et al., 1987). Likewise Mg concentrations < 400 mg/L, K concentrations around 200 mg/L and Br concentrations mainly < 20 mg/L do not equate with seawater values which are approximately 1300 mg/L, 427 mg/L and 72 mg/L in Mg, K and Br respectively. Additionally, sulphate concentrations in Group A waters reach 5900 mg/L, whereas a value of 2880 mg/L would be expected for SO_4 in seawater. Group A chemistry, combined with physical knowledge of basin uplifts and isotopic values would indicate these waters reflect a meteoric endmember infiltrating the basin in the west and southwest, and possibly at the eastern margin.

This conclusion is consistent with other studies, including Benn and Rostron (1998), whose class 1 waters with TDS $< 30,000$ mg/L correspond to the Group A TDS description (Table 5.2), but contain more calcium than sodium and more sulphate than chloride. Higher sodium and chloride values in Group A waters compared to Class 1 waters of Benn and Rostron (1998), are due to the limited number of samples in the southwest in this study. Group A waters are equivalent to Na-Ca-Mg-Cl-SO_4-HCO_3 type waters in the Silurian to Devonian units described as Facies 1 meteoric waters by Busby et al. (1995). Although not enough of these waters have been sampled in this study to ascertain whether this endmember is present in all pre-Mississippian formations, this has previously been documented (Busby et al., 1995; Benn and Rostron, 1998).

6.2 BRINES DERIVED FROM SALT DISSOLUTION

As meteoric water enters rock formations it may dissolve the rock matrix through which it passes, becoming concentrated through reaction and even achieving brine salinities above 100,000 mg/L. The infiltrating water dissolves minerals according to their solubility constants, attempting to achieve equilibria along the flow path. The formation water can gain many types of solutes as it travels, but generally increases in the amount of total dissolved solids until it is at equilibrium with respect to the minerals in the rock. Brines derived from salt dissolution are especially conceivable in basins with large evaporite deposits containing the most soluble minerals, such as the Williston Basin. Formation water becomes increasingly concentrated as it dissolves more of the soluble minerals such as chloride salts, while gaining relatively little of the less soluble species such as Ca, CO3 and SO4.

6.2.1 MAJOR IONS IN GROUP B BRINES

Group B brine compositions are consistent with salt dissolution. Group B chloride concentrations range from 181,000 to 192,000 mg/L and Na concentrations range from 104000 to 113000 mg/L. These two major ion concentrations are close to 1:1 on a molar basis (Figure 6.1), indicating these waters could be derived mainly from halite dissolution. Indeed, although saturation indices are difficult to calculate due to the high temperatures and high ionic strengths of these waters, with concentrations of Cl around 190,000 mg/L, Na around 110,000 mg/L and TDS approximately 300,000 mg/L, samples in this group are considered to be at halite saturation (Hanor, 1994). Nevertheless, progressive seawater evaporation can also increase Na and Cl concentrations to the point of halite saturation (McCaffrey et al., 1987), so other major ions are considered. Group B sulphate concentrations around 650 mg/L comprise less than 1% of the total anions. Other cation concentrations account for the remaining ionic balance: Group B calcium averages around 6000 mg/L, magnesium ranges from 800 to 4500 mg/L and potassium concentrations average around 5500 mg/L. These values are not consistent with those in evaporated seawater with TDS = 300,000 mg/L (McCaffrey et al, 1987).

6.2.2. MINOR IONS IN GROUP B BRINES

To further evaluate the compositional source of these brines Na-Br-Cl systematics have been applied. As discussed in Chapter 3, bromine does not become incorporated into the halite lattice with the exception of minor inclusions. Thus, a brine derived from halite dissolution is generally low in Br compared to evaporated seawater. Group B bromine concentrations range from 188 to 622 mg/L. Given the high Group B Cl and Na concentrations, Cl/Br and Na/Br ratios for the Group B endmember are much greater than those for seawater (Figure 6.2) (seawater data from McCaffrey et al., 1987), strongly indicating that halite dissolution is the source of solutes within these waters.

6.3 BRINES DERIVED FROM EVAPORATED SEAWATER

Seawater, at an evaporation degree of around 4x, is concentrated enough to be classified as a brine (McCaffrey et al, 1987). In a sedimentary basin, seawater may either evaporate at surface, or may evaporate subaerially. As a brine evaporates, there is a succession of minerals that precipitate with progressive evaporation according to the solubility constant/precipitation equilibria. The remaining brine retains some species in relatively high amounts, but retains little of other less soluble mineral forming species (McCaffrey et al., 1987). Thus, brines, with progressive evaporation, have chemical signatures increasingly different than the original composition of seawater. The tracers that can be used to indicate an evaporated seawater signature include: major ions, minor ions and isotopes. (The latter will not be discussed in this thesis; rather, future publications, including Holmden and Rostron, in prep, will contain a discussion of isotopes in the basin).

6.3.1 MAJOR IONS IN GROUP C BRINES

Major ions can be used as tracers of evaporated seawater involvement in brine formation, as during seawater evaporation, mineral saturations control solute abundance and a definite evaporated seawater signature develops. With progressive evaporation of seawater, Ca and CO_3 drop out of solution and the dominant ions become SO_4, Cl, Na, Mg and K. At around 10x the concentration of seawater Na and Cl start to precipitate together forming halite (Figure 6.3). Thereafter, because Na is the limiting ion, the Na concentration starts to decrease, while Cl continues to rise until at an evaporation ratio of about 80x, magnesium and potassium chlorides start to precipitate (Figure 6.3). Thus in a brine derived from seawater evaporated past halite saturation one would expect to find little Ca, lower amounts of Na and high amounts of Mg, K and Cl, compared to seawater (at an evaporation degree below halite saturation) and meteoric water.

Most major ion concentrations in the Group C endmember are within 10 to 20% of seawater values for equivalent salinities (taken from McCaffrey et al., 1987) even though some are not wholly consistent with evaporated seawater. Potassium, with a concentration range of around 3000 mg/L to 10,000 mg/L, closely approximates K concentrations in seawater evaporated by 10 to 40x, even though some Group C concentrations may be a bit higher (Figure 6.4). Group C Na concentrations can be up to 20,000 mg/L lower, than those in seawater evaporated by 10 to 40 times, and fall within the range of 58,000 to 88,000 mg/L (Figure 6.4). Group C Cl concentrations ranging from 193,000 to 215,000 mg/L are up to 20,000 mg/L higher than those for seawater evaporated by 10 to 40 times (Figure 6.4). Despite the variation, these concentrations are still reasonably close to the seawater trajectory (Figure 6.3), especially given 10% analytical error, and are definitely not indicative of 1:1 NaCl dissolution.

Higher discrepancy occurs between the evaporation trajectory and the remaining major ions. Ca is a major cation in Group C waters, with concentrations of 40,000 to 59,000 mg/L, ranging from 20% to 58% of the cations on a milliequivalent basis. These values are enriched by 10 to 100 times that of seawater at evaporation degrees of 10 to 40 (McCaffrey et al., 1987) (Figure 6.5). Meanwhile, magnesium concentrations ranging from 3000 to 5000 mg/L and sulphate concentrations less than 350 mg/L, are ten times and one hundred times lower respectively than predicted by seawater evaporation degrees of 10 to 40 (McCaffrey et al., 1987) (Figure 6.5).

6.3.2 REACTIONS AFFECTING GROUP C MAJOR IONS

These deviations may be explained by several reactions including: anhydrite precipitation, anhydrite dissolution, thermochemical sulphate reduction, dolomitization, and albitization (for further description and discussion see Appendix E). Sulphate values and calcium values are three orders of magnitude different (Figure 6.6) indicating if anhydrite precipitation is the cause of SO_4 depletion, another process is responsible for the great calcium enrichment. Conversely, if anhydrite dissolution is responsible for calcium excess relative to seawater, vast amounts of sulphate have been removed via another process. Neither anhydrite precipitation nor dissolution can solely explain Group C deviation from seawater compositions. The occurrence of thermochemical sulphate reduction is acknowledged in the basin, but it is not known to transpire on a large scale, and therefore not likely the mechanism responsible for sulphate removal.

Multiple reactions are more plausible for the explanation of Group C compositions. Anhydrite precipitation may occur in conjunction with dolomitization

(Carpenter, 1978) accounting for reduced sulphate concentrations. Fairly widespread dolomitization has occurred in much of the pre-Mississippian, and may account for both enriched calcium and depleted magnesium values with respect to seawater (Kent, 1960; Thiede, 1975; Perrin, 1982; Kendall, 1989; Chow, 1991). A plot of Log Ca+Mg-SO4 (meq/L) vs. Log Br (mg/L) should produce a straight line regardless of what dolomitization related reactions have occurred at any evaporation degree, as mass is conserved in the brine (Carpenter, 1978; Connolly, 1990). A plot of Group C waters is close to the 1:1 line and dolomitization is reasonable; however, the slight elevation in the factor Log $Ca+Mg-SO_4$ suggests yet another process is involved (Figure 6.7). A comparison of Ca excess versus Mg depletion on a milliequivalence basis (for definitions, equations and calculations see Appendix F) also shows that although Ca excess and Mg depletion are strongly related. However, a slope of 1.19 rather than 1 indicates that some of the calcium in the brine has been derived from another process, as not enough Mg depletion has occurred to account for the calcium enrichment (Figure 6.8).

Multiple reactions affecting Group C major ions potentially include not only dolomitizing related reactions, but also sodium – calcium exchange reactions. However, a plot of Ca excess versus Na depletion (for definitions, equations and calculations see Appendix F) for the Group C endmember shows a highly evolved brine affected by reaction(s) involving calcium, but relatively independent of reactions involving sodium (Figure 6.9). Albitization may be indicated on a plot of Na/Br vs. Cl/Br (Figure 6.10) as values plot to the left of seawater data indicating lower values of Na/Br, but this feature can also be a product of the elevated Cl values. If Na-Ca exchange reactions have affected Group C compositions to slightly elevate Ca and lower Na concentrations, it is not to a large extent. Unfortunately, as yet there is no known recorded core data to support either the presence of abundant feldspars or that an albitization reaction contributed ionic Ca to the deep basinal brines while removing sodium.

6.3.3 MINOR IONS IN GROUP C BRINES

Minor ions may also be used to trace the Group C endmember to an evaporated seawater origin, as they are not affected by reactions in the same manner as major ion compositions. Samples from pre-Mississippian units show lithium, strontium and iodide concentrations are generally the highest in Group C waters. Group C lithium concentrations range from 40 to 200 mg/L. Group C strontium concentrations range from 1100 to 2700 mg/L. Group C Iodine concentrations average around 30 mg/L. These elevated concentrations are thought to be consistent with evaporated seawater (Davisson and Criss, 1996).

Bromine, another minor ion, has been used as a tracer to indicate the presence of seawater in many studies (Carpenter, 1978; Stueber and Walter, 1994; etc.). As discussed in Chapter 3, bromine behaves conservatively during the progressive evaporation of seawater, as it does not form salts. Loss of bromine during seawater evaporation generally occurs through minor inclusion in other evaporite minerals. Due to bromine's non-reactive nature, its concentration increases during seawater evaporation as more water molecules are lost and bromine is left behind (Figure 6.3). Group C bromine concentrations range from 700 to 1600 mg/L, which correspond to seawater evaporation degrees of 12 to 25x seawater (McCaffrey et al., 1987).

Cl/Br and Na/Br ratios also support the occurrence of residual seawater, as they plot well below the normal seawater value (Figure 6.10) taken from McCaffrey et al. (1987). Although it is known that mixing of brines derived from evaporated seawater with brines derived from halite dissolution can alter the location of data points on a Cl/Br vs. Na/Br plot (Chi and Savard, 1997), data plotting below seawater implies that at least some proportion of evaporated seawater is still left. In the Group C endmember, representing the greatest proportion of residual seawater left in the basin, it appears that at least up to 40% of formation water (by comparison with Chi and Savard (1997)) is residual seawater remaining in the pre-Mississippian. Not enough Group C waters have been sampled to unequivocally conclude a seawater endmember is present in all pre-Mississippian formations, but these residual seawaters are present in at least three aquifers, both above and below the Prairie Aquitard.

DISTINCTION BETWEEN BROMINE SOURCES IN ENDMEMBERS

Halite dissolution has been cited to generate both high Br and low Br waters (Stoessell and Carpenter, 1986; Chipley and Kyser, 1991). To use bromine to trace brine origin with confidence, a distinction between these two cases must be made. High bromide values are produced during repeated dissolution and recrystallization as the halite lattice is slowly, but preferentially rid of impurities such as Br (Stoessell and Moore, 1983). This mechanism requires a strongly rock-dominated system for halite recrystallization to yield a formation water composition with a Cl/Br ratio less than seawater (Stoessell and Carpenter, 1986). In such a system, little water escapes from the halite and therefore can only locally affect the surrounding brine content.

Incongruent halite recrystallization (preferential release of Br into solution) may have taken place in the Williston Basin (Kreis et al., 1991; Chipley and Kyser, 1991) over a lengthy period (300 million years) of minimal early flow. In spite of this possibility, there is no evidence to indicate that recrystallization has elevated Br concentrations. Br-rich brines are not uniformly found across the basin in the vicinity of the Prairie Formation. Major ion compositions show Group B waters appear to be derived from congruent dissolution and Na-Cl-Br systematics confirm they are not elevated in bromine (Figure 6.2). If waters known to be derived from halite are not elevated in bromine (particularly in adjacent formations, e.g. the Winnipegosis which shows low bromine concentrations), it is entirely unreasonable that Group C waters falling on or slightly to the right of the Br vs. Cl seawater trend (Figure 6.11) have been elevated in bromine by incongruent halite dissolution. Additionally, the K/Br ratio is high for Group C waters, as both solute concentrations have increased during seawater evaporation; in contrast, low K/Br ratios would be associated with incongruent recrystallization as no K is involved (Stoessell and Carpenter, 1986; Connolly, 1990). Therefore, all evidence points toward highly saline Group C waters in the basin being derived from evaporated seawater.

6.4 ENDMEMBER MIXING

Formation water chemistry establishes zones of mixing between freshwater and waters with higher TDS or mixing between high TDS waters of different origin. Mixing relationships are indicated if two end-members produce compositions that plot along a straight line or if three endmembers produce compositions that fall within a triangle on a comparison plot (Spencer, 1987). This thesis hypothesizes three endmember compositions exist in the basin: meteoric water, halite-saturated water and evaporated seawater, therefore mixtures of the three should produce intermediate compositions in which the endmembers are reflected.

6.4.1 MIXING BETWEEN GROUP A AND B ENDMEMBERS

Collected data demonstrate mixing between the Group A and Group B endmembers. Linearly increasing amounts of Na and Cl can be observed as the degree of halite dissolution increases (Figure 6.12). Ca concentrations for Mix AB waters are generally in between those for the meteoric endmember and halite-saturated water and also show that mixing/dilution is the process responsible for these waters (Figure 6.13). Furthermore, Na/Br and Cl/Br ratios for Mix AB waters are all greater than those corresponding to seawater (Figure 6.14), supporting the combination of meteoric water and halite-saturated water to create those mixtures.

6.4.2 MIXING BETWEEN GROUP A AND C ENDMEMBERS

Transitional compositions between Group A meteoric water and Group C residual seawater can also be explained by mixing between these two groups. Mix AC waters contain less TDS, sodium and chloride than those in Group C indicating mixing with some proportion of meteoric water (Figure 6.12). It should be noted from Figure 6.12 that meteoric water does not invade right into the basin center without gaining solute, as evidenced by a mixing line that does not go through the origin {0,0}. Rather, Group C is mixing with meteoric water that has gained some Na and Cl, but is still relatively fresh. In spite of this dilution by the fresher water, Mix AC waters still exhibit a strong residual seawater signature. Signs of Group C evolution are still evident in significant Ca concentrations (> 20,000 mg/L) and low Mg (< 5000 mg/L) and sulphur (500 mg/L) concentrations. Mix AC major ion concentrations e.g., Ca, have been shifted only slightly towards the meteoric endmember from those in Group C, showing the major component of the mixtures is residual seawater and not as much mixing of evaporated seawater with meteoric water has occurred (Figure 6.13). Na/Br and Cl/Br ratios for Mix AC plot below values for normal seawater, and since ratios are unaffected by dilution, Mix AC Na/Br and Cl/Br ratios are equivalent to those in the Group C endmember from which they were derived (Figure 6.15).

6.4.3 MIXING BETWEEN GROUP B AND C ENDMEMBERS

Mixing also occurs between the Group B endmember associated with halite saturation and the Group C residual seawater endmember. Na-Cl-Br systematics for Mix BC artificially split the group in two, as some samples lie below seawater and some above seawater on a Cl/Br vs. Na/Br plot (Figure 6.16). Closer inspection reveals that the range of Na/Br and Cl/Br is continuous and there is a gradual change from Group C type waters to Group B type waters. Major ion concentrations for Mix BC also show a gradual change from Group C values to Group B values, particularly for calcium. Ca values greater than 30,000 mg/L correspond to low Cl/Br ratios, but a few samples that plot above seawater also contain > 30,000 mg/L in Ca, and blend with a 10,000 to 20,000 mg/L Ca range for the remaining samples (Figure 6.17). This signifies some calcium has moved out from the center of the basin through mixing, providing a mechanism through which high calcium waters from Group C may affect some Group B sulphate values. Along the mixing zone, high sulphate from Group B and high calcium from Group C may be precipitated to form anhydrite, explaining low sulphate near the residual brines, while SO_4 concentrations are still reasonably high further away from the center. Plots of Ca excess vs. Mg depletion and Ca excess vs. Na depletion also demonstrate how waters with decidedly different origin and evolutionary mechanisms are now blending compositions via mixing (Figure 6.18 and 6.19).

6.5 SPATIAL DISTRIBUTION OF ENDMEMBERS AND MIXTURES

Visible mixing trends between endmembers explained in the previous sections are summarized in Table 6.1 and are also documented spatially (Figure 6.20). The Group C endmember lies in the very center of the basin. Surrounding this endmember immediately to the north is Mix BC, produced where halite saturated waters of Group B, yet further to the north, are mixing with the residual seawater brine forming intermediate compositions. Southwest of the residual slug, meteoric water (Group A) mixes directly with evaporated seawater where mixing Group AC can be found. Further southwest, samples are representative of the intruding meteoric water. In the west, the meteoric endmember has dissolved halite to produce the compositions characteristic of Mix AB. No abrupt boundaries exist between water types and their mixtures, as distinct zonations are blurred through mixing.

6.6 IMPLICATIONS FOR FLUID FLOW IN THE WILLISTON BASIN

Pre-Mississippian chemistry indicates a more active gravity-driven flow system has altered uniform distributions of evaporated seawater-derived salinity indicative of an ancient, relatively inactive flow system. This involves the replacement of formerly widespread seawater by freshwater and active halite dissolution. One can speculate that considering the basin has not been flushed of residual seawater, it is doubtful that any pre-Cretaceous fluid flow events were either pervasive or completely regional. A proportion of residual seawater is now isolated in the basin center and lies surrounded by water not of seawater origin. The evaporated seawater-derived brine does not appear to be moving although with the decrease in residual brine over time, a new steady state may not have been reached and the pressure of the entering column of water could be pushing it up-dip slightly.

In order for this evaporated seawater slug to persist while flushing has occurred in other areas, flow must be continuing preferentially around it to the north and south, and to some degree possibly over and under it. Within the pre-Mississippian hydrostratigraphic units, a higher percentage of residual brine seems to lie within the Manitoba, Duperow, Ordo-Silurian and Yeoman aquifers, suggesting that permeabilities and flow rates are lower in these formations. Meanwhile the Bakken and Birdbear aquifers at the top of the section, the Winnipegosis Aquifer just below the Prairie Evaporite and the Cambro-Ordovician aquifer at the bottom of the section have lower percentages of residual seawater, and therefore indicate a higher degree of flushing and faster flow through these units. In general flow above the Prairie is more sluggish and flow below the Prairie is slightly faster.

Flow in pre-Mississippian units at the western margin includes a large component of cross-formational flow as evidence of mixing is found in all hydrostratigraphic units and not just right above and below the salt. Chemistry indicates all seawater beyond the slug at the eastern margin has been discharged since dominant ions present at discharge points in Manitoba are Na and Cl (Grasby and Betcher, 2000). Thus the flow system must be fairly active in the east (Grasby and Betcher, 2000). Flow rates associated with recharge and discharge areas are on the order of m/yr (Downey et al., 1987).

6.7 SUMMARY OF ORIGIN AND EVOLUTION AND IMPLICATIONS FOR FLUID FLOW

Salinity distributions in pre-Mississippian formations can be explained in terms of two brine origin mechanisms, halite dissolution and seawater evaporation, and in terms of two major evolutionary processes, reaction and mixing. Major ion chemistry and Na-Cl-Br systematics show brines throughout much of the basin have derived their salinity from halite dissolution. Major ion chemistry and bromine data also provide evidence that brines in the center of the basin have derived their salinity from evaporated seawater and mixtures. Approximately 40% of the samples show a residual seawater signature based on Na-Cl-Br systematics (Figure 6.21).

Diagenetic reactions have significantly lowered magnesium and sulphate concentrations, and minutely lowered sodium concentrations, while increasing calcium concentrations in the residual seawater endmember. Dolomitization, albitization and anhydrite precipitation appear to have taken place prior to Laramide flow system development, as these reactions have not affected compositions elsewhere in the basin.

Mixing has blurred the spatial distinction between the two types of genetic mechanisms and is evident in the gradual transition from major and minor ion compositions characteristic of altered seawater in the center, out to the north where compositions are characteristic of halite dissolution. Mixing has also diluted basin salinity in the west where meteoric water encounters halite and in the southwest where meteoric water encounters the residual seawater slug. Such mixing indicates that since uplift in the Laramide, meteoric fluids have migrated down deep into the basin, gradually flushing the seawater, first at the margins and gradually further into the center of the basin and have presently left only a remnant of evaporated seawater in the basin center. During seawater flushing, meteoric fluids have encountered a second source of salinity in halite and more recently formed brines have developed.

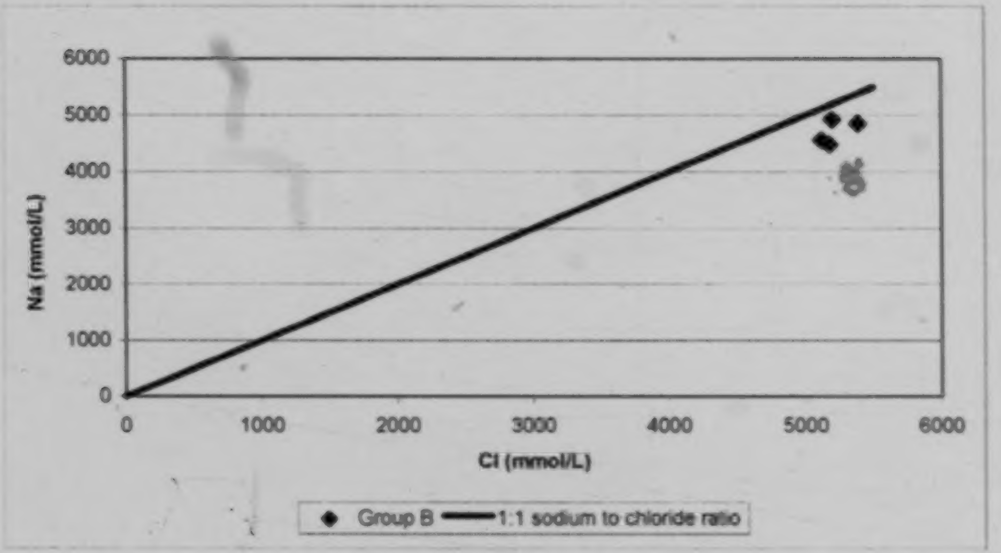

Figure 6.1. Position of Group B endmember relative to the 1:1 halite dissolution line.

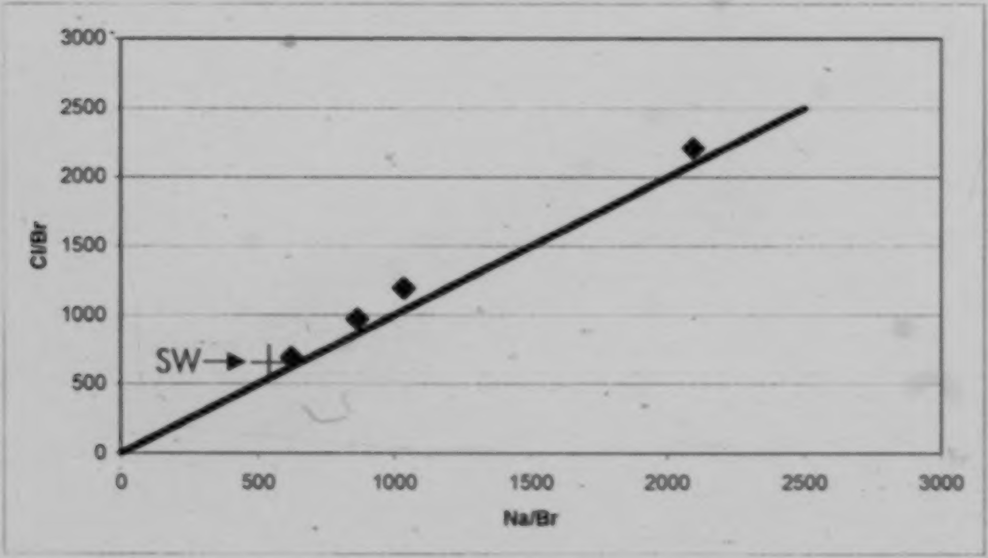

Figure 6.2. Group B endmember Na/Br and Cl/Br molar ratios compared to seawater. The green line represent Na:Cl = 1:1

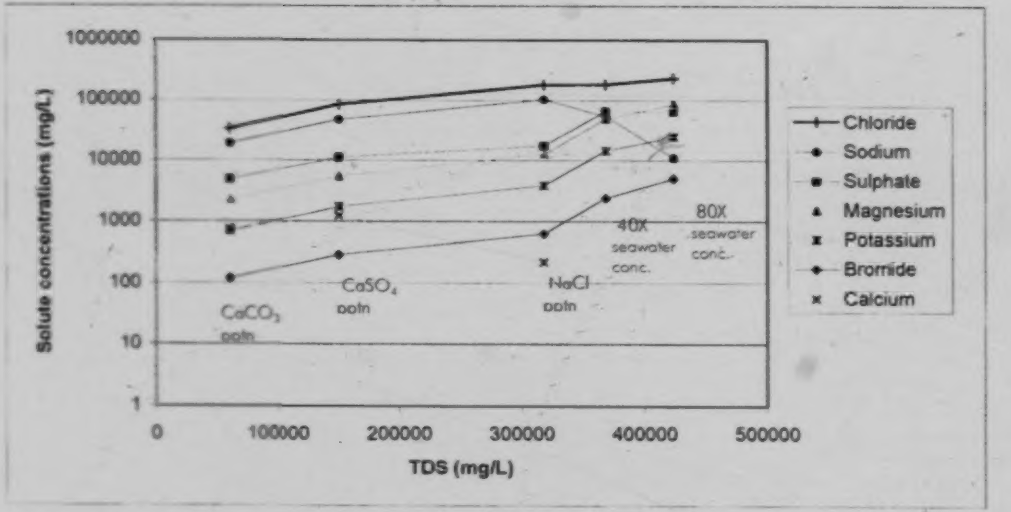

Figure 6.3. The behavior of solutes during progressive seawater evaporation (data taken from McCaffrey et al, 1987).

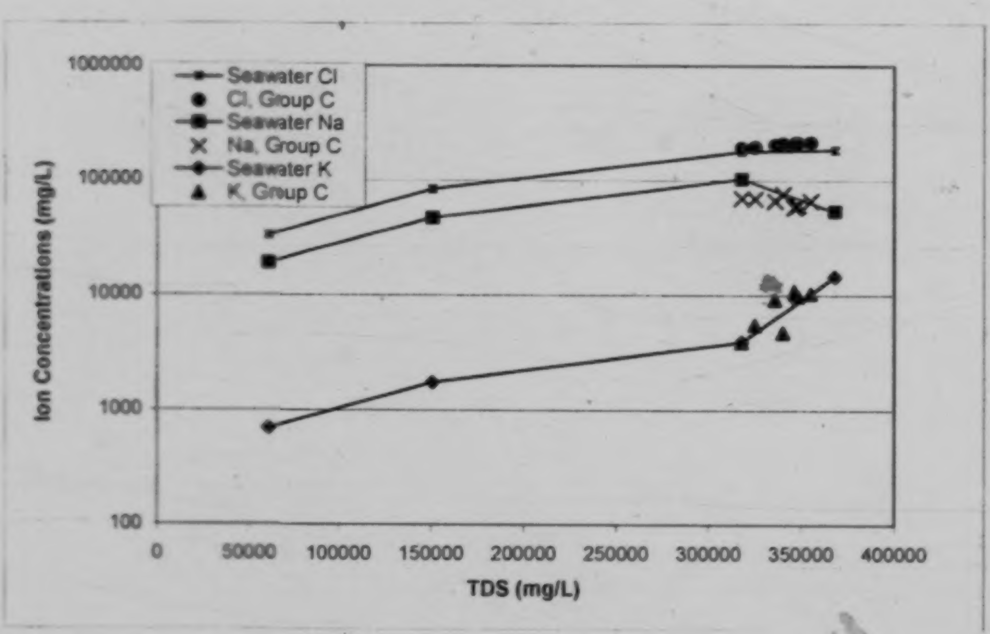

Figure 6.4. Comparison of Group C chloride, sodium and potassium concentrations with the seawater evaporation trends.

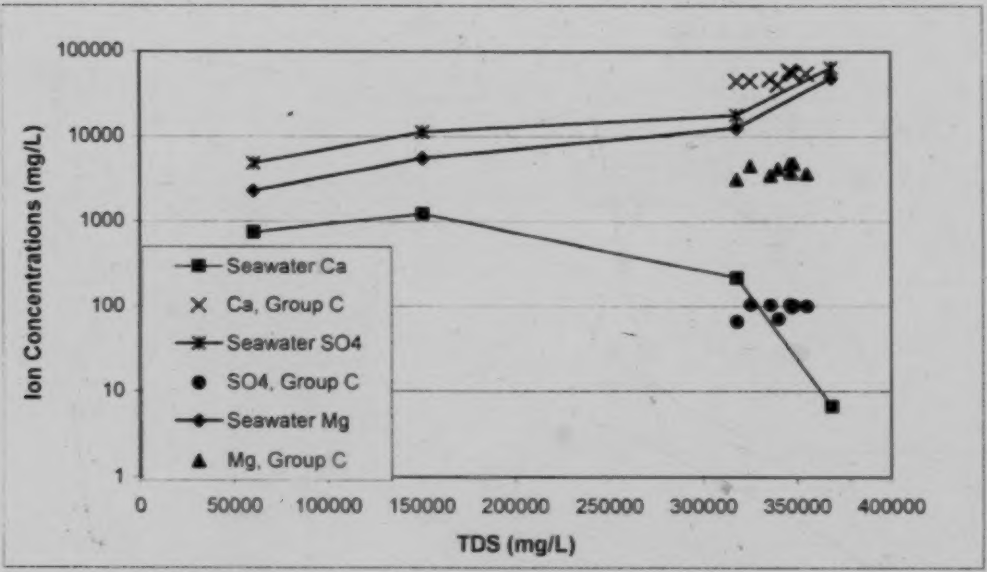

Figure 6.5. Comparison of Group C calcium, sulphate and magnesium concentrations with the seawater evaporation trend.

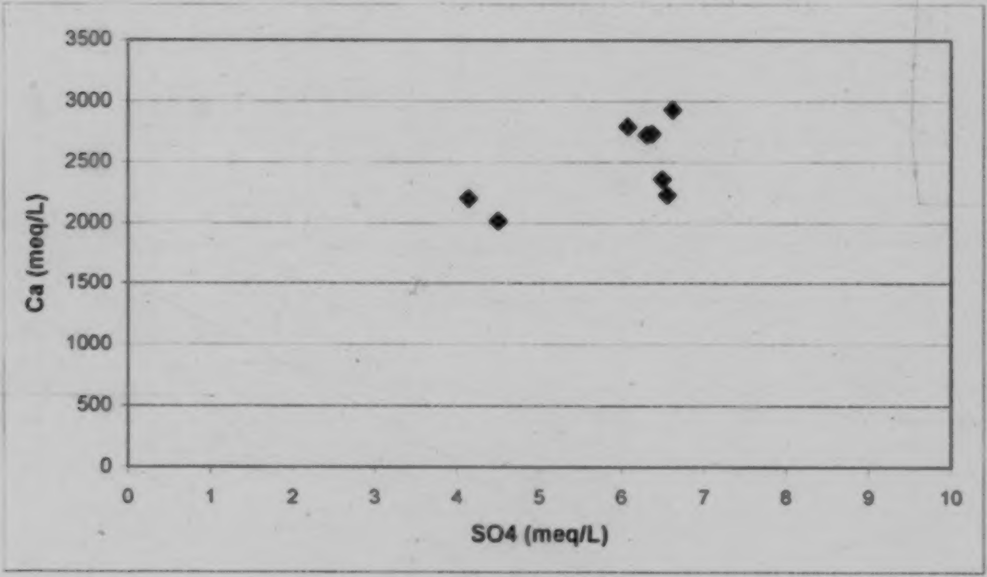

Figure 6.6. Calcium vs. sulphate in Group C waters.

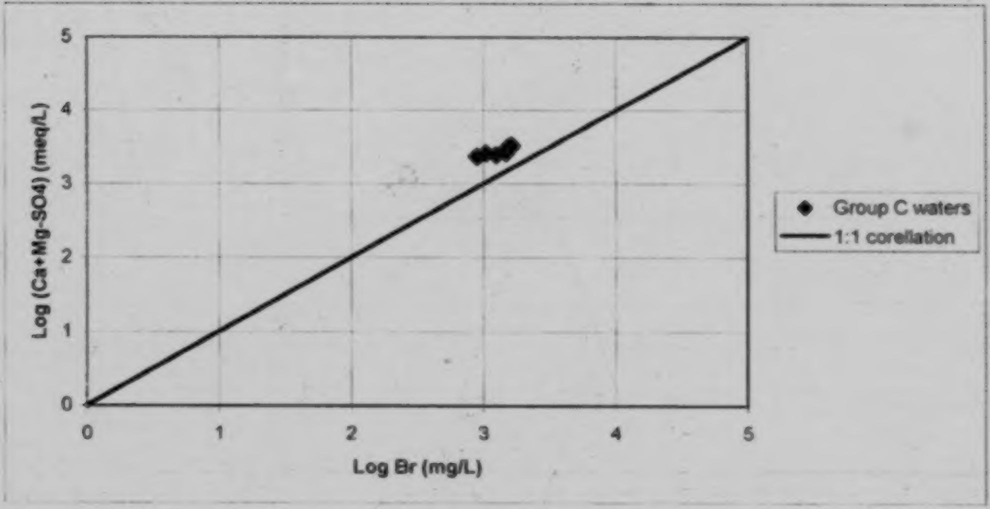

Figure 6.7. Log (Ca+Mg-SO_4) vs. Log Br for Group C values.

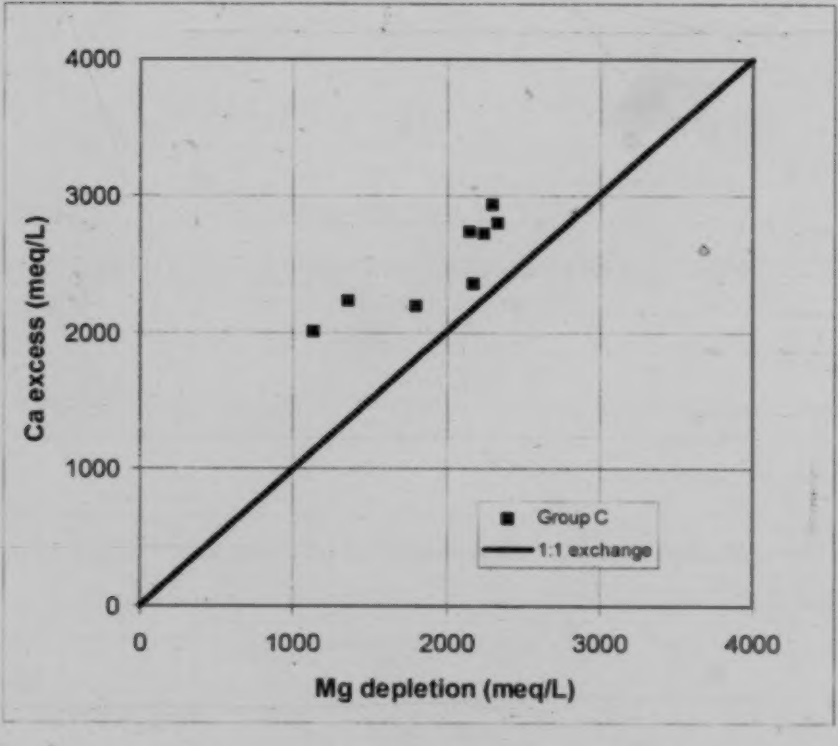

Figure 6.8. Ca excess vs. Mg depletion compared to evaporated seawater.

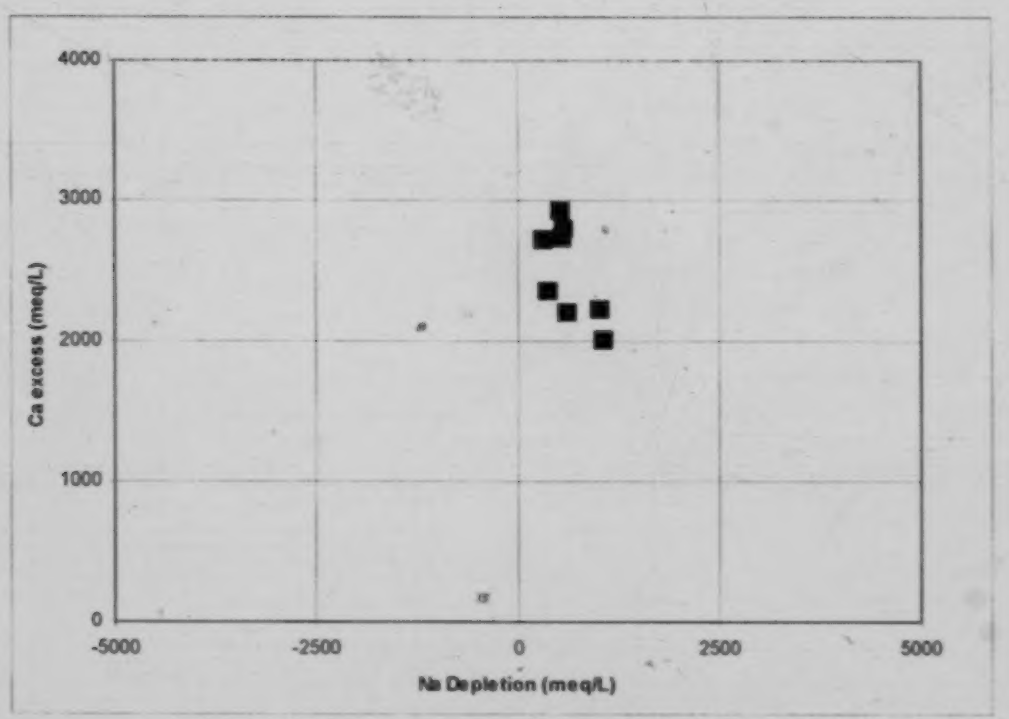

Figure 6.9. Ca Excess vs. Na Depletion in Group C samples compared to evaporated seawater.

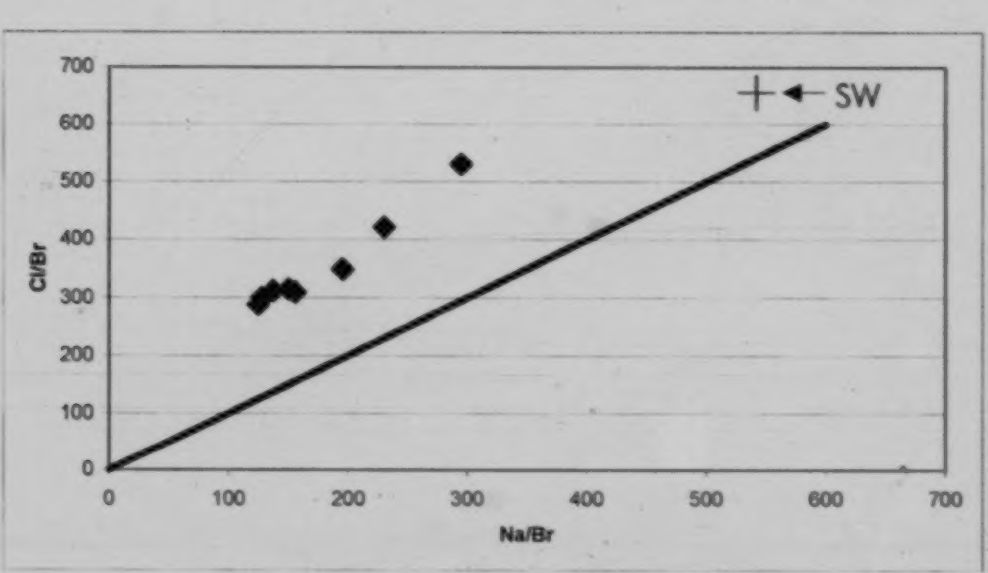

Figure 6.10. Group C endmember Na/Br and Cl/Br molar ratios compared to seawater.

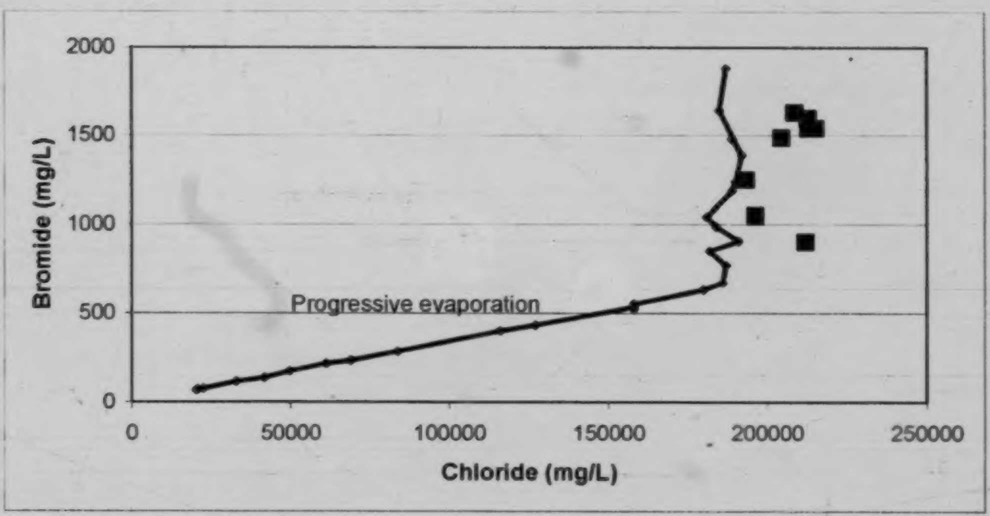

Figure 6.11. Bromide vs. chloride for the Group C endmember relative to seawater evaporation. Data taken from McCaffrey et al., 1987.

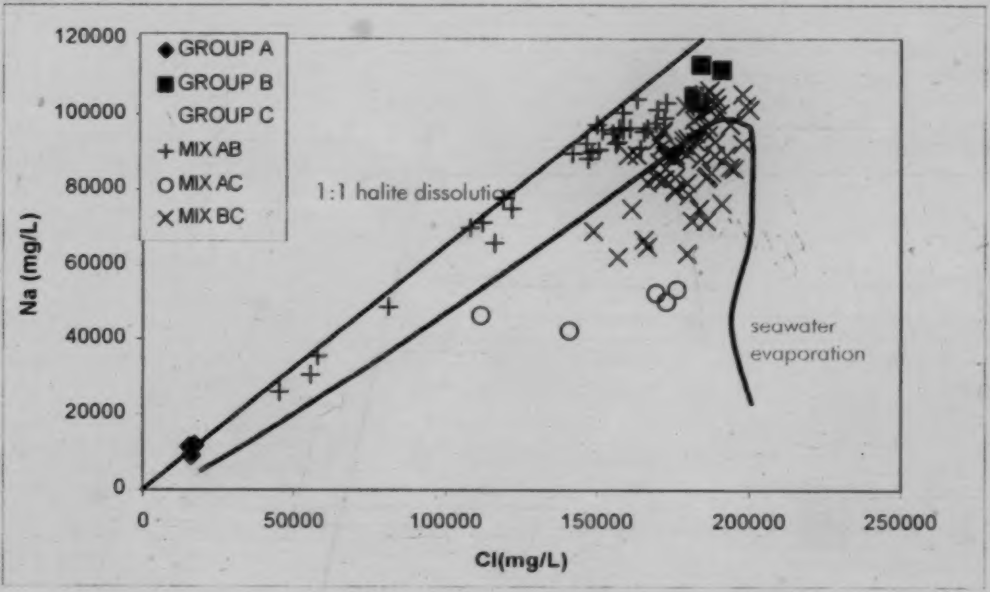

Figure 6.12. Endmember groupings and mixtures on a sodium vs. chloride plot.

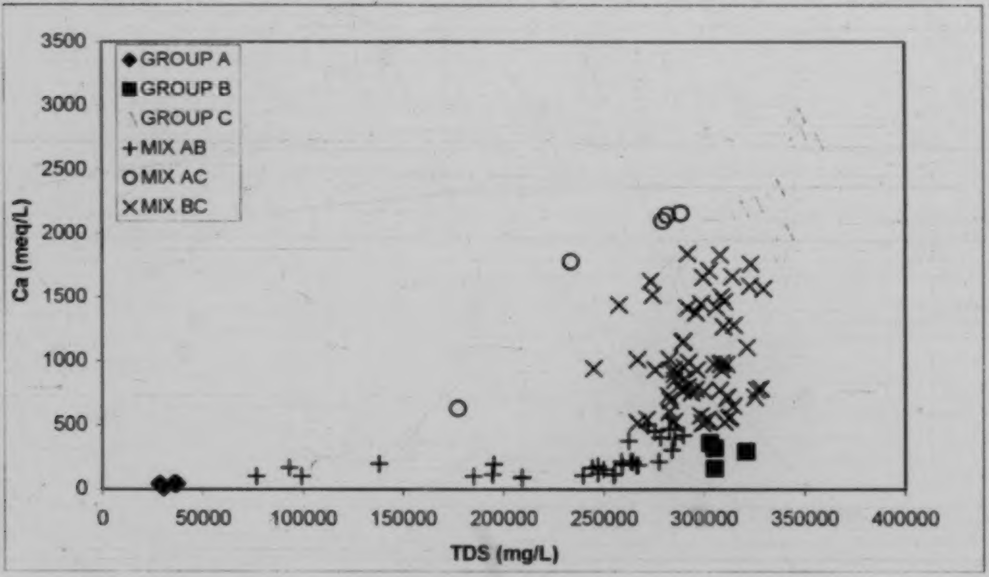

Figure 6.13. Endmember groupings and mixtures on a calcium vs. TDS plot.

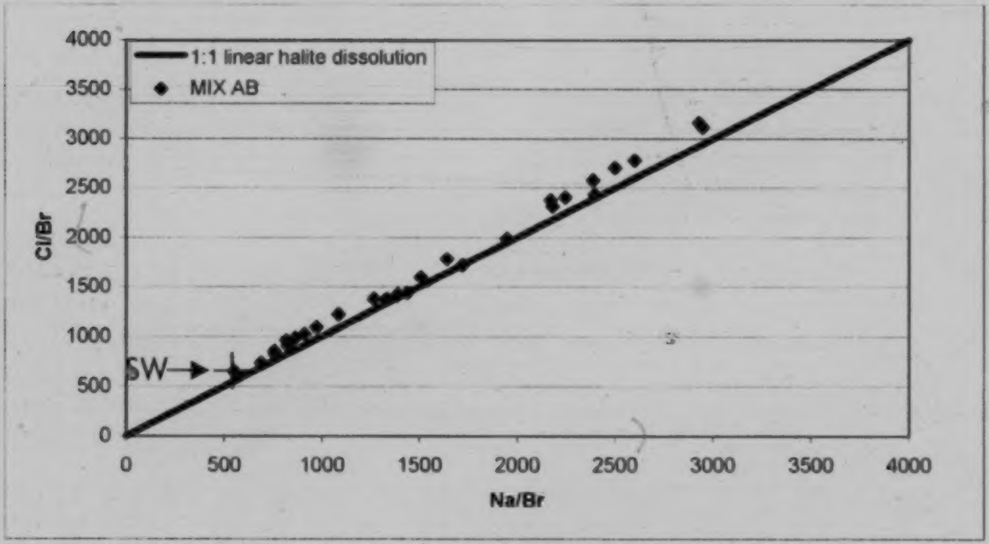

Figure 6.14. Mix AB Na/Br and Cl/Br molar ratios compared to seawater.

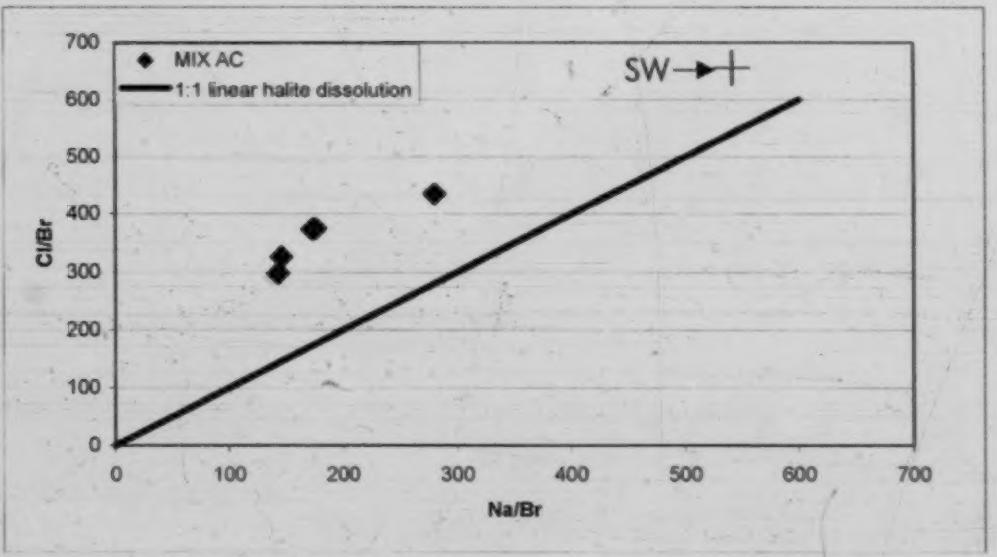

Figure 6.15. Mix AC Na/Br and Cl/Br molar ratios compared to seawater.

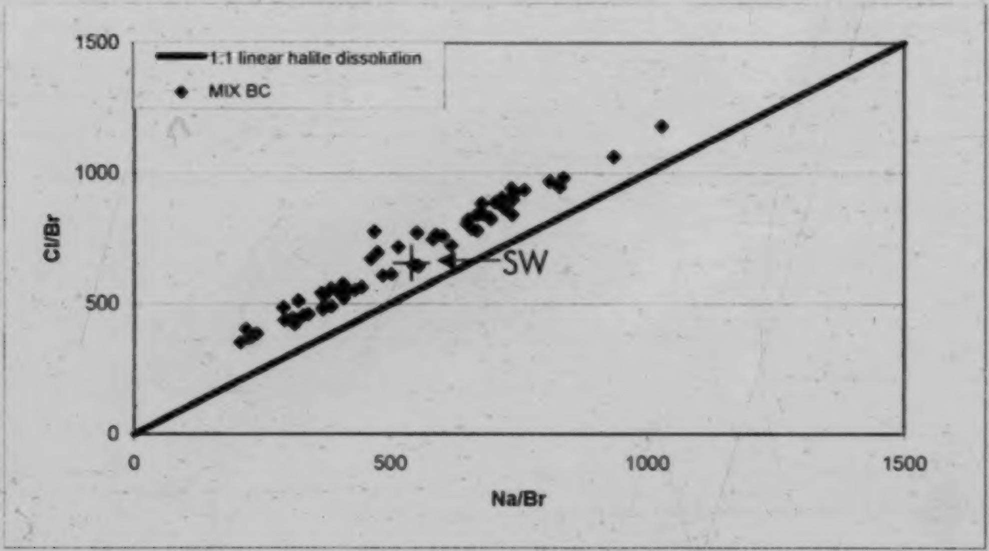

Figure 6.16. Mix BC Na/Br and Cl/Br molar ratios compared to seawater.

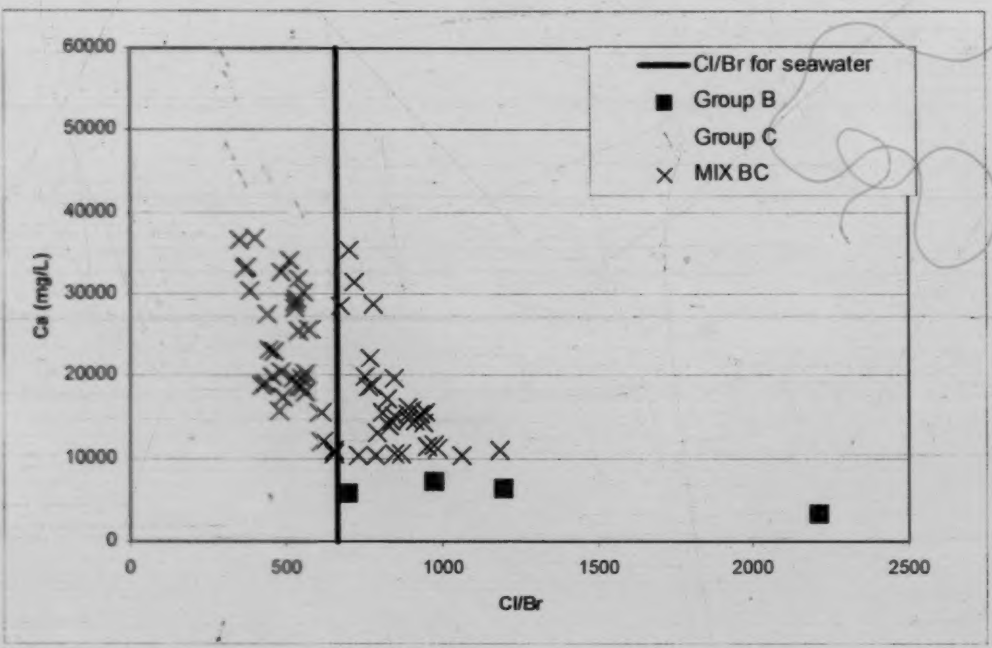

Figure 6.17. Ca vs. Cl/Br for saline endmembers and intermediate compositions compared to seawater.

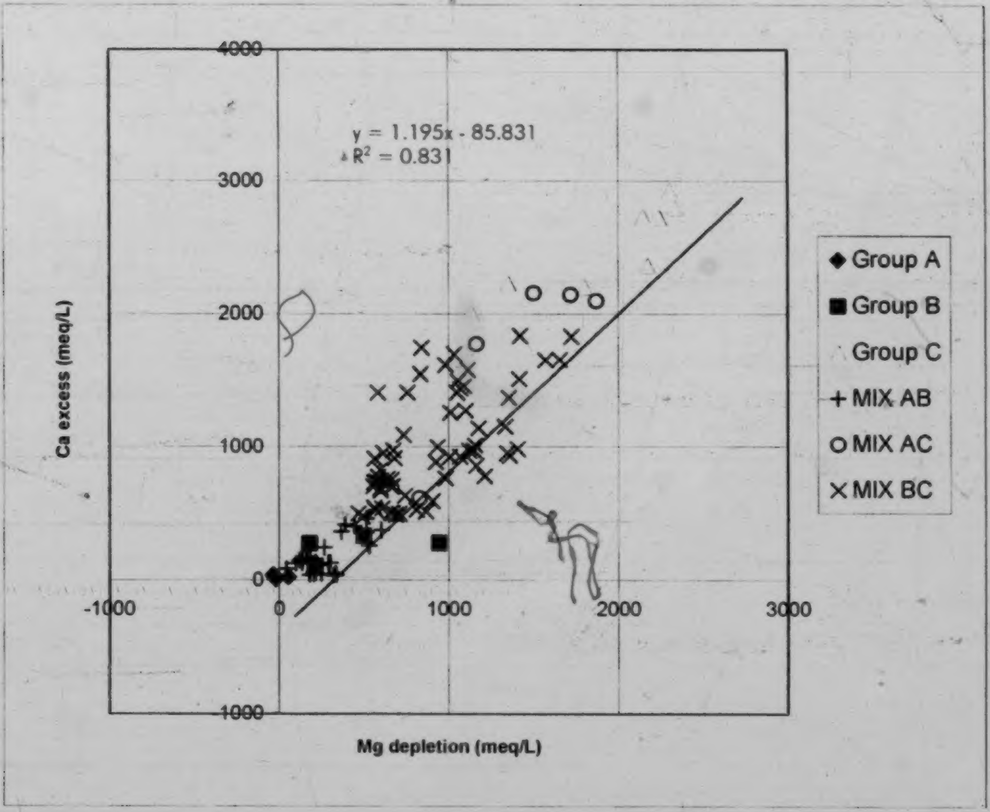

Figure. 6.18. Ca excess vs. Mg depletion in WB samples compared to evaporated seawater.

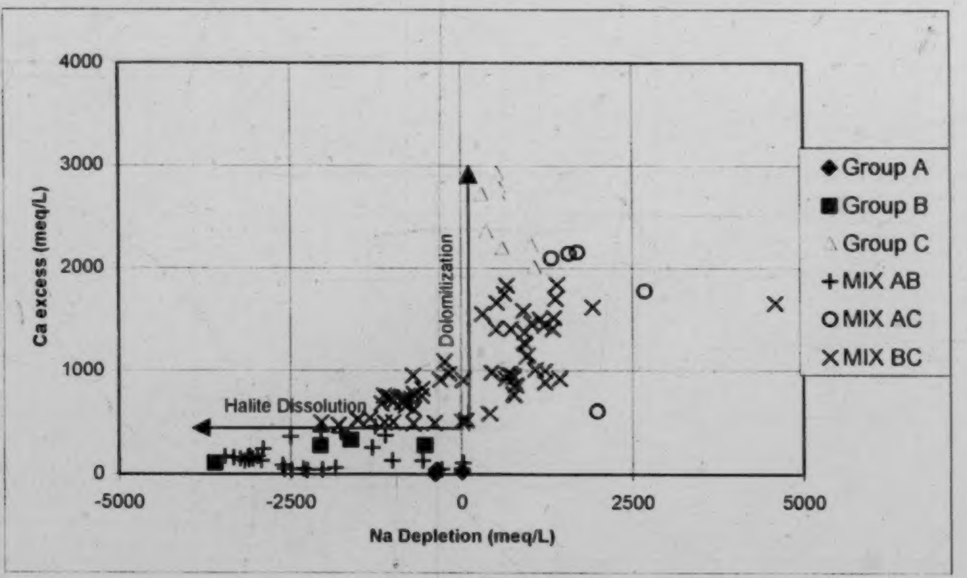

Figure 6.19. Ca Excess vs. Na Depletion in WB samples compared to evaporated seawater. Please note, although similar to a Davisson and Criss (1996) excess-deficit plot, this diagram is not equivalent, for further discussion please see Appendix F.

Group	A	Mix AB	B	Mix BC	C	Mix AC
Type	Na-Ca-Mg-Cl-SO_4	Na-Cl	Na-Cl	Na-(Ca)-Cl	Ca-Na-Cl	Na-Ca-Cl
Cl/Br	> SW	> SW	> SW	> SW	< SW	< SW
Ca % meq	<10	< 10	<10	10 - 20	> 20	>20
TDS (mg/L)	<40,000	40,000- 300,000	> 300,000	200,000 - 300,000	> 300,000	200,000 - 300,000

Table 6.1. Summary of water and mixing group classifications.

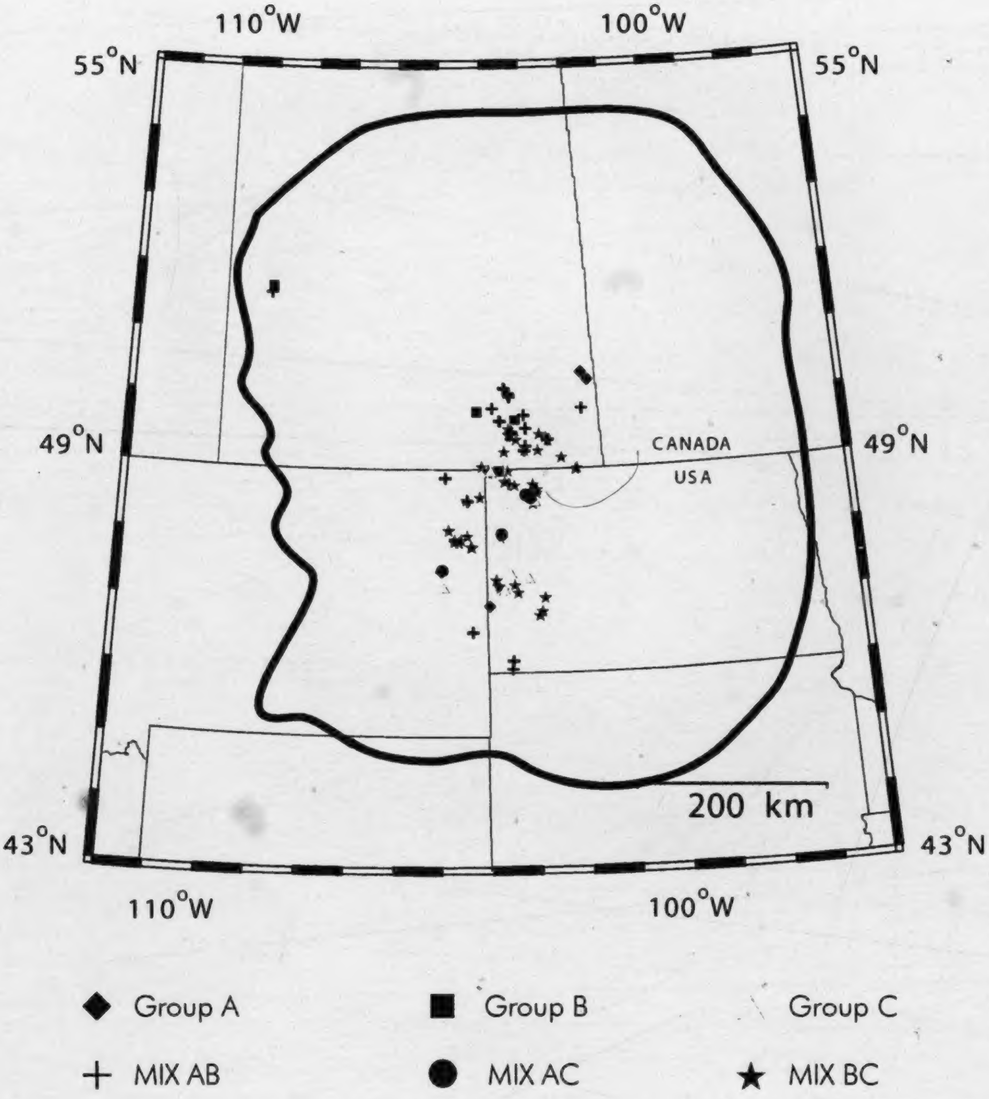
110°W
100°W
55°N
55°N
49°N
CANADA
USA
49°N
200 km
43°N
43°N
110°W
100°W
◆ Group A
■ Group B
Group C
+ MIX AB
● MIX AC
★ MIX BC

Figure 6.20. Spatial distributions of water groups and mixing zones for all formations within the Williston Basin Study Area boundary.

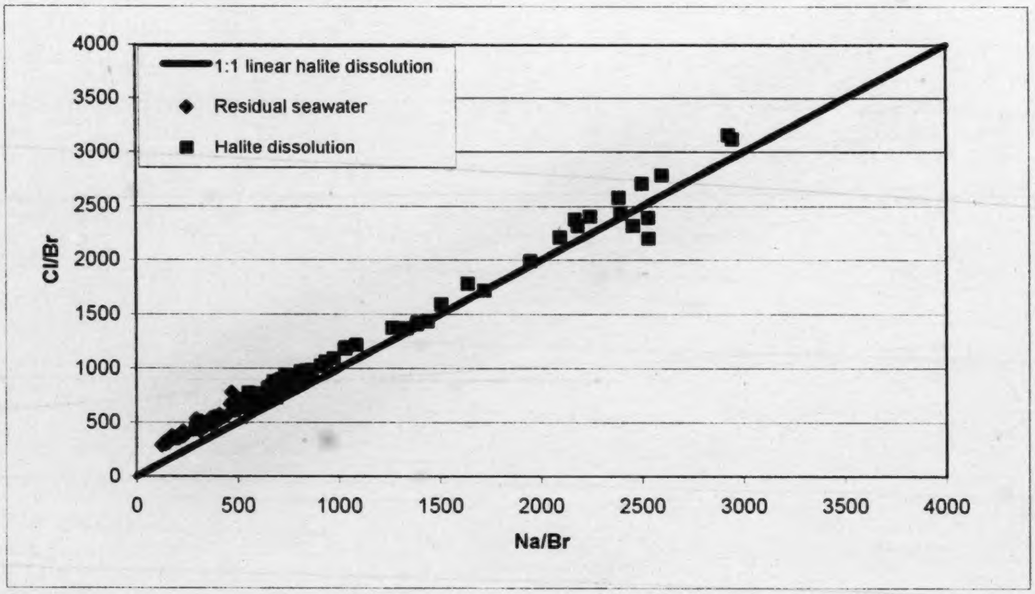

Figure 6.21. Cl/Br vs. Na/Br molar ratios for all pre-Mississippian samples.

CHAPTER 7

7. CONCLUSIONS

Analysis of new wellhead geochemical data from the pre-Mississippian formations of the Williston Basin has resulted in the following conclusions.

1) Major ion chemistry and Na-Cl-Br systematics indicate the presence of residual evaporated seawater in the basin center and refute the widely accepted idea that halite dissolution has solely generated Williston Basin brines.

2) These residual seawater-derived brines have undergone dolomitization, albitization and anhydrite precipitation, reflected by high calcium concentrations and low magnesium and sulphate concentrations.

3) Brines surrounding the residual seawater slug to the north and east do originate from the dissolution of salt. These brines form a Na-Cl dominated transition zone between meteoric water entering in the southwest and halite saturated waters in the north.

4) Brackish water in the southwest represents fairly recent meteoric infiltration as indicated by the lack of extensive interaction. Brackish water compositions seem to be controlled chiefly by the composition of the infiltrating water, and the lithology of the aquifer through which they have passed.

5) Mixing zones exist among residual seawater, Na-Cl dominated water and brackish meteoric water forming intermediary compositions (Figure 7.1).

6) The presence of a seawater-derived brine slug in the basin center today, suggests paleo-fluid flow was relatively minimal and limited to localized, episodic events of short duration. High calcium concentrations in the residual

brine slug indicate the remnant brine acted as a dolomitizing fluid signifying early fluid refluxing or vertical migration during deposition and burial likely occurred.

7) The present-day flow system originated during Laramide uplift as meteoric water moved into the basin, very slowly eroding and flushing the relatively stagnant seawater through mixing. The large density contrast prohibited the meteoric waters from invading the evaporative seawater area rapidly, and except for a small amount of mixing, fresher water was diverted around the slug to the north, south and into the overlying formations, instigating dissolution of the Prairie Evaporite. Evidence of this continuing process can be observed in the inactive, residual remnant brine in the basin center (Figure 7.1).

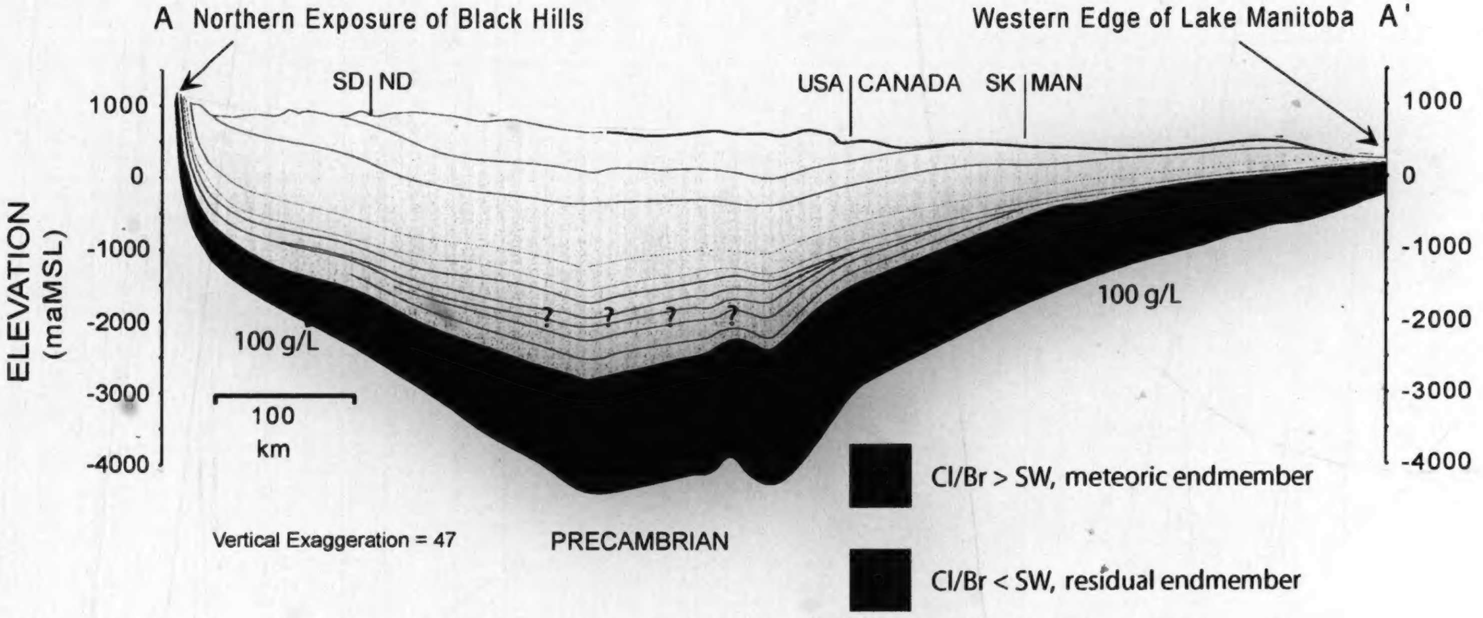
A Northern Exposure of Black Hills
Western Edge of Lake Manitoba A'
SD | ND
USA | CANADA
SK | MAN
ELEVATION (maMSL)
1000
0
-1000
-2000
-3000
-4000
100 g/L
100 g/L
?
100 km
Vertical Exaggeration = 47
PRECAMBRIAN
Cl/Br > SW, meteoric endmember
Cl/Br < SW, residual endmember

Figure 7.1. Schematic drawing of new flow model and brine composition. Based on data collected in this study. A greater degree of mixing is indicated in aquifers highlighted with a deeper shade. Estimated by comparison with Chi and Savard (1997). 100 g/L contour approximately represents the updip limit of TDS = 100 g/L. Brine compositions not evaluated above the Bakken Formation.

REFERENCES

Bachu, S. and Hitchon, B., 1996. Regional-scale flow of formation waters in the Williston Basin. AAPG Bulletin, 80(2): 248-264.

Benn, A.A. and Rostron, B.J., 1997. Regional scale groundwater geochemistry of the Lower Paleozoic Formations of the Williston Basin, Canada-USA: Preliminary results. Abstract and poster in: Fifth International Williston Basin Horizontal Well Workshop. Regina, Saskatchewan, April 13-16.

Benn, A.A. and Rostron, B.J., 1998. Regional hydrochemistry of Cambrian to Devonian aquifers in the Williston basin, Canada-USA. In: J.E. Christopher, C.F. Gilboy, D.F. Paterson and S.L. Bend (Editors), Eighth International Williston Basin Symposium. Special Publication. Saskatchewan Geological Society, Regina, pp. 238-246.

Berg, R.R., DeMis, W.D. and Mitsdarffer, A.R., 1994. Hydrodynamic effects on Mission Canyon (Mississippian) oil accumulations, Billings Nose Area, North Dakota. AAPG Bulletin, 78(4): 501-518.

Bernatsky, R., 1998. Hydrogeochemistry of Formation Waters in Southern Saskatchewan. Masters of Science Thesis, University of Regina, Regina, 206 pp.

Bredehoeft, J.D., Neuzil, C.E., Milly, P.C., 1983. Regional Flow in the Dakota Aquifer: A study on the role of confining layers. U.S. Geological Survey Supply Paper, 2237. U.S. Geological Survey, 45 pp.

Brown, D. and Brown, D., 1987. Wrench style deformation and paleostructural influence on sedimentation in and around a cratonic basin. In: M. Longman (Editor), Williston Basin - Anatomy of a cratonic oil province, Rocky Mountain Association of Geologists, pp. 57-70.

Busby, J.F., Kimball, B.A. and Downey, J.S., 1995. Geochemistry of water in aquifers and confining units of the Northern Great Plains in parts of Montana, North Dakota, South Dakota, and Wyoming. U.S. Geological Survey Professional Paper, 1402-F. U.S. Geological Survey, 146 pp.

Carlson, C.G., 1967. Cross-section of Paleozoic rocks of western North Dakota. 34, North Dakota Geological Survey, Grand Forks, North Dakota.

Carlson, C.G. and Eastwood, W.P., 1962. Upper Ordovician and Silurian Rocks of North Dakota. North Dakota Geological Survey Bulletin, pp. 52.

Carpenter, A.B., 1978. Origin and Chemical Evolution of Brines in Sedimenatry Basins. Oklahoma Geological Survey Circular, 79: 60-77.

Chi, G. and Savard, M.M., 1997. Sources of basinal and Mississippi Valley-type mineralizing brines: mixing of evaporated seawater and halite-dissolution brine. Chemical Geology, 143 (3-4): 121-125.

Chipley, D. and Kyser, T.K., 1991. Large scale fluid movement in the Western Canadian Sedimentary Basin as recorded by fluid inclusions in evaporites. In: J.E. Christopher and F.M. Haidl (Editors), Sixth International Williston Basin Symposium. Saskatchewan Geological Society Special Publication. Regina, Saskatchewan Geological Society, Regina, Saskatchewan, pp. 265-269.

Chow, N., 1991. Dolomitization in Middle Devonian platform carbonates, Elm Point Formation, Interlake area , Manitoba. In: J.E. Christopher and F.M. Haidl (Editors), Sixth international Williston Basin symposium. Saskatchewan Geological Society, Regina, SK, pp. 34-39.

Clayton, R.N., Friedman, I., Graf, D.L, Mayeda, T.K., Meents, W.F., Shimp, N.F., 1966. The origin of saline formation waters 1 Isotopic composition. Journal of Geophysical Research, 71(16): 3869-3882.

Collins, A.G., 1967. Geochemistry of Some Tertiary and Cretaceous Age Oil-Bearing Formation Waters. Environmental Science and Technology, 1(9): 725-730.

Connolly, C.A., Walter, L.M., Baadsgaard, H. and Longstaffe, F.J., 1990. Origin and evolution of formation waters, Alberta Basin, Western Canada Sedimentary Basin. I. Chemistry. Applied Geochemistry, 5: 375-395.

Darton, N.H., 1906. The Great Plains of the central United States. Scottish Geographical Magazine., 32: 9-18.

Davisson, M.L. and Criss, R.E., 1996. Na-Ca-Cl relations in basinal fluids. Geochimica et Cosmochimica Acta, 60(15): 2743-2752.

Downey, J.S., 1982. Geohydrology of the Madison and associated aquifers in parts of Montana, North Dakota, South Dakota, and Wyoming. Open-File Report - U. S. Geological Survey., 120 pp.

Downey, J.S., 1984. Geohydrology of the Madison and associated aquifers in parts of Montana, North Dakota, South Dakota, and Wyoming. U.S. Geological Survey Professional Paper, 1273-G. U.S. Geological Survey, 47 pp.

Downey, J.S., Busby, J.F. and Dinwiddie, G.A., 1987. Regional aquifers and petroleum in the Williston Basin region of the United States, 1987 Symposium of the Rocky Mountain Association of Geologists, pp. 299-312.

Duke, M.J. and Rostron, B.J., 2002. Determination of bromine, iodine, chloride and sodium in highly saline formation waters by epithermal Neutron Activation Analysis. In press.

Edie, R.W., 1959. Middle Devonian sedimentation and oil possibilities, central Saskatchewan, Canada. AAPG Bulletin, 43(5): 1026-1057.

Fisher, R.S. and Kreitler, C.W., 1987. Origin and evolution of deep-basin brines, Palo Duro Basin, Texas. 166, Bureau of Economic Geology.

Fuller, J.G., 1961. Ordovician and contiguous formations in North Dakota, South Dakota, Montana and adjoining areas of Canada and the United States. Bulletin of the American Association of Petroleum Geologists, 45(8): 1334-1363.

Fuller, J.G. and Porter, J.W., 1962. Cambrian, Ordovician and Silurian formations of the northern Great Plains and their regional connections. Journal of the Alberta Society of Petroleum Geologists, 10(8): 455-485.

Gerhard, L.C. and Anderson, S.B., 1988. Geology of the Williston Basin (United States portion). In: L.L. Sloss (Editor), Sedimentary Cover - North American Craton: U.S. Geological Society of America, pp. 221-241.

Gosnold, W.D., 1990. Heat flow in the Great Plains of the United States. Journal of Geophyscical Research, 95(B1): 353-374.

Haidl, F.M., 1990. Ordovician hydrocarbon reservoirs, Herald and Yeoman Formations (Red River), southeastern Saskatchewan. Summary of Investigations 1990, Saskatchewan Geological Survey: 176-185.

Haidl, F.M., Kreis, L.K. and Dancsok, E.F.R., 1996. New oil discoveries in Ordovician Red River strata, southeastern Saskatchewan. Summary of Investigations, Saskachewan Geological Survey, Miscellaneous Report 96-4: 136-144.

Hannon, N., 1987. Subsurface water flow patterns in the Canadian sector of the Williston Basin, 1987 Symposium of the Rocky Mountain Association of Geologists, pp. 313-321.

Hanor, J.S., 1994. Origin of saline fluids in sedimentary basins. Geofluids: Origin, Migration and Evolution of Fluids in Sedimentary Basins, 78: 151-174.

Hitchon, B. and Friedman, I., 1969. Geochemistry and origin of formation waters in the Western Canada Sedimentary Basin - I. Stable isotopes of hydrogen and oxygen. Geochimica et Cosmochimica Acta, 33: 1321-1349.

Ingebritsen, S.E. and Sanford, W.E., 1998. Groundwater in geologic processes., 1 ed.

Kendall, A.C., 1989. Brine mixing in the middle Devonian of western Canada and its possible significance to regional dolomitization. Sedimentary Geology, 64: 271-285.

Kent, 1960. The evaporites of the Upper Ordovician strata in the northern part of the Williston Basin. Regina : Dept. of Mineral Resources, Petroleum and Natural Gas Branch, Geology Division Publication, 1960.

Kesler, S.E. et al., 1995. Na-Cl-Br systematics of mineralizing brines in Mississippi Valley-type deposits. Geology, 23(7): 641-644.

Kreis, L.K., Gent, M. and Vigrass, L.W., 1991. Subsurface brines in southern Saskatchewan. In: J.E. Christopher and F. Haidl (Editors), Sixth International Williston Basin Symposium. Saskatchewan Geological Society Special Publication, Regina, SK, pp. 283-292.

Laird, W.M., 1952. Geology of the Williston Basin in North Dakota. World Petroleum, 23(1): 42-44.

Land, L.S., 1987. The major ion chemistry of saline brines on sedimentary basins. In: J.R. Banavar, J. Koplik and K.W. Winkler (Editors), Physics and Chemistry of Porous Media II. American Institute of Physics, Ridgefield, CT, pp. 160-179.

Land, L.S. and Macpherson, G.L. 1992. Origin of Saline Formation Waters, Cenozoic Section, Gulf of Mexico Sedimentary Basin. Bulletin of the American Association of Petroleum Geologists, 76(9): 1344-1362.

LeFever, R.D., 1996. Sedimentology and stratigraphy of the Deadwood-Winnipeg Interval (Cambro-Ordovician), Williston Basin. In: M.W. Longman and M.D. Sonnenfeld (Editors), Paleozoic systems of the Rocky Mountain region. Society for Sedimentary Geology, Rocky Mountain Section, United States, pp. 11-28.

LeFever, R.D., 1998. Hydrodynamics of formation waters in the North Dakota Williston Basin. In: J. Christopher, C. Gilboy, D. Paterson and S. Bend (Editors), Eighth international Williston Basin symposium. Saskatchewan Geological Society. Regina, SK, Canada. 1998. PY: 1998, Regina, SK, Canada., pp. 229-237.

Lico, M.S., Kharaka, Y.K., Carothers, W.W. and Wright, V.A., 1982. Methods for collection and analysis of geopressured geothermal and oil field waters. U. S. Geological Survey Water-Supply Paper., 34 pp.

Lisenbee, A.L. and Dewitt, E., 1993. Laramide evolution of the Black Hills Uplift. In: A.W. Snoke, J.R. Steidtmann and S.M. Roberts (Editors), Geology of Wyoming. Memoir - Geological Survey of Wyoming, pp. 375-412.

LoBue, C., 1982. Depositional environments and diagenesis of the Silurian Interlake Formation, Williston Basin, western North Dakota. In: J. Christopher, J. Kaldi, C. Dunn, D. Kent, J. Lorsong (Editors), Fourth International Williston Basin Symposium. Saskatchewan Geological Society. Regina, SK, Canada. 1992. PY: 1992, Regina, SK, Canada, pp. 29-42.

McCaffrey, M.A., Lazar, B. and Holland, H.D., 1987. The Evaporation Path of Seawater and the Coprecipitation of Br- and K+ with Halite. Journal of Sedimentary Petrology, 57(5): 928-937.

Mossop, G. and Shetsen, I.e., 1994. Geological Atlas of the Western Canada Sedimentary Basin, 510 pp.

Paterson, D.F., 1988. Review of regional stratigraphy relationships of the Winnipeg Group (Ordovician), the Deadwood Formation (Cambro-Ordovician) and underlying strata in Saskatchewan. In: L.p. Beck (Editor), Summary of investigations 1988, Saskatchewan Geologic Survey., pp. 224-225.

Perrin, N.A., 1982. Environments of Deposition and Diagenesis of the Winnipegosis Formation (Middle Devonian), Williston Basin, North Dakota. In: J.E. Christopher and J. Kaldi (Editors), Fourth International Williston Basin Symposium. Saskatchewan Geological Society Special Publication. Saskatchewan Geological Society, Regina, Saskatchewan, pp. 51-66.

Peterson, J.A. and MacCary, L.M., 1987. Regional stratigraphy and general petroleum geology, Williston Basin, United States and adjacent area. In: M. Longman (Editor), Williston Basin - Anatomy of a cratonic oil province, Rocky Mountain Association of Geologists, pp. 9-44.

Rostron, B.J., Holmden, C. and Kreis, L.K., 1998. Hydrogen and oxygen isotope compositions of Cambrian to Devonian formation waters, Midale area, Saskatchewan. In: J.E. Christopher, C.F. Gilboy, D.F. Paterson and S.L. Bend (Editors), Eighth International Williston Basin Symposium. Special Publication. Saskatchewan Geological Society, Regina, pp. 267-273.

Rostron, B., Kreis, L.K., Holmden, C., 1999. The Saskatchewan brine sampling program. In: Summary of Investigations 1999, Saskatchewan Geological Survey, Sask. Energy and Mines, Miscellaneous Report 99(4-1): 85-85.

Rostron, B.J., and Holmden, C. 2000. Fingerprinting formation waters using stable isotopes, Midale area, Williston Basin, Canada. Journal of Geochemical Exploration, 69-70: 219-223.

Sandberg, C.A. and Hammond, C.R., 1958. Devonian system in Williston Basin and central Montana. AAPG Bulletin, 42(10): 2293-2334.

Seaber, P.R., 1997. Mapping of hydrostratigraphic units. Abstracts with Programs - Geological Society of America, 29(6): 472.

Sloss, L.L., 1987. Williston in the family of cratonic basins. In: M. Longman (Editor), Williston Basin - Anatomy of a cratonic oil province, Rocky Mountain Associatio of Geologists, pp. 1-8.

Spencer, R.J., 1987. Origin of Ca-Cl brines in Devonian formations, western Canada sedimentary basin. Applied Geochemistry, 2: 373-384.

Stoessell, R.K. and Moore, C.H., 1983. Chemical constraints and origins of four groups of Gulf Coast reservoir fluids. American Association of Petroleum Geologists Bulletin, 67 (6): 896 -906.

Stoessell, R.K. and Carpenter, A.B., 1986. Stoichiometric saturation tests of $NaCl_{1-x}Br_x$ and $KCl_{1-x}Br_x$. Geochimica et Cosmochimica Acta, 50: 1465-1474.

Stueber, A.M. and Walter, L.M., 1994. Glacial recharge and paleohydrologic flow systems in the Illinois basin: Evidence from chemistry of Ordovician carbonate (Galena) formation waters. Geological Society of America Bulletin, 106: 1430-1439.

Stueber, A.M., Saller, A.H. and Ishida, H., 1998. Origin, Migration and Mixing of Brines in the Permian Basin: Geochemical Evidence from the Eastern Central Basin Platform, Texas. American Association of Petroleum Geologists, 82(9): 1652-1672.

Thiede, D.S., 1975. Geological implications of variation in heavy metal content in the elk point evaporite sequence, Saskatchewan, Canada. Masters Thesis, University of Wisconsin-Madison, Madison, Wisconsin, 192 pp.

Tóth, J., 1984. The role of regional gravity flow in the chemical and thermal evolution of groundwater. In: B. Hitchon and E. Wallick (Editors), First Canadian/American conference on hydrogeology; practical applications of groundwater geochemistry, Banff, AB, Canada, pp. 3-39.

Wade, W.J., Hanor, J.S. and Sassen, R., 1989. Controls on H_2S Concentration and Hydrocarbon Destruction in the Eastern Smackover Trend, Transactions - Gulf Coast Association of Geological Societies, pp. 309-320.

Wilson, T.P. and Long, D.T., 1993. Geochemistry and isotope chemistry of Michigan Basin brines: Devonian formations. Applied Geochemistry, 8: 81-100.

Wittrup, M.B. and Kyser, T.K., 1990. The petrogenesis of brines in Devonian potash deposits of western Canada. Chemical Geology, 82: 103-128.

Worden, R.H., 1996. Controls on Halogen Concentrations in Sedimentary Formation Waters, Mineralogical Magazine, pp. 259-274.

Zhu, C. and Hajnal, Z., 1993. Tectonic development of the northern Williston basin: a seismic interpretation of an east-west regional profile. Canadian Journal of Earth Sciences, 30: 621-630.

Appendix A. Well Location, Well Name, Well Operators and Comments.

Sample ID		LSD	Sec	TWP	RNG	Mer	Latitude	Longitude	Well Name	Operator	Comments
UofA 9969	SW	SW	3	157	95		48.446633	102.948017	H. Borstad #1	Texakota	Wellhead
UofA 9948	NE	SE	8	159	95		48.609738	102.975287	Toftness #9-8	Galaxy Oil Co. (Jettison)	Wellhead
UofA 9951	SE	SE	31	26	55		47.959641	104.417040	Finnicum #31-44	Headington Oil	Wellhead
UofA 9979	31	13	22	16	32	1	50.385273	101.820732		Cherryhill Resources	Wellhead
UofA 9978	21	5	15	15	31	1	50.274494	101.680893		Cherryhill Resources	Wellhead
UofA 9977	31	4	15	15	31	1	50.271954	101.681892		Cherryhill Resources	Wellhead
UofA 9821	21	3	11	7	11	2	49.538330	103.400307		Berkley Petroleum	Wellhead, 17/8/98
UofA 9820	41	13	34	6	11	2	49.521324	103.415526		Berkley Petroleum	Wellhead, 17/8/98
UofA 9856	32	11	34	6	11	2	49.518188	103.411423		Berkley Petroleum	Wellhead, Aug 21/98
UofA 9843	NW	SW	8	159	94		48.609378	102.861117	Peterson 13-8	Williston Industrial Supply	Wellhead, Aug 20/98, 3 forks @ 9258
UofS 9723	31	11	34	6	11	2	49.519096	103.412277		Berkley Petroleum	Wellhead, july 28/97
UofA 9986	31	13	3	1	16	2	49.013187	104.073563		Wascana Energy	Wellhead
UofA 9925	NW	SE	9	143	103		47.216209	103.736501	Mesa Federal #1-9	Westport Oil and Gas	Wellhead
UofA 9981	41	5	33	10	32	1	49.877064	101.778427		Northrock Resources	Wellhead
UofS 9727	91	4	33	10	32	1	49.874062	101.778412		Northrock Resources	Wellhead
UofA 9839	1	8	30	7	8	2	49.586559	103.070190		Sceptre Resources	Wellhead, 21/8/98, disposal well 2 miles east
UofS 9616	11	7	3	7	11	2	49.527451	103.413361		Berkley Petroleum	r 1050m
UofS 9714	31	11	35	6	11	2	49.517406	103.388321		Berkley Petroleum	Wellhead
UofS 9732	31	11	35	6	11	2	49.517406	103.388321		Berkley	Wellhead
UofA9842	SE	SW	8	161	99		48.780689	103.566182	Johnson #1	Continental Operating Corp	Tank sample, 1 month old, aug 20/98
UofA 9829	NW	NW	18	163	99		48.950545	103.593376	Pederson 11-18#1	Colt Resources Corp	Wellhead, 19/8/98
UofA 9841	SE	NW	8	161	99		48.788027	103.566838	Johnson 22-8 #1	Eland Energy Corp	Wellhead, aug 20/98
UofA 9995	SE	NE	7	143	100		47.222039	103.396170	MOI Firehole 42-7	Burlington Resources	Wellhead
UofA 9828	SW	NE	14	163	99		48.947282	103.494608	State-Henning 32-14#1	Colt Resources Corp	Wellhead, 19/8/98
UofA 9942	SW	NW	23	142	100		47.105564	103.325994	Anna Osadchuk B-1	Petro Hunt LLC	Wellhead
UofA 9973	SE	SW	22	32	56		48.507100	104.423400	Sunmark Benson #3	Flying J Oil and Gas	Wellhead
UofA 9947	NW	SW	19	159	95		48.580284	103.009738	F.E. McCoy #2	Condor Petroleum	Wellhead
UofA 9926	SE	NE	26	143	103		47.176046	103.690634	Williamson Federal #42-26R	Summit Resources	Wellhead
UofA 9941	SE	NW	13	152	102		47.989253	103.684444	Helgeson-Hoehn #1	Westport Oil and Gas	Wellhead
UofA 9946	SW	SE	5	159	96		48.619942	103.111918	Hansen #5D-3-1	Petro Hunt LLC	Wellhead
UofA 9950	NW	NW	30	159	95		48.573595	103.009807	Mccoy-Koshman #2	Mayson Inc	Wellhead
UofA 9940	NE	NE	9	144	98		47.309711	103.098512	Tarnavsky #3-9-2B	Petro Hunt LLC	Wellhead
UofA 9996	SE	SE	12	145	101		47.388809	103.484374	Edgar Federal 16-12	Burlington Resources	Wellhead
UofA 9949	NE	SW	26	158	95		48.479378	102.920693	Lalim Ives 'A' #1	Amerada Hess	Wellhead
UofA 9953	SW	NE	9	151	102		47.914583	103.740757	Simpson #9-32	Headington Oil	Wellhead
UofA 9952	NE	NE	35	158	95		48.472110	102.909722	n Bohrstad #35-41(thrond lalim	Amerada Hess	Wellhead
UofA 9980	11	4	33	10	32	1	49.874062	101.778397		Northrock Resources	Wellhead
UofS 9711	1	12	30	30	21	3	51.600140	108.953270	Suncor (Danoil Energy Ltd)	Suncor (Danoil Energy Ltd)	Wellhead, 7/1/1997
UofA 9840	SW	NE	30	163	100		48.918436	103.711772	Mosser 32-30 #1	Colt Resources Corp	Wellhead, aug 19/98
UofA 9966	NE	NE	11	32	58		48.545800	104.129000	Cenex Sorenson #1-11	Basic Earth Science	Wellhead
UofA 00201	NE	SE	33	20	53		47.448430	104.966966	McGarty 1-33-3B	Berco Resources Ltd	wellhead, 12/9/00
UofA 9957	NE	NE	35	25	54		47.876400	104.710300	BN VAIRA B-1	Flying J Oil and Gas	Wellhead

Appendix A. Well Location, Well Name, Well Operators and Comments.

Sample ID		LSD	Sec	TWP	RNG	Mer	Latitude	Longitude	Well Name	Operator	Comments
UofA 9956	SE	NE	23	25	54		47.903587	104.696000	BN #8-23	Flying J Oil and Gas	Wellhead
UofA 9967	NW	SE	27	36	52		48.843049	104.894667	Loucks #33-27	Summit Resources	Wellhead
UofA 9971	NW	NE	27	32	56		48.488789	104.403333	Land Tronson #1	Flying J Oil and Gas	Wellhead
UofA 9991	1	16	26	5	5	2	49.418842	102.570282		Berkley Petroleum	Wellhead
UofA 9993	11	5	26	5	5	2	49.410427	102.585716		Berkley Petroleum	Wellhead
UofA 9975	11	9	18	7	11	2	49.821278	104.181145	4A9 Re-entry	Berkley Petroleum	Wellhead
UofA 9982	31	4	30	4	8	2	49.321461	103.081352		Anderson Exploration	Wellhead
UofS 9731	31	8	35	3	9	2	49.252655	103.108696		Stampeder	Wellhead
UofA 9990	11	7	26	5	5	2	49.410992	102.574883		Berkley Petroleum	Wellhead
UofS 9731	31	8	35	3	9	2	49.252655	103.108696		Stampeder	Wellhead
UofA 9983	21	16	13	4	9	2	49.301960	103.087730		Anderson Exploration	Wellhead
UofA 9848	11	7	26	5	5	2	49.410992	102.574883		Berkley Petroleum	Wellhead, Aug 21/98
UofS 9725	32	12	31	3	6	2	49.255241	103.292389		Cavell	Wellhead
UofS 9728	31	10	24	2	3	2	49.142189	102.283730		Duce	Wellhead
UofS 9726	21	15	23	5	5	2	49.403923	102.576569		Berkley Petroleum	Wellhead
UofA 9992	21	15	23	5	5	2	49.403923	102.576569		Berkley Petroleum	Wellhead
UofA 9846	SW	NW	36	161	98		48.729322	103.352540	Wildrose #36-5	Petro Hunt Corp	Treater tank, 20/8/98
UofA 9845	NE	SE	25	161	95		48.740368	102.942189	Kjelshus#1		Wellhead, Aug 20/98
UofA 9858	92	2	32	8	10	2	49.684620	103.324142	4b7-32-8b2-32 Hz	Berkley Petroleum	Wellhead, Aug 21/98
UofA 9936	NW	SE	17	141	95		47.028692	102.742773	S.E. Russian Creek #33-17	Armstrong Operating	Wellhead
UofA 9961	NE	NE	31	24	58		47.792100	104.319700	Allison #1	Flying J Oil and Gas	Wellhead
UofA 9935	NW	NW	33	139	96		46.815203	102.806281	Kostelecky #11-33	Wesco Operating	Wellhead
UofA 9934	NE	NW	24	138	97		46.758286	102.865124	Heidt #24-1	Armstrong Operating	Wellhead
UofA 9955	SE	SW	20	160	94		48.664943	102.856115	Spangrud #1	Petro Hunt LLC	Wellhead
UofA 9937	NE	NE	31	140	105		46.901836	103.969572	Mertz #41-31	Best Pacific Resources	Wellhead
UofA 00200	NE	SE	4	19	53		47.430493	104.988779	Raisl 1-4-3C	Berco Resources Ltd	wellhead, 4/9/00
UofA 9963	NW	NE	25	161	99		48.749035	103.471523	Plumer Lundquist #25-2	Lyco Energy Corp	Wellhead
UofA 9970	NE	SE	6	16	54		47.174888	104.940667	Elpel #2	Berco Resources Ltd	Wellhead
UofA 9851	1	14	36	8	13	2	49.695293	103.645561		Berkley Petroleum	Wellhead, Aug 21/98
UofA 9852	91	1	2	9	13	2	49.699303	103.657364	4d7-2-3d1-2	Berkley Petroleum	Wellhead, Aug 21/98, split & filtered in lab later
UofA 9850	92	2	9	6	5	2	49.455532	102.611972		Upton Resources Ltd.	Wellhead, Aug 21/98
UofA 9836	11	15	20	7	11	2	49.577914	103.458939		Tarragon Oil and Gas	Wellhead, 20/8/98
UofA 9832	11	1	29	6	11	2	49.495598	103.443825		Berkley Petroleum	Wellhead, 19/8/98
UofA 9847	91	9	29	6	6	2	49.503769	102.769981	3d8-29-3d9-29	Shell	Wellhead, Aug 21/98
UofS 9720	11	15	34	6	11	2	49.520481	103.402122		Berkley Petroleum	Wellhead
UofS 9716	41	10	29	6	11	2	49.504410	103.448776		Berkley Petroleum	Wellhead
UofS 9719	11	7	3	7	11	2	49.527451	103.413361		Berkley Petroleum	Wellhead
UofS 9715	41	4	35	6	11	2	49.510906	103.392258		Berkley Petroleum	Wellhead
UofA 9825	21	4	28	6	11	2	49.494781	103.439262		Berkley Petroleum	Wellhead, 18/8/98
UofA 9833	91	12	12	6	11	2	49.459076	103.370735	8b2-13/4c12-12	Berkely Petroleum	Wellhead, 19/8/98, actually 91/12-12-6-11 HZ, 8b2-13-4c12-12
UofA 9831	31	7	15	6	11	2	49.470039	103.402618	DD 4A7-15/1C7-15	Berkley Petroleum	Wellhead, 19/8/98
UofA 9830	31	3	14	6	11	2	49.466760	103.387642		Berkley Petroleum	Wellhead, 19/8/98

Appendix A. Well Location, Well Name, Well Operators and Comments.

Sample ID		LSD	Sec	TWP	RNG	Mer	Latitude	Longitude	Well Name	Operator	Comments
UofA 9835	SE	SE	19	163	101		48.925473	103.840115	Wehrman #1-19	Colt Resources Corp	Wellhead, 19/8/98, filtered 20/8/98
UofA 9838	91	11	28	3	12	2	49.240749	103.566925	4d4-28-11-28	Wascana Energy Inc	Wellhead, 21/8/98, deviated hole (4-28, maybe 6-28 = surface location)
UofA 9962	SW	SE	35	27	53		48.044843	104.826667	Gifford #34-35	Panterra/Nance Pet.	Wellhead
UofA 9959	NE	NW	21	25	55		47.899103	104.560000	Bidegaray #1-21-21	Ocean Energy	Wellhead
UofA 9958	NW	SW	34	25	55		47.867719	104.606667	Kemp #1-34	Ocean Energy	Wellhead
UofA 0093	41	1	27	14	12	2	50.195808	103.555664		Trilink	
UofA 0094	31	16	14	14	12	2	50.177029	103.533920		Trilink	
UofA 0092	21	6	28	13	11	2	50.110104	103.455482		Trilink	
UofA 0090	21	8	21	13	11	2	50.095932	103.442558		Trilink	
UofA 9930	SE	NE	22	23	5		45.948500	103.481400	Otterness #41-22	Luff Exploration	Wellhead
UofA 9987	21	5	11	11	14	2	49.891533	103.824425		Husky Oil	Wellhead
UofA 0091	11	6	10	13	11	2	50.065613	103.429390		Trilink	
UofA 00189	91	8	16	6	11	2	49.470123	103.421448	1d7-16/3a8-6-11W2, sub	Berkley Petroleum	
UofA 00192	92	8	16	6	11	2	49.470104	103.421410	3A9-16/1B8-16, submersible	Berkley Petroleum	Wellhead
UofS 9729	21	15	28	5	10	2	49.418600	103.295799		Cavell	Wellhead
UofA 9927	NW	NE	6	142	102		47.150468	103.652171	9210 JVP Federal DM#1	BTA	Wellhead
UofA 9931	NW	NE	20	130	102		46.073321	103.459158	M.L. Peters #1-20	Luff Exploration	Wellhead
UofA 9994	NE	NE	25	9	58		46.502252	104.311685	Monarch 41-25HR	Burlington Resources	Wellhead
UofA 9939	SE	SE	12	144	104		47.298929	103.793683	Federal/Hall Bros. #1-12	Wesco Operating	Wellhead
UofA 9964	SE	NE	28	163	102		48.918224	103.929994	Gjesdal 28 #1	Omimex Petroleum	Wellhead
UofA 9965	NE	SE	9	163	102		48.958039	103.927674	Drawbond 9 #3	Omimex Petroleum	Wellhead
UofA 9834	SW	SW	24	163	102		48.925803	103.877541	Wehrman 14-24 #1	Colt Resources Corp	Wellhead?, 19/8/98, filtered @UofA
UofA 9928	SW	SE	4	142	102		47.140136	103.613007	Cenex Federal Twin #34-4	Summit Resources	Wellhead
UofA 9960	C	SW	29	24	58		47.798500	104.310300	Dynneson 1-29 A-1	Flying J Oil and Gas	Wellhead
UofA 9972	NE	NW	27	32	56		48.501700	104.423100	Land Tronson #4	Flying J Oil and Gas	Wellhead
UofA 9989	32	7C	2	10	9	2	49.786762	103.110489		Founders Energy	Wellhead
UofA 9810	42	4	35	6	11	2	49.510319	103.392258	4A-35T	Berkley et al	Wellhead, 4-35T, sample collected by Berkley, June 11/98
UofA 9824	11	16	20	6	11	2	49.490215	103.442787		Berkley Petroleum	Wellhead, 18/8/98
UofA 9976	31	8	16	6	11	2	49.470688	103.423599		Berkley Petroleum	
UofS 9609	2	12	21	31	21	3	51.672020	108.929581		Annuity et al	Wellhead, 8/1/1996
UofA 9822	SW	NE	3	163	87		48.976666	101.939347	Mott #32X-3	Geo Resources Inc	Storage tank, 18/8/98, well making >90% oil, tank emptied recently
UofA 9823	NE	SW	9	163	87		48.955811	101.970479	E-M Larson #9-11R	Eagle Operating Inc	Storage tank, 18/8/98, well shut in ~5 days prior,

Appendix B. Neutron Activation Analysis (NAA) of Highly Saline Brines.

Theory

The University of Alberta *SLOWPOKE* Reactor Facility has a low power, research nuclear reactor and several computerized, highly sensitive radiation detectors. Samples for analysis are made radioactive by irradiating them in the reactor. Subsequent measurement of this induced radioactivity, specifically the gamma-rays emitted by the samples, affords the means of elemental analysis: the energies of the gamma-rays are used to identify the elements present, and the intensity or number gamma-rays detected used to determine the concentration of elements. Using this method of analysis (referred to as Neutron Activation Analysis, or NAA) the *SLOWPOKE* Facility can analyze samples for a number of elements simultaneously, with sensitivity in many instances at the part per million (ppm) to part per billion (ppb) level. The method requires minimal sample preparation and is non-destructive which permits retention of valuable samples or their reuse for additional analysis once the induced radioactivity decays away.

The neutrons produced by the nuclear reactor show a range of energies subdivided into three main groups, namely: fast neutrons, intermediate (or epithermal) neutrons, and slow (or thermal) neutrons. Activation of the components of a sample is largely accomplished by the more abundant low energy thermal neutrons. This is especially so with elements such as Na and Cl, the two major ions in many brines. Unfortunately, activation of these two elements produces a significant background component which makes it difficult to determine trace levels of elements such as Br and I in the presence of macro quantities of Na and Cl because of poor signal-to-background ratios. Fortunately, both Br and I, in addition to being activated by thermal neutrons, are activated to a large degree by the intermediate or epithermal neutrons (unlike Na and Cl). By filtering out most of the thermal neutrons in the neutron flux (thus permitting the epithermal (and fast) neutrons to activate a sample) one can preferentially enhance the activation of Br and I over Na and Cl, for example. In this manner it is possible to quantify μg/mL levels of I and Br in brines with Cl/I and Cl/Br ratios > 20,000 and 400, respectively, while simultaneously quantifying the Na and Cl using the residual thermal neutron flux. In this work boron-carbide (B_4C) was used as the neutron filter or shield. This variation of NAA is referred to as Epithermal Neutron Activation Analysis (ENAA) because of the dominant usage of the epithermal neutrons.

Experimental

Aliquots of the brine samples measuring 250 μL were pipetted into polyethylene micro-centrifuge tubes previously washed in nitric-acid and rinsed in deionized water and hermetically sealed. Individual samples were placed in the central cavity of a B_4C shield and irradiated at a nominal thermal neutron flux of 1×10^{11} n cm^{-2} s^{-1} in the University of Alberta SLOWPOKE Nuclear Reactor for 360 seconds (6 mins). Following irradiation the samples were permitted to decay for 10-15 minutes, during which time the irradiated sample was removed from the irradiation shield and placed in front of a gamma-ray detector at a sample-to-detector distance of 5 mm. Following the timed decay period each sample was counted for 360 seconds (6 mins) using a 41% hyperpure Ge detector housed in a 10 cm lead cave[1]. Relevant nuclear data for the radionuclides used to quantify the Br, I, Cl, Na (± Sr) contents of the brines are listed in Table 1.

Table 1. Selected nuclear data for Br, I, Cl, Na and Sr.

Element	Radionuclide	Half-life	Principal γ-ray(s)
Br	^{80}Br	17.68 min	616.3, 665.8
I	^{128}I	24.99 min	442.9
Cl	^{38}Cl	37.21 min	1642.4, 2167.5
Na	^{24}Na	14.959 hrs	1368.6
Sr	^{87m}Sr	2.805 hrs	388.4

Elemental standards were prepared from pure (*i.e.*, > 99.999% purity) salts of KI, KCl, KBr, and NaCl, and in the case of Sr from commercially available atomic absorption standards (*e.g.*, SPEX). Analysis was performed by the semi-absolute method of activation analysis (Bergerioux, *et al.*, 1979).

In NAA the detection limit for an element is dependent on the background component (Currie, 1968) and therefore varies with sample composition. In Table 2 the detection limits for Br, I, Cl, Na and Sr are listed for three brines showing a wide range of Na+Cl content.

Table 2. Detection limits for Br, I, Cl, Na and Sr in brines of differing Na+Cl content (250 μL brine sample, nominal flux 1 x 10^{11} n cm^{-2} s^{-1}).

Element	Sodium + Chloride content		
	300 mg/mL	100 mg/mL	30 mg/mL
Br (μg/mL)	6	3.2	1.7
I (μg/mL)	1.45	0.83	0.59
Cl (mg/mL)	1.9	1.0	0.47
Na (mg/mL)	1.1	0.63	0.31
Sr (μg/mL)	165	80	57

As can be seen from Table 2 the detection limits increase with increasing Na and Cl content. Fortunately, however, the trace elements Br and I invariably increase with increasing TDS content too. For all of the brines analyzed to date in this study Br and I have not been below the detection limits. In instances where this might be the case increasing the neutron flux from 1 to 5 x 10^{11} n cm^{-2} s^{-1} would result in a decrease in the detection limits listed in Table 2 by a factor of 0.45, thus the detection limit for I in the most dilute of the three brines listed in Table 2 would be 0.266 µg/L (ppm) or 266 µg/L (ppb).

---

[1] Initial analyses were performed with a 20 % hyperpure Ge detector but for increased sensitivity a 41% efficient detector was utilized for the majority of the analyses.

Comparison of the Sr concentration of a number of brines determined by ENAA with those determined by ICP-AES from a commercial laboratory showed very good agreement over a wide concentration range with a correlation coefficient, r = 0.979.

References

Currie, L.A. (1968) Limits for qualitative detection and quantitative determination – application to radiochemistry. *Anal. Chem.*, **40**, 586-593.

Bergerioux, C., Kennedy, G., and Zikovsky, L. (1979) Use of the semi-absolute method in neutron activation analysis. *J. Radioanal. Chem.*, **50**, 229-234.

Appendix C. Densities, Temperature, Depths and Classification Data.

Sample ID	Formation	Depth	Temp	pH	Density	Na/Br	Cl/Br	GROUP by Ca
UofA 9969	Bakken	2942.5	99	6.10	1.1951	503	612	MIX BC
UofA 9948	Bakken	2822.1	107	6.01	1.1957	369	478	MIX BC
UofA 9951	Bakken	2978.2	98	5.74	1.2110	385	557	MIX BC
UofA 9979	Bakken	711.0	38	7.12	1.0214	2457	2318	GROUP A
UofA 9978	Bakken	716.0	38	7.39	1.0251	2533	2395	GROUP A
UofA 9977	Bakken	724.3	34	7.25	1.0250	2533	2198	GROUP A
UofA 9821	Bakken	1702.5	71	nd	nd	1334	1373	MIX AB
UofA 9820	Bakken	1718.0	71	nd	nd	1390	1424	MIX AB
UofA 9856	Bakken	1719.5	71	nd	nd	1439	1439	MIX AB
UofA 9843	Bakken, 3 Forks	2809.3	98	6.06	nd	331	456	MIX BC
UofS 9723	Bakken	1719.0	71	6.42	1.1600	1327	1370	MIX AB
UofA 9986	Birdbear	2407.0	92	6.14	1.12-1.19	555	645	MIX BC
UofA 9925	Birdbear	3218.1	116	6.01	1.1976	385	492	MIX BC
UofA 9981	Birdbear	1078.3	42	6.83	1.12-1.19	1720	1717	MIX AB
UofS 9727	Birdbear	1078.3	42	6.35	1.1380	1507	1594	MIX AB
UofA 9839	Birdbear	1676.2	69	nd	nd	826	908	MIX AB
UofS 9616	Birdbear	2565.5	75	nd	nd	910	1026	MIX AB
UofS 9714	Birdbear	1790.0	75	6.00	1.1840	669	781	MIX BC
UofS 9732	Birdbear	1790.0	75	nd	nd	723	865	MIX BC
UofA 9842	Duperow	2808.4	88	5.58	1.9013	486	608	MIX BC
UofA 9829	Duperow	2549.3	94	5.82	1.1940	445	564	MIX BC
UofA 9841	Duperow	2800.2	88	5.59	1.1976	431	551	MIX AC
UofA 9995	Duperow	3458.7	127	nd	nd	310	445	MIX BC
UofA 9828	Duperow	2568.5	88	5.34	nd	400	543	MIX BC
UofA 9942	Duperow	3445.9	129	6.27	1.1949	240	387	MIX BC
UofA 9973	Duperow	2860.5	104	6.25	1.2068	224	369	MIX BC
UofA 9947	Duperow	3091.0	112	6.13	1.12-1.19	173	373	MIX AC
UofA 9926	Duperow	3373.1	110	5.72	1.2200	209	353	MIX BC
UofA 9941	Duperow	3488.1	119	5.87	1.12-1.19	143	299	MIX AC
UofA 9946	Duperow	3087.0	113	5.79	1.2015	146	326	MIX AC
UofA 9950	Duperow	3093.4	111	5.79	1.2015	175	375	MIX AC

Appendix C. Densities, Temperature, Depths and Classification Data.

Sample ID	Formation	Depth	Temp	pH	Density	Na/Br	Cl/Br	GROUP by Ca
UofA 9940	Duperow	3489.0	117	5.65	1.2360	156	310	GROUP B
UofA 9996	Duperow	3410.0	126	nd	nd	150	315	GROUP C
UofA 9949	Duperow	3090.1	117	5.28	1.2403	138	312	GROUP C
UofA 9953	Duperow	3483.6	119	5.19	1.2429	128	300	GROUP C
UofA 9952	Duperow	3092.5	120	5.25	1.2461	125	289	GROUP C
UofA 9980	Duperow	1082.0	42	6.81	1.12-1.19	1385	1410	MIX AB
UofS 9711	Duperow	1111.5	40	nd	nd	864	988	MIX AB
UofA 9840	Duperow	2616.4	91	5.66	1.2071	623	692	GROUP C
UofA 9966	Duperow+Nisku	2848.7	87	5.75	1.2006	341	461	MIX BC
UofA 00201	Dawson Bay	3130	109	nd	nd	280	435	MIX AC
UofA 9957	Dawson Bay	3290.2	107	5.97	1.1949	314	423	MIX BC
UofA 9956	Dawson Bay	3218.1	107	5.99	1.1936	318	435	MIX BC
UofA 9967	Winnipegosis	2713	87	6.94	1.1170	4279	4319	MIX AB
UofA 9971	Winnipegosis	3119.6	109	6.45	1.12-1.19	2948	3119	MIX AB
UofA 9991	Winnipegosis	2191.0	81	6.50	1.12-1.19	2395	2434	MIX AB
UofA 9993	Winnipegosis	2199.8	82	6.51	1.12-1.19	1640	1783	MIX AB
UofA 9975	Winnipegosis	2251.5	81	6.69	1.1990	864	972	GROUP B
UofA 9982	Winnipegosis	2408.8	100	6.36	1.12-1.19	759	852	MIX AB
UofS 9731	Winnipegosis	2465.0	100	6.20	nd	820	963	MIX AB
UofA 9990	Winnipegosis	2196.0	81	6.28	1.1952	935	1062	MIX BC
UofS 9731	Winnipegosis	2465.0	100	6.20	nd	619	724	MIX BC
UofA 9983	Winnipegosis	2424.8	97	6.24	1.2084	738	842	MIX BC
UofA 9848	Winnipegosis	2196.0	81	5.82	1.1949	837	982	MIX BC
UofS 9725	Winnipegosis	2368.2	89	5.94	nd	830	947	MIX BC
UofS 9728	Winnipegosis	2309.5	82	5.85	nd	718	907	MIX BC
UofS 9726	Winnipegosis	2195.0	81	5.56	1.2380	736	942	MIX BC
UofA 9992	Winnipegosis	2195.0	81	6.08	1.2053	738	898	MIX BC
UofA 9846	Winnipegosis	3193.4	104	6.05	nd	553	772	MIX BC
UofA 9845	Winnipegosis	3274.8	104	5.78	1.1656	469	765	MIX BC
UofA 9858	Winnipegosis	2085.0	75	6.08	1.1901	1035	1197	GROUP B
UofA 9936	Interlake	3493.8	113	6.36	1.12-1.90	410	542	MIX BC

Appendix C. Densities, Temperature, Depths and Classification Data.

Sample ID	Formation	Depth	Temp	pH	Density	Na/Br	Cl/Br	GROUP by Ca
UofA 9961	Interlake	3538.7	112	5.85	1.2102	419	553	MIX BC
UofA 9935	Interlake	3382.8	127	6.01	1.12-1.19	369	487	MIX BC
UofA 9934	Interlake	3337.4	128	5.79	1.1992	294	439	MIX BC
UofA 9955	Interlake	3669.5	122	nd	nd	371	529	MIX BC
UofA 9937	Interlake	3254.7	117	7.11	1.0161	565	660	GROUP A
UofA 00200	Interlake	3218.4	112	nd	nd	552	656	MIX AB
UofA 9963	Interlake	3186.4	107	6.38	1.12-1.19	2183	2316	MIX AB
UofA 9970	Interlake	2859.3	89	5.33	1.2321	230	422	MIX BC
UofA 9851	Yeoman	2448.5	87	6.03	1.1777	974	1093	MIX AB
UofA 9852	Yeoman	2441.0	87	nd	nd	1084	1220	MIX AB
UofA 9850	Yeoman	2496.8	81	6.09	1.2139	658	787	MIX BC
UofA 9836	Yeoman	2563.3	92	nd	nd	696	824	MIX BC
UofA 9832	Yeoman	2581.0	92	nd	nd	761	937	MIX BC
UofA 9847	Yeoman	2480.5	81	6.06	1.1936	693	830	MIX BC
UofS 9720	Yeoman	2577.5	92	5.80	1.1840	710	889	MIX BC
UofS 9716	Yeoman	2601.0	92	5.90	1.1900	680	844	MIX BC
UofS 9719	Yeoman	2575.0	92	6.19	1.1840	742	924	MIX BC
UofS 9715	Yeoman	2582.5	92	6.08	1.1750	704	890	MIX BC
UofA 9825	Yeoman	2602.5	92	5.48	nd	649	806	MIX BC
UofA 9833	Yeoman	2575.0	92	nd	nd	603	760	MIX BC
UofA 9831	Yeoman	2635.5	92	nd	nd	669	842	MIX BC
UofA 9830	Yeoman	2623.0	92	nd	nd	583	746	MIX BC
UofA 9838	Yeoman	2850.0	95	nd	nd	589	765	MIX BC
UofA 9962	Red River	3337.6	112	5.86	1.12-1.19	404	563	MIX BC
UofA 9835	Red River	3318.7	107	nd	nd	408	575	MIX BC
UofA 9959	Red River	3584.8	122	5.67	1.2110	371	530	MIX BC
UofA 9958	Red River	3609.4	123	5.77	1.2120	372	538	MIX BC
UofA 0093	Red River	2120.5	73	6.76	nd	2929	3162	MIX AB
UofA 0094	Red River	2118.5	71	6.69	nd	2387	2581	MIX AB
UofA 0092	Red River	2157.5	72	6.72	nd	2599	2782	MIX AB
UofA 0090	Red River	2150.0	72	6.70	nd	2500	2707	MIX AB

Appendix C. Densities, Temperature, Depths and Classification Data.

Sample ID	Formation	Depth	Temp	pH	Density	Na/Br	Cl/Br	GROUP by Ca
UofA 9930	Red River	2813.3	123	6.53	1.0915	764	821	MIX AB
UofA 9987	Red River	2293.5	75	6.59	1.12-1.19	2245	2406	MIX AB
UofA 0091	Red River	2173.0	72	6.64	nd	2170	2376	MIX AB
UofA 00189	Red River	2600.0	92	nd	nd	811	970	MIX BC
UofA 00192	Red River	2600.0	92	nd	nd	678	885	MIX BC
UofS 9729	Red River	2727.0	95	5.78	1.1950	462	672	MIX BC
UofA 9927	Red River A,B,C,D	3769.9	129	5.91	1.1932	219	404	MIX BC
UofA 9931	Red River B	2899.3	102	6.93	1.0659	691	731	MIX AB
UofA 9994	Red River 'B'	2824.9	106			561	628	MIX AB
UofA 9939	Red River B,C,D	3861.1	123	5.46	1.12-1.19	230	373	MIX BC
UofA 9964	Red River C	3259.8	97	6.43	1.1908	292	487	MIX BC
UofA 9965	Red River C	3215.9	98	5.86	1.2161	321	511	MIX BC
UofA 9834	Red River 'C'	3254.2	107	nd	nd	295	531	GROUP C
UofA 9928	Red River D	3855.7	126	5.80	1.2226	196	349	GROUP C
UofA 9960	Red River	3828.3	114	5.88	1.2073	409	523	MIX BC
UofA 9972	Red River	3389.4	109	5.68	1.2213	366	542	MIX BC
UofA 9976	Red River	2600.0	92	6.46	1.1901	652	822	MIX BC
UofA 9989	Winnipeg	2416.5	88	6.36	1.12-1.19	1948	1990	MIX AB
UofA 9810	Winnipeg	2694.5	95	nd	nd	1265	1378	MIX AB
UofA 9824	Winnipeg	2700.5	95	nd	nd	1028	1182	MIX BC
UofS 9609	Deadwood	2037.8	69	nd	nd	2094	2210	GROUP B
UofA 9822	Deadwood	2794.3	90	5.20	nd	516	717	MIX BC
UofA 9823	Deadwood	2918.2	94	5.27	1.2130	475	697	MIX BC

Appendix D. Minor Elements: results in mg/L.

Sample ID	Al	Sb	As	Ba	Be	Bi	Cd	Cr	Co	Cu	Fe	Pb
UofA 9969	6.80	<1.2	<2	1.13	<0.1	<2	<0.1	<0.20	0.45	<0.3	4.20	<0.5
UofA 9948	4.20	<1.2	<2	5.20	<0.1	<2	<0.1	<0.20	0.50	<0.3	99.00	<0.5
UofA 9951	<2	<1	<2	33.30	<0.1	<2	<0.1	<0.2	0.55	0.33	45.50	<0.5
UofA 9979	7.20	<1	<2	0.75	<0.1	<2	<0.1	<0.2	0.25	<0.3	<0.8	<0.5
UofA 9978	6.90	<1	<2	<0.05	<0.1	<2	<0.1	<0.2	0.18	<0.3	<0.8	0.98
UofA 9977	8.30	<1	<2	<0.05	<0.1	<2	<0.1	<0.2	<0.2	<0.3	0.78	<0.5
UofA 9821	0.78	0.15	0.06	0.12	0.01	<0.007	0.01	<0.0008	0.16	<0.001	6.39	0.24
UofA 9820	1.04	0.05	<0.01	0.62	<0.0005	<0.007	0.01	<0.0008	0.15	<0.001	88.80	0.08
UofA 9856	0.54	<0.005	<0.01	0.63	<0.0005	<0.007	0.01	<0.0008	0.16	0.02	59.10	0.10
UofA 9843	0.36	0.13	0.05	19.80	<0.0005	<0.007	0.01	<0.0008	0.13	0.21	39.20	0.26
UofS 9723	0.71	0.15	<0.01	0.40	<0.0005	<0.007	<0.0005	<0.0008	0.15	<0.001	1.54	0.15
UofA 9986	11.00	<1	<2	5.60	<0.1	<2	<0.1	<0.20	0.57	<0.3	23.00	0.68
UofA 9925	4.30	<1	<2	15.70	<0.1	2.50	<0.1	<0.2	0.65	<0.3	24.60	1.40
UofA 9981	9.60	<1	<2	<0.05	<0.1	<2	<0.1	<0.2	0.50	<0.3	<0.8	0.83
UofS 9727	1.02	0.07	0.31	0.01	<0.0005	<0.007	<0.0005	<0.0008	0.13	<0.001	0.11	0.27
UofA 9839	0.47	0.08	0.03	1.85	<0.0005	<0.007	<0.0005	<0.0008	0.13	0.04	0.17	0.14
UofS 9616	<0.008	<0.005	0.24	0.95	0.01	<0.007	0.02	<0.0008	0.15	0.05	0.57	0.25
UofS 9714	0.03	0.04	<0.01	1.00	<0.0005	<0.007	0.01	<0.0008	0.15	<0.001	1.03	0.17
UofS 9732	0.10	0.09	0.01	1.01	<0.0005	<0.007	<0.0005	<0.0008	0.15	0.03	1.00	0.26
UofA 9842	1.57	0.01	0.07	10.50	<0.0005	<0.007	<0.0005	<0.0008	0.13	0.13	0.25	0.17
UofA 9829	1.92	0.03	0.08	14.40	<0.0005	<0.007	<0.0005	<0.0008	0.14	0.12	19.00	0.12
UofA 9841	0.62	<0.005	<0.01	10.10	<0.0005	<0.007	<0.0005	<0.0008	0.13	0.13	0.18	0.10
UofA 9995	<2	<1.2	<2	30.00	<0.1	<2	<0.1	<0.20	0.45	0.45	56.20	<0.5
UofA 9828	0.65	<0.005	0.16	23.50	<0.0005	<0.007	<0.0005	<0.0008	0.12	0.13	22.40	0.02
UofA 9942	<2	<1	<2	4.47	<0.1	<2	<0.1	<0.20	0.40	<0.3	28.30	<0.5
UofA 9973	<2	<1	<2	23.20	<0.1	<2	<0.1	<0.20	0.40	0.40	2.00	<0.5
UofA 9947	14.00	<1	<2	5.93	<0.1	<2	<0.1	<0.20	0.35	0.30	22.80	<0.5
UofA 9926	<2.0	<1	<2	18.90	<0.1	<2	<0.1	<0.20	0.45	<0.3	26.90	<0.5
UofA 9941	<2	<1	<2	51.90	<0.1	<2	<0.1	<0.20	0.48	0.33	73.50	<0.5
UofA 9946	<2	<1	<2	36.20	<0.1	<2	<0.1	<0.2	<0.2	0.53	<0.8	<0.5
UofA 9950	<2	<1	<2	6.80	<0.1	<2	<0.1	<0.20	0.40	<0.3	35.20	<0.5

Appendix D. Minor Elements: results in mg/L.

Sample ID	Al	Sb	As	Ba	Be	Bi	Cd	Cr	Co	Cu	Fe	Pb
UofA 9940	<2	<1	<2	36.70	<0.1	<2	<0.1	<0.20	0.45	0.38	83.80	<0.5
UofA 9996	2.70	<1.2	2.60	69.50	<0.1	<2	<0.1	<0.20	0.45	0.30	32.60	<0.5
UofA 9949	2.60	<1	<2	43.40	<0.1	<2	<0.1	<0.20	0.40	0.33	35.10	<0.5
UofA 9953	<2	<1	<2	43.50	<0.1	<2	<0.1	<0.20	0.35	0.45	69.20	<0.5
UofA 9952	<2	<1	<2	50.00	<0.1	<2	<0.1	<0.20	0.40	0.28	64.50	<0.5
UofA 9980	10.00	<1.2	<2	<0.05	<0.1	2.00	<0.1	<0.2	0.53	<0.25	<0.8	0.73
UofS 9711	0.85	0.06	0.10	0.04	<0.0005	<0.007	0.01	<0.0008	0.15	<0.001	0.22	0.24
UofA 9840	<0.008	0.04	0.08	3.86	<0.0005	<0.007	0.01	<0.0008	0.18	0.05	0.47	0.15
UofA 9966	9.20	<1	<2	20.70	<0.1	<2	<0.1	<0.20	0.48	<0.3	7.98	<0.5
UofA 00201	2.10	<0.5	<1.0	9.87	<0.05	<0.7	<0.05	<0.08	0.15	0.12	7.14	<0.2
UofA 9957	<2	<1	<2	10.70	<0.1	<2	<0.1	<0.20	0.45	<0.3	27.60	<0.5
UofA 9956	<2	<1	<2	20.00	<0.1	<2	<0.1	<0.20	0.53	<0.3	35.20	<0.5
UofA 9967	8.80	<1	<2	1.03	<0.1	<2	<0.1	<0.2	0.45	<0.3	1.70	<0.5
UofA 9971	8.00	<1	<2	4.77	<0.1	<2	<0.1	<0.2	0.45	<0.3	24.00	<0.5
UofA 9991	7.90	<1	<2	1.90	<0.1	<2	<0.1	<0.2	0.45	<0.3	23.80	0.73
UofA 9993	8.70	<1.2	<2	2.88	<0.1	<2	<0.1	<0.2	0.40	<0.3	27.00	0.50
UofA 9975	11.00	<1.2	<2	4.58	<0.1	<2	<0.1	<0.2	0.60	<0.3	40.10	0.68
UofA 9982	11.00	<1	<2	8.53	<0.1	<2	<0.1	<0.2	0.53	<0.3	60.70	0.60
UofS 9731	1.42	0.10	<0.01	11.00	<0.0005	<0.007	<0.0005	<0.0008	0.15	0.07	6.02	0.27
UofA 9990	7.20	<1	<2	4.98	<0.1	<2	<0.1	<0.2	0.40	<0.3	16.50	0.65
UofS 9731	0.91	0.12	0.14	11.20	<0.0005	<0.007	<0.0005	<0.0008	0.17	0.06	0.56	0.23
UofA 9983	11.00	<1	<2	11.10	<0.1	<2	<0.1	<0.2	0.65	<0.3	29.20	<0.5
UofA 9848	1.68	0.02	0.09	5.89	<0.0005	0.84	<0.0005	<0.0008	0.16	0.10	3.21	0.23
UofS 9725	1.29	0.08	<0.01	9.39	<0.0005	<0.007	<0.0005	<0.0008	0.15	0.02	1.40	0.19
UofS 9728	0.56	0.09	0.14	9.51	<0.0005	<0.007	<0.0005	<0.0008	0.14	0.08	5.16	0.21
UofS 9726	0.47	0.09	0.20	8.70	<0.0005	<0.007	<0.0005	<0.0008	0.15	0.02	0.15	0.14
UofA 9992	3.90	<1	<2	8.15	<0.1	<2	<0.1	<0.2	0.48	<0.3	8.75	<0.5
UofA 9846	1.61	0.10	0.04	9.24	<0.0005	<0.007	<0.0005	<0.0008	0.13	0.10	4.25	0.18
UofA 9845	0.87	<0.005	<0.01	25.90	0.01	<0.007	0.02	<0.0008	0.13	0.14	6.05	0.14
UofA 9858	0.08	0.02	<0.01	2.45	<0.0005	<0.007	<0.0005	<0.0008	0.12	0.07	45.40	0.19
UofA 9936	3.80	<1	<2	25.80	<0.1	<2	<0.1	<0.2	0.40	0.40	2.70	<0.5

Appendix D. Minor Elements: results in mg/L.

Sample ID	Al	Sb	As	Ba	Be	Bi	Cd	Cr	Co	Cu	Fe	Pb
UofA 9961	<2	<1	<2	9.28	<0.1	<2	<0.1	<0.20	0.45	<0.3	10.60	<0.5
UofA 9935	<2	<1.2	<2	22.30	<0.1	<2	<0.1	<0.20	0.43	0.33	0.95	<0.5
UofA 9934	<2	<1.2	<2	11.50	<0.1	<2	<0.1	<0.20	0.50	<0.3	2.70	<0.5
UofA 9955	<2.0	<1.2	<2	12.20	<0.1	<2	<0.1	<0.2	0.40	<0.3	15.10	<0.5
UofA 9937	3.40	<1	<2	0.58	<0.1	<2	<0.1	<0.2	<0.2	<0.3	21.00	<0.5
UofA 00200	2.20	<0.5	<1.0	2.90	<0.05	<0.7	<0.05	<0.08	0.13	0.23	4.23	<0.2
UofA 9963	12.00	<1.2	<2	4.90	<0.1	<2	<0.1	<0.2	0.57	<0.3	18.00	0.73
UofA 9970	<2.0	<1	<2	1.43	<0.1	3.70	<0.1	<0.2	0.55	0.30	20.70	<0.5
UofA 9851	1.98	<0.005	0.19	6.43	0.01	0.11	0.01	<0.0008	0.15	0.10	20.20	0.32
UofA 9852	1.09	<0.005	0.14	6.49	<0.0005	<0.007	0.01	<0.0008	0.15	0.16	69.10	0.23
UofA 9850	1.16	0.02	<0.01	8.39	0.01	<0.007	<0.0005	<0.0008	0.14	0.10	35.00	0.20
UofA 9836	1.23	0.09	0.08	8.97	<0.0005	<0.007	<0.0005	<0.0008	0.15	0.10	0.27	0.27
UofA 9832	1.36	0.06	<0.01	10.60	<0.0005	<0.007	<0.0005	<0.0008	0.14	0.14	0.13	0.21
UofA 9847	1.12	0.06	0.08	8.89	<0.0005	<0.007	<0.0005	<0.0008	0.15	0.08	28.20	0.22
UofS 9720	1.06	0.07	<0.01	9.80	<0.0005	<0.007	<0.0005	<0.0008	0.13	0.06	2.66	0.27
UofS 9716	0.57	0.07	0.16	10.90	<0.0005	<0.007	<0.0005	<0.0008	0.15	0.03	5.07	0.19
UofS 9719	1.11	0.09	0.17	9.91	<0.0005	<0.007	0.01	<0.0008	0.15	0.04	6.89	0.26
UofS 9715	1.39	<0.005	<0.01	10.10	<0.0005	<0.007	<0.0005	<0.0008	0.14	0.03	3.05	0.20
UofA 9825	1.50	0.16	<0.01	11.20	<0.0005	<0.007	0.01	<0.0008	0.15	0.06	22.30	0.22
UofA 9833	1.56	0.04	0.14	13.80	<0.0005	<0.007	<0.0005	<0.0008	0.15	0.13	0.29	0.28
UofA 9831	1.53	0.11	0.09	14.80	<0.0005	<0.007	<0.0005	<0.0008	0.16	0.11	0.21	0.22
UofA 9830	0.86	0.13	<0.01	15.30	<0.0005	<0.007	<0.0005	<0.0008	0.12	0.12	22.40	0.03
UofA 9838	0.84	<0.005	0.25	19.80	<0.0005	<0.007	<0.0005	<0.0008	0.14	0.15	0.28	0.10
UofA 9962	<2	<1	<2	89.10	<0.1	<2	<0.1	<0.2	0.30	0.50	1.50	<0.5
UofA 9835	<0.080	<0.050	<0.10	6.32	<0.0050	87.90	<0.0050	<0.0080	<0.0070	<0.010	121.00	0.03
UofA 9959	<2.0	<1	<2	13.80	<0.1	<2	<0.1	<0.2	0.35	<0.3	25.60	<0.5
UofA 9958	<2.0	<1	<2	13.90	<0.1	<2	<0.1	<0.2	0.40	<0.3	16.20	<0.5
UofA 0093	1.40	<0.5	<1.0	0.78	<0.05	<0.7	<0.05	<0.08	0.19	<0.1	19.20	<0.2
UofA 0094	1.40	<0.5	<1.0	0.87	<0.05	<0.7	<0.05	<0.08	0.18	<0.1	22.20	<0.2
UofA 0092	0.98	<0.5	<1.0	0.98	<0.05	<0.7	<0.05	<0.08	0.19	<0.1	2.10	<0.2
UofA 0090	1.10	<0.5	<1.0	1.04	<0.05	<0.7	<0.05	<0.08	0.17	<0.1	8.59	<0.2

Appendix D. Minor Elements: results in mg/L.

Sample ID	Al	Sb	As	Ba	Be	Bi	Cd	Cr	Co	Cu	Fe	Pb
UofA 9930	8.30	<1	<2	3.23	<0.1	<2	<0.1	<0.2	0.25	<0.3	61.90	0.53
UofA 9987	9.20	<1	<2	1.83	<0.1	<2	<0.1	<0.2	0.43	<0.3	27.70	<0.5
UofA 0091	<0.8	<0.5	<1.0	1.26	<0.05	<0.7	<0.05	<0.08	0.20	<0.1	25.30	<0.2
UofA 00189	2.40	<0.5	<1.0	7.77	<0.05	<0.7	<0.05	<0.08	0.20	0.28	18.90	0.20
UofA 00192	3.00	<0.5	<1.0	11.20	<0.05	<0.7	<0.05	<0.08	0.21	0.15	8.55	0.24
UofS 9729	1.35	0.09	<0.01	20.10	<0.0005	<0.007	<0.0005	<0.0008	0.12	0.02	1.09	0.23
UofA 9927	<2.0	<1	<2	13.20	<0.1	<2	<0.1	<0.2	0.33	<0.3	10.30	<0.5
UofA 9931	5.60	<1	<2	1.43	<0.1	<2	<0.1	<0.20	0.18	<0.3	30.00	<0.5
UofA 9994	6.00	<1	<2	0.75	<0.1	<2	<0.1	<0.20	0.25	<0.3	2.90	<0.5
UofA 9939	<2	<1	<2	28.50	<0.1	<2	<0.1	<0.20	0.53	0.30	16.70	<0.5
UofA 9964	15.00	<1	<2	27.60	<0.1	<2	<0.1	<0.2	0.63	<0.3	91.80	0.53
UofA 9965	14.00	<1.2	<2	29.60	<0.1	<2	<0.1	<0.2	0.55	<0.3	18.70	0.78
UofA 9834	0.55	0.09	0.23	25.70	<0.0005	<0.007	<0.0005	<0.0008	0.14	0.04	2.39	0.18
UofA 9928	<2	<1	<2	33.00	<0.1	<2	<0.1	<0.2	0.38	0.43	60.30	<0.5
UofA 9960	<2	<1	<2	9.53	<0.1	<2	<0.1	<0.20	0.40	<0.3	9.32	<0.5
UofA 9972	<2	<1.2	<2	17.10	<0.1	<2	<0.1	<0.2	0.48	<0.3	23.30	<0.5
UofA 9976	9.90	<1	<2	11.90	<0.1	<2	<0.1	0.30	0.63	<0.3	75.70	1.20
UofA 9989	9.70	<1	<2	1.58	<0.1	<2	<0.1	<0.2	0.55	<0.3	94.50	0.68
UofA 9810	3.50	0.01	0.13	6.51	<0.0005	<0.007	0.01	<0.0008	0.17	0.21	16.80	0.29
UofA 9824	1.00	0.12	0.25	8.48	<0.0005	<0.007	0.02	<0.0008	0.16	0.05	131.00	0.25
UofS 9609	0.44	0.16	<0.01	0.46	0.01	0.79	0.01	0.03	0.16	<0.001	23.50	0.32
UofA 9822	1.37	0.11	0.04	21.90	0.01	<0.007	0.03	<0.0008	0.14	0.18	256.00	0.71
UofA 9823	<0.008	0.04	0.08	30.30	0.02	<0.007	0.02	<0.0008	0.15	0.02	183.00	0.25

Appendix D. Minor Elements: results in mg/L.

Sample ID	Mn	Mo	Ni	P	Se	Si	Ag	Tl	Sn	Ti	V	Zn
UofA 9969	1.15	<0.25	<0.3	15.00	2.80	14.60	<0.3	2.20	1.10	<0.10	<0.25	<0.2
UofA 9948	4.60	<0.3	<0.3	73.00	<1	19.20	<0.3	1.30	1.10	<0.10	<0.3	0.18
UofA 9951	2.48	<0.3	<0.3	<7	1.40	31.40	<0.3	1.90	1.10	<0.100	<0.25	1.00
UofA 9979	0.05	<0.3	<0.3	<7	<1.0	5.80	<0.3	<1	<0.8	<0.100	0.75	<0.2
UofA 9978	0.20	<0.3	<0.3	<7	<1.0	6.40	<0.3	<1	<0.8	<0.100	0.38	<0.2
UofA 9977	0.38	<0.3	<0.3	<7	<1	6.70	<0.3	1.50	<0.8	<0.100	0.75	0.20
UofA 9821	0.29	<0.001	0.09	8.03	<0.004	7.53	<0.001	0.13	0.07	<0.0004	<0.001	0.01
UofA 9820	1.13	<0.001	0.17	3.96	<0.004	7.05	<0.001	0.17	0.09	<0.0004	<0.001	0.13
UofA 9856	0.90	<0.001	0.10	4.41	<0.004	7.01	<0.001	0.12	<0.003	<0.0004	<0.001	0.02
UofA 9843	17.10	<0.001	0.10	27.80	<0.004	3.41	<0.001	0.47	0.07	<0.0004	<0.001	6.51
UofS 9723	0.28	<0.001	0.07	8.53	<0.004	8.29	<0.001	0.31	0.04	<0.0004	<0.001	0.13
UofA 9986	0.43	<0.3	<0.3	16.00	<1.0	13.10	<0.3	<1	<0.8	<0.100	0.53	0.53
UofA 9925	1.40	<0.3	<0.3	18.00	2.60	19.70	<0.3	3.40	0.98	<0.10	0.38	1.78
UofA 9981	<0.05	<0.3	<0.3	<7	<1	5.30	<0.3	1.70	<0.8	<0.100	1.10	<0.2
UofS 9727	0.03	<0.001	0.04	3.46	<0.004	6.25	<0.001	0.25	0.05	<0.0004	0.03	0.03
UofA 9839	0.21	<0.001	0.10	8.40	<0.004	5.43	<0.001	0.24	0.13	<0.0004	0.05	0.08
UofS 9616	1.15	<0.001	0.14	10.10	<0.004	1.11	<0.001	0.18	0.17	<0.0004	0.07	3.06
UofS 9714	0.27	<0.001	0.14	9.91	0.15	5.24	<0.001	0.06	0.01	<0.0004	<0.001	0.14
UofS 9732	0.28	<0.001	0.12	9.86	0.23	3.99	<0.001	0.08	0.01	<0.0004	<0.001	0.20
UofA 9842	2.05	<0.001	0.08	9.03	<0.004	9.13	<0.001	0.19	0.09	<0.0004	0.05	0.03
UofA 9829	0.64	<0.001	0.07	14.20	0.18	10.80	<0.001	0.40	0.12	<0.0004	<0.001	0.76
UofA 9841	0.70	<0.001	0.17	8.40	<0.004	12.60	<0.001	0.43	0.11	<0.0004	<0.001	<0.0006
UofA 9995	2.28	<0.3	<0.3	14.00	1.50	18.50	<0.3	1.20	1.00	<0.100	<0.25	5.53
UofA 9828	0.81	<0.001	0.20	14.50	<0.004	12.90	<0.001	0.26	0.13	<0.0004	<0.001	1.61
UofA 9942	1.65	<0.25	<0.3	11.00	<1	22.40	<0.3	1.50	0.83	<0.100	<0.25	9.48
UofA 9973	0.45	<0.25	<0.3	<7	2.10	19.00	<0.3	1.30	1.00	<0.100	<0.25	<0.2
UofA 9947	2.08	<0.3	1.50	12.00	<1	18.50	<0.3	2.10	1.00	<0.1000	0.38	1.10
UofA 9926	1.15	<0.3	<0.3	<7	<1	16.00	<0.3	1.20	<0.8	<0.100	<0.3	5.25
UofA 9941	1.95	<0.25	<0.3	11.00	<1	14.70	<0.3	1.80	1.20	<0.100	0.38	6.15
UofA 9946	1.58	<0.3	<0.3	8.50	1.20	13.10	<0.3	2.90	<0.8	<0.10	<0.3	16.00
UofA 9950	1.83	<0.25	<0.3	9.80	<1	14.00	<0.3	<1	1.10	<0.100	<0.3	7.73

Appendix D. Minor Elements: results in mg/L.

Sample ID	Mn	Mo	Ni	P	Se	Si	Ag	Tl	Sn	Ti	V	Zn
UofA 9940	3.03	<0.25	0.30	13.00	<1	22.70	<0.3	1.80	1.60	<0.100	<0.3	15.70
UofA 9996	2.50	<0.25	<0.3	11.00	<1	23.00	<0.3	2.00	1.40	<0.1000	<0.25	23.00
UofA 9949	1.68	<0.3	<0.3	13.00	<1	10.90	<0.3	1.40	0.88	<0.1000	<0.3	9.10
UofA 9953	3.15	<0.3	<0.3	11.00	<1	20.80	<0.3	2.10	0.93	<0.100	<0.25	14.10
UofA 9952	1.95	<0.25	<0.3	8.50	2.30	14.60	<0.3	2.80	0.98	<0.1000	<0.25	8.95
UofA 9980	0.08	<0.3	<0.3	13.00	<1	5.30	<0.3	<1	<0.8	<0.100	<0.3	<0.2
UofS 9711	0.04	<0.001	0.10	3.27	<0.004	3.14	0.04	0.36	<0.003	<0.0004	<0.001	0.04
UofA 9840	1.38	<0.001	0.05	8.43	<0.004	0.68	<0.001	0.24	0.11	<0.0004	<0.001	4.97
UofA 9966	0.78	<0.3	<0.3	22.00	<1.0	15.00	<0.3	<1	<0.8	<0.100	0.33	<0.2
UofA 00201	0.82	<0.1	<0.1	<3	<0.4	13.70	<0.1	<0.4	<0.3	<0.040	<0.1	0.08
UofA 9957	1.15	<0.3	<0.3	<7	<1	25.30	<0.3	2.60	0.78	<0.100	<0.25	<0.2
UofA 9956	1.22	<0.25	<0.3	<7	1.50	25.70	<0.3	1.30	<0.8	<0.100	<0.3	0.18
UofA 9967	0.25	<0.3	<0.3	<7	<1	22.90	<0.3	<1	<0.8	<0.100	0.57	0.20
UofA 9971	1.68	<0.3	<0.3	<7	1.80	20.80	<0.3	<1	<0.8	<0.10	<0.25	0.18
UofA 9991	0.33	<0.3	<0.3	<7	<1	11.40	<0.3	1.70	1.40	<0.10	<0.3	<0.2
UofA 9993	0.35	<0.3	<0.3	<7	<1	10.00	<0.3	2.00	1.10	<0.100	<0.3	0.63
UofA 9975	0.95	<0.3	<0.3	47.00	<1	8.20	<0.3	1.10	<0.8	<0.100	0.38	0.60
UofA 9982	1.10	<0.3	<0.3	<7	<1	8.40	<0.3	<1	0.95	<0.100	<0.3	1.30
UofS 9731	0.70	<0.001	0.16	3.13	<0.004	9.51	<0.001	0.32	0.04	<0.0004	0.04	0.06
UofA 9990	0.33	<0.25	<0.3	<7	<1	9.50	<0.3	1.00	<0.8	<0.10	<0.3	0.35
UofS 9731	0.69	<0.001	0.17	3.38	<0.004	6.49	<0.001	0.38	0.14	<0.0004	<0.001	0.22
UofA 9983	0.63	<0.3	<0.3	<7	<1.0	13.40	<0.3	1.30	<0.8	<0.100	0.38	0.45
UofA 9848	0.20	<0.001	0.10	3.03	<0.004	7.86	<0.001	0.26	0.15	<0.0004	0.01	0.38
UofS 9725	0.57	<0.001	0.11	2.99	<0.004	5.97	<0.001	0.23	0.04	<0.0004	<0.001	0.59
UofS 9728	0.65	<0.001	0.11	3.21	<0.004	7.24	<0.001	0.46	0.08	<0.0004	<0.001	0.44
UofS 9726	0.30	<0.001	0.14	3.10	<0.004	7.20	<0.001	0.29	0.09	<0.0004	0.01	0.30
UofA 9992	0.38	<0.3	<0.3	<7	<1	8.60	<0.3	<1	0.93	0.18	<0.3	0.18
UofA 9846	5.05	<0.001	0.17	5.38	0.03	4.24	<0.001	0.19	<0.003	<0.0004	<0.001	4.72
UofA 9845	4.16	<0.001	0.15	3.00	<0.004	4.57	<0.001	0.44	0.09	<0.0004	<0.001	15.80
UofA 9858	0.73	<0.001	0.07	3.97	<0.004	7.89	<0.001	0.19	0.15	<0.0004	0.08	0.29
UofA 9936	0.73	<0.3	<0.3	8.40	1.80	14.80	<0.3	1.70	0.88	<0.100	<0.25	<0.2

Appendix D. Minor Elements: results in mg/L.

Sample ID	Mn	Mo	Ni	P	Se	Si	Ag	Tl	Sn	Ti	V	Zn
UofA 9961	0.35	<0.3	<0.3	<7	<1	23.20	<0.3	1.80	<0.8	<0.100	<0.25	1.50
UofA 9935	0.35	<0.25	<0.3	<7	2.00	22.30	<0.3	2.30	1.10	<0.100	<0.25	<0.2
UofA 9934	1.28	<0.3	<0.3	<7	2.00	19.70	<0.3	2.20	1.10	<0.100	0.40	<0.2
UofA 9955	2.83	<0.3	<0.3	<7	<1.0	28.00	<0.3	1.10	0.80	<0.100	<0.25	0.23
UofA 9937	0.50	<0.3	<0.3	<7	<1	39.30	<0.3	2.10	<0.8	0.15	<0.25	0.20
UofA 00200	0.23	<0.1	<0.1	<3	<0.4	24.00	<0.1	<0.4	<0.3	<0.040	<0.1	0.08
UofA 9963	0.38	<0.3	<0.3	<7	<1	25.40	<0.3	1.70	0.95	<0.100	0.68	0.65
UofA 9970	1.53	<0.3	0.30	13.00	<1	11.40	<0.3	2.20	1.40	<0.100	<0.3	3.53
UofA 9851	0.55	<0.001	0.16	2.97	<0.004	12.00	<0.001	0.32	0.11	<0.0004	0.06	0.48
UofA 9852	0.88	<0.001	0.05	3.74	<0.004	10.60	<0.001	0.25	0.08	<0.0004	<0.001	0.42
UofA 9850	0.67	<0.001	0.07	3.87	0.10	8.86	<0.001	0.33	0.10	<0.0004	0.03	0.83
UofA 9836	0.62	<0.001	0.10	2.20	<0.004	6.26	<0.001	0.34	0.09	<0.0004	<0.001	0.30
UofA 9832	0.75	<0.001	0.12	1.88	<0.004	6.79	<0.001	0.32	0.09	<0.0004	<0.001	1.04
UofA 9847	0.79	<0.001	0.10	3.53	<0.004	8.85	<0.001	0.31	0.15	<0.0004	0.02	1.10
UofS 9720	0.77	<0.001	0.13	2.07	<0.004	5.95	<0.001	0.40	0.12	<0.0004	<0.001	0.83
UofS 9716	0.68	<0.001	0.09	2.93	<0.004	6.31	<0.001	0.16	0.17	<0.0004	0.09	0.63
UofS 9719	0.74	<0.001	0.11	2.33	<0.004	6.45	<0.001	0.19	0.02	<0.0004	<0.001	0.46
UofS 9715	0.77	<0.001	0.11	1.96	<0.004	8.10	<0.001	0.12	0.11	<0.0004	<0.001	0.95
UofA 9825	0.63	<0.001	0.14	2.08	<0.004	10.10	<0.001	0.22	<0.003	<0.0004	<0.001	0.58
UofA 9833	0.95	<0.001	0.09	2.81	0.05	6.99	<0.001	0.35	0.11	<0.0004	<0.001	1.58
UofA 9831	0.94	<0.001	0.11	1.94	0.08	7.84	<0.001	0.23	0.14	<0.0004	<0.001	0.93
UofA 9830	0.93	<0.001	0.15	2.38	<0.004	10.30	<0.001	0.17	0.14	<0.0004	0.01	1.02
UofA 9838	1.46	<0.001	0.14	2.15	<0.004	2.87	<0.001	0.43	0.12	<0.0004	0.06	1.99
UofA 9962	2.68	<0.25	<0.3	<7	<1	37.10	<0.3	<1	<0.8	<0.10	<0.3	<0.2
UofA 9835	1.72	0.02	0.02	<0.30	0.05	6.86	<0.010	<0.040	<0.030	<0.0040	<0.010	2.13
UofA 9959	2.13	<0.3	<0.3	<7	2.60	25.90	<0.3	2.60	<0.8	<0.100	0.35	5.38
UofA 9958	1.88	<0.3	<0.3	<7	<1	25.30	<0.3	<1	<0.8	<0.100	<0.3	5.28
UofA 0093	0.40	<0.1	<0.1	<3	<0.40	7.71	<0.1	<0.4	<0.3	<0.040	<0.1	0.12
UofA 0094	0.37	<0.1	<0.1	<3	<0.4	7.89	<0.1	<0.4	<0.3	<0.040	<0.1	0.09
UofA 0092	0.12	<0.1	0.14	<3	<0.4	8.15	<0.1	<0.4	<0.3	<0.040	<0.1	0.07
UofA 0090	0.23	<0.1	<0.1	<3	<0.4	8.31	0.23	0.91	<0.3	<0.040	<0.1	0.08

Appendix D. Minor Elements: results in mg/L.

Sample ID	Mn	Mo	Ni	P	Se	Si	Ag	Tl	Sn	Ti	V	Zn
UofA 9930	0.90	<0.3	<0.3	<7	<1	27.30	<0.3	1.50	1.00	0.38	0.38	<0.2
UofA 9987	0.63	<0.3	<0.3	<7	<1.0	12.10	<0.3	<1	<0.8	<0.100	0.55	3.15
UofA 0091	0.35	<0.1	<0.1	<3	<0.4	8.45	<0.1	0.44	<0.3	<0.040	<0.1	0.17
UofA 00189	0.54	<0.1	<0.1	<3	<0.4	10.30	<0.1	<0.4	<0.3	<0.040	<0.1	0.90
UofA 00192	0.71	<0.1	<0.1	<3	<0.40	9.63	<0.1	<0.4	<0.3	<0.040	<0.1	1.02
UofS 9729	1.22	<0.001	0.18	2.11	0.05	7.03	<0.001	0.06	0.04	<0.0004	0.02	1.75
UofA 9927	5.10	<0.3	<0.3	<7	<1	17.30	<0.3	2.50	1.60	<0.100	<0.3	3.95
UofA 9931	0.45	<0.3	<0.3	<7	<1	33.30	<0.3	<1	<0.8	0.75	<0.3	<0.2
UofA 9994	0.18	<0.3	<0.3	<7	1.10	26.90	<0.3	2.20	<0.8	0.30	<0.25	<0.2
UofA 9939	1.40	<0.3	<0.3	9.30	2.00	18.60	<0.3	1.80	1.20	<0.10	<0.25	6.20
UofA 9964	3.70	<0.3	0.33	<7	<1	6.40	<0.3	1.40	0.80	<0.100	1.10	1.50
UofA 9965	1.83	<0.3	<0.3	<7	<1.0	15.70	<0.3	<1	<0.8	<0.100	0.68	3.35
UofA 9834	2.63	<0.001	0.19	2.11	<0.004	2.77	0.01	0.32	0.12	<0.0004	0.03	2.91
UofA 9928	9.10	<0.3	<0.3	<7	<1	17.20	0.28	1.90	1.10	<0.100	<0.25	4.85
UofA 9960	0.35	<0.3	<0.3	<7	<1	23.80	<0.3	1.20	<0.8	<0.100	<0.25	1.55
UofA 9972	2.32	<0.3	<0.3	<7	1.80	19.80	<0.3	2.00	1.10	<0.100	<0.3	<0.2
UofA 9976	1.75	<0.3	0.30	<7	<1.0	9.80	<0.3	2.10	0.78	<0.100	0.65	1.30
UofA 9989	3.35	<0.3	<0.3	<7	<1.0	11.40	<0.3	1.00	<0.8	<0.100	0.90	0.83
UofA 9810	12.80	<0.001	0.27	2.82	<0.004	6.37	<0.001	0.25	0.23	<0.0004	0.05	5.76
UofA 9824	21.10	<0.001	0.11	1.83	<0.004	11.00	<0.001	0.36	0.10	<0.0004	<0.001	2.19
UofS 9609	0.70	<0.001	0.09	<0.03	<0.004	3.14	<0.001	0.22	0.08	<0.0004	<0.001	2.78
UofA 9822	67.90	<0.001	0.03	2.76	<0.004	13.20	<0.001	0.55	0.27	<0.0004	<0.001	7.79
UofA 9823	112.00	<0.001	<0.001	3.41	<0.004	8.31	0.01	0.48	0.34	<0.0004	<0.001	4.51

Appendix E. Details of Reactions Possibly Affecting Group C Major Ions

Several possible processes may be responsible for shifting Ca, Na, Mg and SO_4 compositions of Group C waters from those of seawater including: anhydrite precipitation, anhydrite dissolution, thermochemical sulphate reduction, dolomitization and albitization. Enrichment of Ca in basinal brines via albitization depletes the concentrations of Na while enrichment in Ca during dolomitization results in Mg depletion (Viets et al., 1996). Anhydrite dissolution may also increase Ca values, but cannot account for the low sulphate values. However, sulphate can be removed from solution a number of ways including precipitation of sulphate minerals into evaporite deposits, formation of sulphide minerals, formation of organic sulphur and complete sulphate reduction to H_2S via thermochemical sulphate reduction (Machel, 2001). Precipitation of sulphate minerals and thermochemical sulphate reduction are the only two reactions with the potential to reduce sulphur on a scale corresponding to the size of the Group C zone, therefore sulphide minerals and organic sulphur will not be considered. Which of these evolutionary processes have affected the Group C endmember and to what extent will depend on initial and progressive water compositions.

ALBITIZATION

During albitization, mobile sodium is exchanged for calcium in feldspars in the several possible reactions including (Davisson and Criss, 1996):

$$Na^{+}_{(aq)} + SiO_{2(s)} + 4H^{+}_{(aq)} + Ca(Al_2Si_2O_8)_{(s)} \rightarrow$$

$$Ca^{2+}_{(aq)} + Al^{3+}_{(aq)} + 2H_2O_{(l)} + Na(AlSi_3O_8)_{(s)};$$

and,

$$CaAl_2Si_2O_{8\,(s)} + 4SiO_{2\,(s)} + 2Na^{+}_{(aq)} \rightarrow 2NaAlSi_3O_{8\,(s)} + Ca^{2+}_{(aq)}$$

If the first reaction is responsible for an increase in calcium and decrease in sodium, then the molar ratio of Ca_{excess} to $Na_{depletion}$ (for definitions see Appendix F) should be 1:1, as defined by the exchange reaction. If the second reaction is responsible for and increase in calcium and decrease in sodium, then the molar ratio of Ca_{excess} to $Na_{depletion}$ should be 1:2.

ANHYDRITE DISSOLUTION

Calcium may be mobilized during the dissolution of anhydrite, by the reaction:

$$CaSO_{4\,(s)} \leftrightarrow Ca^{2+}{}_{(aq)} + SO_4{}^{2-}{}_{(aq)}$$

This reaction would release one mole of both sulphate and calcium per mole of anhydrite dissolved. Assuming similar initial concentrations of sulphate and calcium (as would be found in seawater or halite-saturated water), the molar amount of calcium observed would approximately equal the molar amount of sulphate observed.

DOLOMITIZATION

Calcium enrichment may also occur through dolomitization as magnesium is substituted for calcium in a 1:1 ratio during interaction with calcite (Hardie, 1987):

$$Mg^{2+}{}_{(aq)} + 2CaCO_{3\,(s)} \rightarrow Ca^{2+}{}_{(aq)} + MgCa(CO_3)_{2\,(s)}$$

If this reaction is responsible for an increase in calcium and decrease in magnesium, then the molar ratio of Ca_{excess} to $Mg_{depletion}$ (for definitions see Appendix F) should be 1:1, as defined by the exchange reaction.

THERMOCHEMICAL SULPHATE REDUCTION

Low concentrations of SO_4 and high concentrations of H_2S at 3-5 km depths of the subsurface are thought to arise from a reaction that is abiotically controlled and involves the oxidation of hydrocarbons, with concurrent reduction of sulphate (Machel, 1992; Goldstein and Aizenshtat, 1994). Previous studies have proposed that large volumes of H_2S in deep reservoirs are formed via TSR of evaporite-derived sulphate, with hydrocarbons acting as the reducing agent (Wade et al., 1989). This sulphate reducing reaction is best represented as (Worden and Smalley, 1996):

$$CaSO_{4\,(s)} + CH_{4\,(g)} \rightarrow CaCO_{3\,(s)} + H_2S_{(g)} + H_2O_{(l)}$$

This reaction can also be written for higher hydrocarbons with the same net result; increasing H_2S while oxidizing the hydrocarbons, and written in aqueous form, clearly shows the role of sulphate (Feely and Kulp, 1952):

$$SO_4^{2-}{}_{(aq)} + 1.33\{CH_2\}_{(l)} + 2H^+{}_{(aq)} \rightarrow H_2S_{(g)} + 1.33CO_{2(g)} + 1.33H_2O_{(l)}$$

Due to the many explanations for sulphate removal from groundwater, the presence of H_2S is actually a better indicator for TSR than the absence of SO_4^{2-}, since there is only this one potential mechanism for non-microbial H_2S production (Feely and Kulp, 1952).

Several previous attempts have been made to define the conditions under which TSR and gas souring can occur. Temperature is viewed as a primary factor (Worden et al., 1995). Both experimental laboratory studies and subsurface evidence have been used to establish the occurrence of TSR in the subsurface. Experimental results have been limited and only show TSR occurring at temperatures as low as 175°C (Orr, 1977). On the basis of fluid inclusion data, petrographical analysis/thin section mineralogy and gas composition data, it has been suggested that the critical minimum temperature for TSR is 140°C (Simpson, 2000). The range of threshold reaction temperatures listed in literature is from a minimum of 80°C to greater than 200°C.

ANHYDRITE PRECIPITATION

Solubility controls on high Ca concentrations may potentially require anhydrite precipitation:

$$Ca^{2+}_{(aq)} + SO_4^{2-}{}_{(aq)} \leftrightarrow CaSO_{4\,(s)}$$

Considering only this reaction, removal of sulphate and calcium from solution would occur on a 1:1 molar basis.

References

Davisson, M.L. and Criss, R.E., 1996. Na-Ca-Cl relations in basinal fluids. Geochimica et Cosmochimica Acta, 60(15): 2743-2752.

Feely, H.W. and Kulp, J.L., 1952. Origin of the Gulf Coast salt-dome sulphur depositis. Bulletin of the American Association of Petroleum Geologists, 41(8): 1803-1853.

Goldstein, T.P. and Aizenshtat, Z., 1994. Thermochemical Sulphate Reduction, a review. Journal of Thermal Analysis, 42: 241-290.

Hardie, L.A., 1987. Dolomitization: A Critical View of Some Current Views. Journal of Sedimentary Petrology, 57(1): 166-183.

Machel, H.G., 1992. Low-Temperature and High-Temperature Origins of Elemental Sulphur in Diagenetic Environments. In: G.R. Wessel and B.H. Wimbley (Editors), Native Sulphur Developments in Geology and Exploration. Society for Mining, Metallurgy and Exploitation, Inc., Littleton, CO, pp. 3-22.

Machel, H.G., 2001. Bacterial and thermochemical sulphate reduction in diagenetic settings – old and new insights. Sedimentary Geology, 140: 143-175.

Orr, W.L., 1977. Geologic and geochemical controls on the distribution of hydrogen sulphide in natural gas. In: R. Campos and J. Goni (Editors), Advances in Organic Geochemistry, Madrid, pp. 571-597.

Simpson, G.P., 2000. Sulphate reduction and fluid chemistry of the Devonian Leduc and Nisku Formations in south-central Alberta. Ph.D. 2000.

Viets, J.G., Hofstra, A.H. and Emsbo, P., 1996. Solute compositions of fluid inclusions in sphalerite from North American and European Mississippi Valley-type ore deposits: ore fluids derived from evaporated seawater. In: D.F. Sangster (Editor), Carbonate Pb-Zn Deposits, SEPM Special Publication No. 4. Society of Economic Geologists, pp. 465-482.

Wade, W.J., Hanor, J.S. and Sassen, R., 1989. Controls on H_2S Concentration and Hydrocarbon Destruction in the Eastern Smackover Trend, Transactions - Gulf Coast Association of Geological Societies, pp. 309-320.

Worden, R.H. and Smalley, P.C., 1996. H2S producing reactions in deep carbonate gas reservoirs: Khuff Formation, Abu Dhabi. Chemical Geology, 133: 151-171.

Worden. R.H., Smalley, P.C., Oxtoby, N.H., 1995. Gas souring by Thermochemical Sulphate Reduction at 140°C. Bulletin of the American Association of Petroleum Geologists, 79(6): 854-863.

Appendix F. Calculations for Estimating Ca Excess, Na Depletion and Mg Depletion.

PART I

Various types of reactions including exchange, dissolution, precipitation and redox govern ion concentrations in formation waters. Many types of reactions may affect one particular species. Amounts of species gained or lost via certain processes can be estimated using Br values to find the predicted major ion concentrations from seawater evaporation data (taken from McCaffrey et al., 1987) since Br has been shown to be conservative in the Group C endmember. These predicted values are quantitatively compared to measured values in the basin today. Although without knowledge of all reactions and amount of solids, many factors remain unknown, and a true mass balance can never be achieved. However, a general idea of solute reactions and history may be obtained through comparison of actual sample concentrations and estimates of what concentrations would be found at an evaporation degree coupled with a given bromine concentration. A mass balance approach has been taken in other brine studies, e.g., Kinsman (1964); Butler (1969) and (1970); Patterson and Kinsman (1982); Spencer (1987) and Carpenter (1978).

The following describes the steps used to estimate Ca excess in pre-Mississippian formation waters.

Step 1. A line of best fit is obtained from the graphical relationship between Ca vs. Br measured in seawater during progressive evaporation from McCaffrey et al (1987), and is used to derive an equation which allows one to predict a Ca concentration for any given Br concentration. Two separate lines are fit since the relationship between Ca and Br, prior to, and after gypsum precipitation, is completely different (Figures 1 and 2). The two equations corresponding to the best-fit line are:

1) $Ca_{seawater}(mg/L) = 6.1938 * Br_{seawater}(mg/L) - 34.153$ {*before gypsum precipitation*}

2) $Ca_{seawater}(mg/L) = 3982.6e^{-0042(Br\ seawater)}$ {*after gypsum precipitation*}

Step 2. Based on the assumption that processes other than seawater evaporation do not affect bromine concentrations, the term $Br_{seawater}$ is replaced by $Br_{measured}$, the Br concentration measured in the sample. This substitution results in an equation describing the predicted or 'unreacted' Ca concentration in evaporated seawater. $Br_{measured}$ is compared to Figures 1 and 2 to determine if it corresponds to a concentration prior to or after gypsum precipitation and then the correct equation below is applied to obtain $Ca_{predicted}$:

3) $Ca_{predicted}(mg/L) = 6.1938 * Br_{measured}(mg/L) - 34.153$ {*before gypsum precipitation*}

4) $Ca_{predicted}(mg/L) = 3982.6e^{-0042(Br\ measured)}$ {*after gypsum precipitation*}

This is the Ca value that should equate with the measured Br concentration; the Ca value that one would expect in that sample if no reactions had taken place.

Step 3. The predicted Ca value is subtracted from the measured Ca value in the same sample, to obtain the Ca excess. This difference is also converted to milliequivalents per liter at this time:

$$5)\ Ca_{excess}\ (meq/L) = [Ca_{measured} - Ca_{predicted}] * 2/40.08$$

The following describes the steps used to estimate Na depletion in pre-Mississippian formation waters.

Step 1. A line of best fit is obtained from the graphical relationship between Na vs. Br measured in seawater during progressive evaporation from McCaffrey et al (1987), and is used to derive an equation which allows one to predict a Na concentration for any given Br concentration. Two separate lines are fit since the relationship between Na and Br, prior to, and after halite precipitation, is completely different (Figures 3 and 4). The two equations corresponding to the best-fit line are:

6) $Na_{seawater}(mg/L) = 158.96*Br_{seawater}(mg/L) + 592.14$ {*before halite precipitation*}
7) $Na_{seawater}(mg/L) = -51395Ln(Br_{seawater}) + 450774$ {*after halite precipitation*}

Step 2. Based on the assumption that processes other than seawater evaporation do not affect bromine concentrations, the term $Br_{seawater}$ is replaced by $Br_{measured}$, the Br concentration measured in the sample. This substitution results in an equation describing the predicted or 'unreacted' Na concentration in evaporated seawater. $Br_{measured}$ is compared to Figures 3 and 4 to determine if it corresponds to a concentration prior to or after halite precipitation and then the correct equation below is applied to obtain $Na_{predicted}$:

8) $Na_{predicted}\ (mg/L) = 158.96*Br_{measured}\ (mg/L) + 592.14$ {*before halite precipitation*
9) $Na_{predicted}\ (mg/L) = -51395Ln(Br_{measured}) + 450774$ {*after halite precipitation*}

This is the Na value that should equate with the measured bromine concentration; the Na value that one would expect in that sample if no reactions had taken place.

Step 3. The measured Na value is subtracted from the predicted Na value in the same sample, to obtain the Na depletion. This difference is also converted to milliequivalents per liter at this time:

$$10)\,Na_{depletion}\ (meq/L) = [Na_{predicted} - Na_{measured}]*1/22.99$$

The following describes the steps used to estimate Mg depletion in pre-Mississippian formation waters.

Step 1. A line of best fit is obtained from the graphical relationship between Mg vs. Br measured in seawater during progressive evaporation from McCaffrey et al (1987), and is used to derive an equation which allows one to predict a Mg concentration for any given Br concentration. Only one line is fit since the relationship between Mg and Br does not change until an evaporation degree of 70 (Figures 5). The equation corresponding to the best-fit line is:

$$11)\ Mg_{seawater}\ (mg/L) = 20.296*Br_{seawater} - 333.5\ \ \{\text{before 70x evaporation}\}$$

Step 2. Based on the assumption that processes other than seawater evaporation do not affect bromine concentrations, the term $Br_{seawater}$ is replaced by $Br_{measured}$, the Br concentration measured in the sample. This substitution results in an equation describing the predicted or 'unreacted' Mg concentration in evaporated seawater.

$$12)\ Mg_{predicted}\ (mg/L) = 20.296*Br_{measured} - 333.5\ \ \{\text{before 70x evaporation}\}$$

Step 3. The measured Mg value is subtracted from the predicted Mg value in the same sample, to obtain the Mg depletion. This difference is also converted to milliequivalents per liter at this time:

$$13)\ Mg_{depletion}\ (meq/L) = [Mg_{predicted} - Mg_{measured}]*2/24.31$$

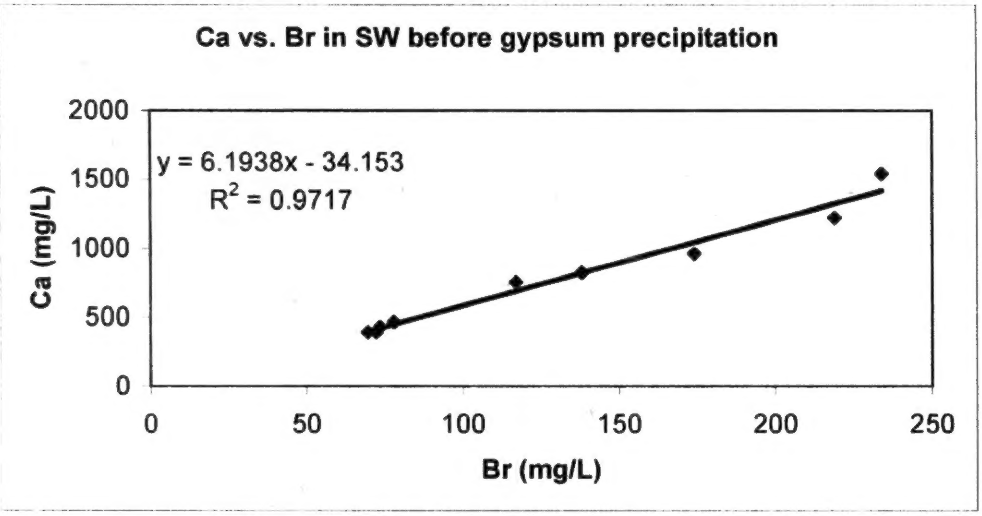

Figure 1. Ca vs. Br trend and corresponding equation for SW at evaporation degrees prior to gypsum precipitation.

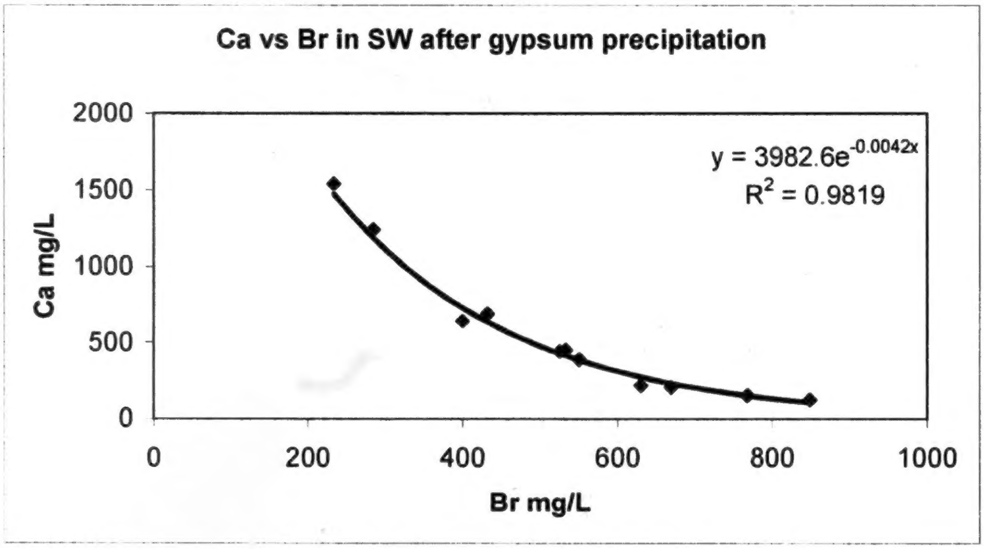

Figure 2. Ca vs. Br trend and corresponding equation for SW at evaporation degrees after gypsum precipitation.

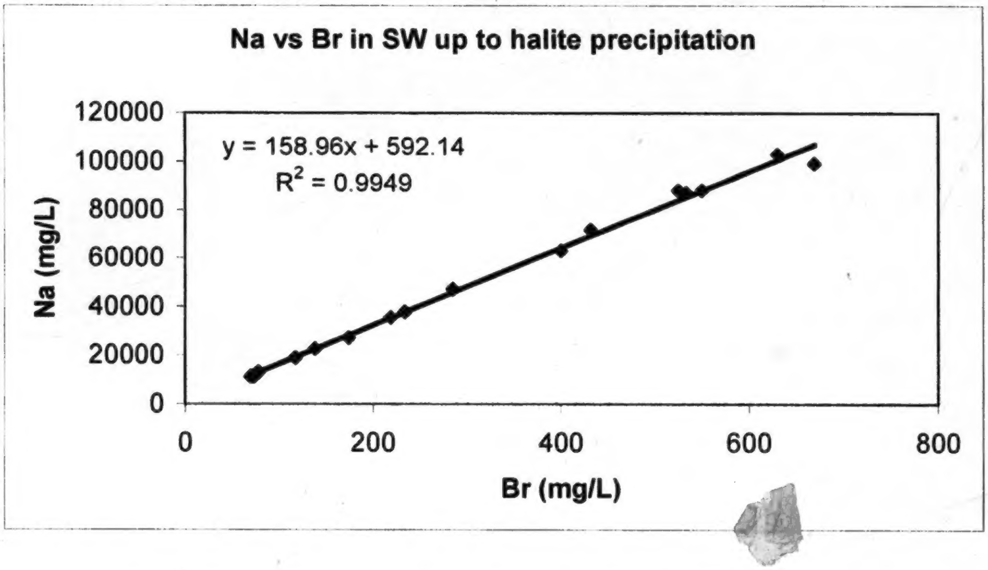

Figure 3. Na vs. Br trend and corresponding equation for SW at evaporation degrees prior to halite precipitation.

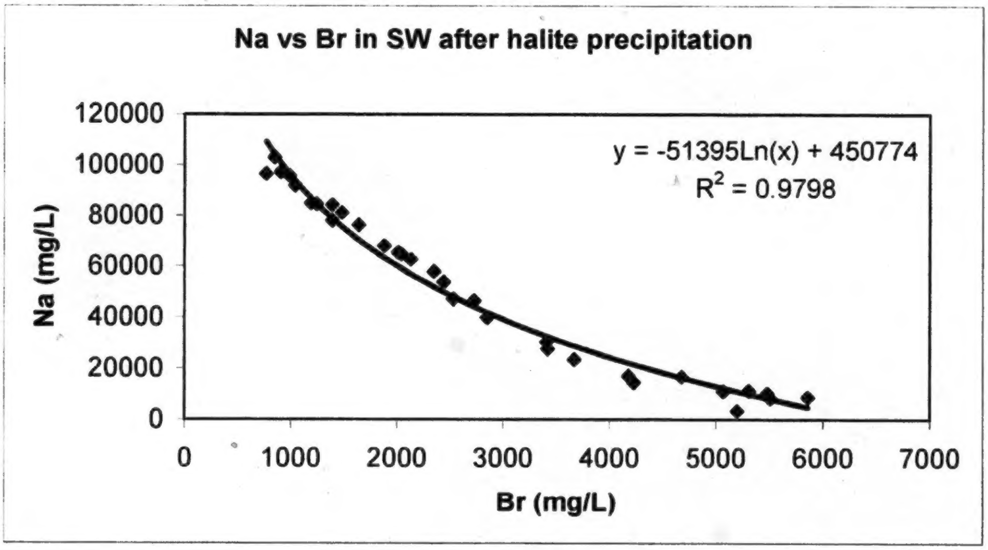

Figure 4. Na vs. Br trend and corresponding equation for SW at evaporation degrees after halite precipitation.

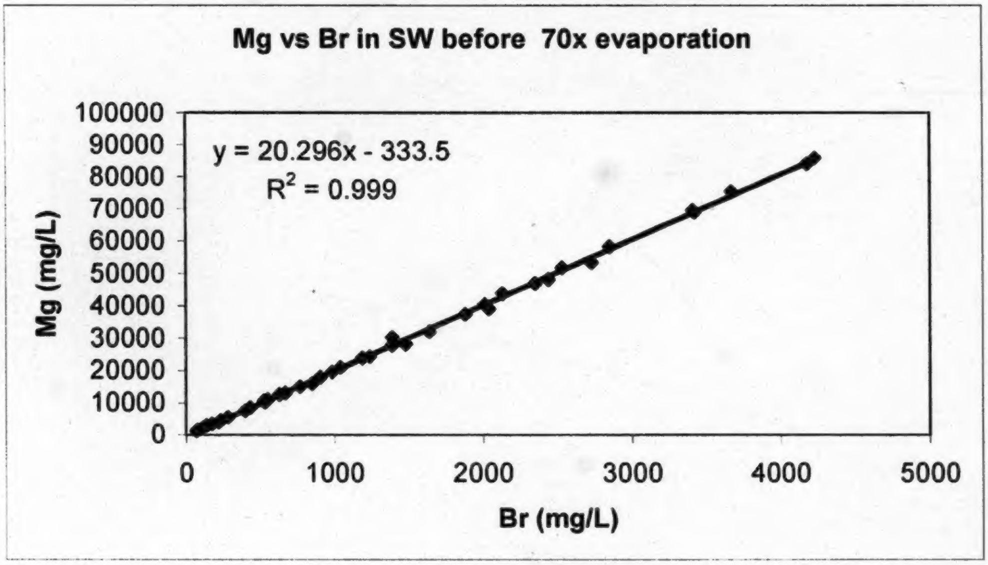

Figure 5. Mg vs. Br trend and corresponding equation for SW at evaporation degrees below 70.

References

Butler, G.P., 1969. Modern evaporite deposition and geochemistry of coexisting brines, the sabkha, Trucial Coast, Arabian Gulf. Journal of Sedimentary Petrology, 39: 70-89.

Butler, G.P., 1970. Holocene gypsum and anhydrite of the Abu Dhabi sabkha, Trucial Coast: an alternative explanation of origin, 3rd symposium on salt. Northern Ohio Geological Society, Cleveland, Ohio, pp. 120-152.

Carpenter, A.B., 1978. Origin and Chemical Evolution of Brines in Sedimenatry Basins. Oklahoma Geological Survey Circular, 79: 60-77.

Kinsman, D.J., 1964. Recent carbonate sedimentation near Abu Dhabi, Trucial Coast, Persian Gulf, Imperial College of Science and Technology, University of London, London.

McCaffrey, M.A., Lazar, B. and Holland, H.D., 1987. The Evaporation Path of Seawater and the Coprecipitation of Br- and K+ with Halite. Journal of Sedimentary Petrology, 57(5): 928-937.

Patterson, R.J. and Kinsman, D.J., 1982. Formation of diagenetic dolomite in coastal sabkha along Arabian Gulf. Americal Association of Petroleum Geologists Bulletin, 66: 28-43.

Spencer, R.J., 1987. Origin of Ca-Cl brines in Devonian formations, western Canada sedimentary basin. Applied Geochemistry, 2: 373-384.

PART II

The reader should note that the steps 1 through 3, used to find Ca excess and Na depletion as defined here, are not equivalent to the steps and calculations used by Davisson and Criss (1996) to find the same terms.

Davisson and Criss (1996) use the following equations.

1) $Ca_{excess} = [Ca_{sample} - ((Ca_{seawater} / Cl_{seawater}) * Cl_{sample})] *2/40.08$
2) $Na_{depleion} = [((Na_{seawater} / Cl_{seawater}) * Cl_{sample}) - Na_{sample}] * 1/22.99$

The Davisson and Criss equations assume chloride is a conservative parameter (instead of bromine), which can be used to estimate either the concentration of Ca, or Na that 'should' be present in the sample. The problem is these equations normalize the estimated concentration by the ratio of the constituents in non-evaporated seawater (with TDS = 35,000 mg/L), and make no allowance for the relative solute concentration changes as seawater evaporates. This normalizing effect can be seen in Figure 1 which uses pre-Mississippian data, and the Davisson and Criss (1996) definitions of Ca excess and Na depletion.

In comparison with Figure 6.19 of Chapter 6, this plot and underlying equations used to derive it, result in a linear trend. However, the linear trend is an artifact of two neglected features, rather than 2:1 exchange of Na for Ca. First, there is little Ca in seawater, so any increase via any reaction appears to be a linear increase when normalized to the seawater value. Second, sodium and chloride are approximately 1:1 during seawater evaporation until the point of halite saturation, but on Figure 1, for Group C samples, decreased Na concentrations due to evaporation past halite precipitation are disguised as apparent deficits in sodium due to 2:1 exchange of Na for Ca.

Due to their limitations, the Davisson and Criss (1996) equations cannot be used for brines, and should not be used for water with salinities much greater than seawater. Instead, predictions of the constituents concentrations originally present prior to reaction in waters of higher salinity should be based equations that account for seawater evaporation, such as the equations presented in Part I.

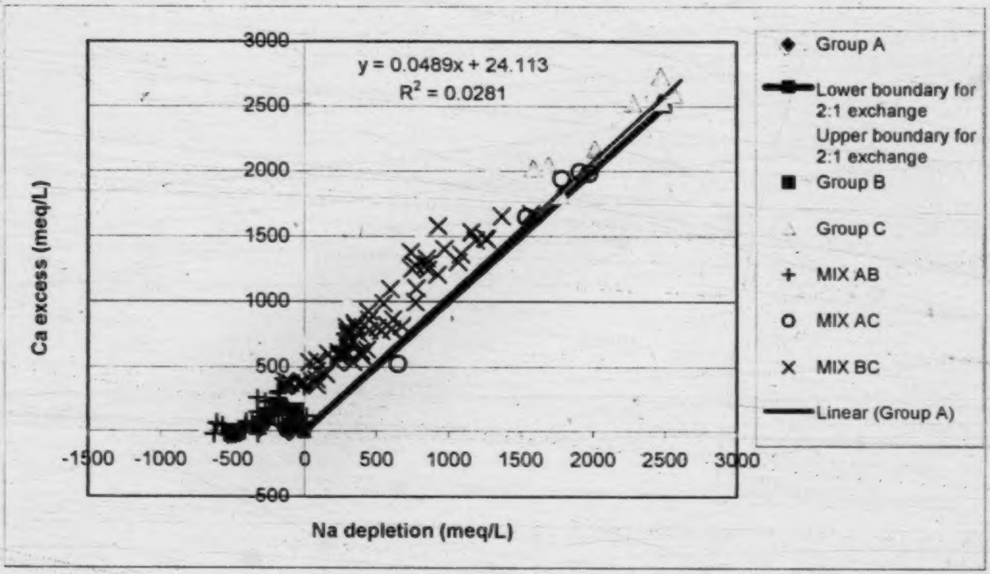

Figure 1. Ca Excess vs. Na Depletion in WB samples compared to non-evaporated seawater using Davisson and Criss (1996) equations.

References

Davisson, M.L. and Criss, R.E., 1996. Na-Ca-Cl relations in basinal fluids. Geochimica et Cosmochimica Acta, 60(15): 2743-2752.